THERMOCHEMICAL CONVERSION OF *CHLORELLA* SPP. INTO BIOCHAR AND ITS POTENTIAL ENVIRONMENTAL APPLICATIONS

YU KAI LING

FACULTY OF SCIENCE
UNIVERSITI MALAYA
KUALA LUMPUR

2021

THERMOCHEMICAL CONVERSION OF *CHLORELLA* SPP. INTO BIOCHAR AND ITS POTENTIAL ENVIRONMENTAL APPLICATIONS

YU KAI LING

THESIS SUBMITTED IN FULFILMENT OF THE REQUIREMENTS FOR THE DEGREE OF DOCTOR OF PHILOSOPHY

INSTITUTE OF BIOLOGICAL SCIENCES
FACULTY OF SCIENCE
UNIVERSITI MALAYA
KUALA LUMPUR

2021

UNIVERSITI MALAYA

ORIGINAL LITERARY WORK DECLARATION

Name of Candidate: **YU KAI LING**

Matric No: **SHC160069 / 17021383**

Name of Degree: **DOCTOR OF PHILOSOPHY**

Title of Project Paper/Research Report/Dissertation/Thesis ("this Work"):

THERMOCHEMICAL CONVERSION OF *CHLORELLA* SPP. INTO BIOCHAR AND ITS POTENTIAL ENVIRONMENTAL APPLICATIONS

Field of Study: **ENVIRONMENTAL SCIENCE AND MANAGEMENT**

I do solemnly and sincerely declare that:

(1) I am the sole author/writer of this Work;
(2) This Work is original;
(3) Any use of any work in which copyright exists was done by way of fair dealing and for permitted purposes and any excerpt or extract from, or reference to or reproduction of any copyright work has been disclosed expressly and sufficiently and the title of the Work and its authorship have been acknowledged in this Work;
(4) I do not have any actual knowledge nor do I ought reasonably to know that the making of this work constitutes an infringement of any copyright work;
(5) I hereby assign all and every rights in the copyright to this Work to the University of Malaya ("UM"), who henceforth shall be owner of the copyright in this Work and that any reproduction or use in any form or by any means whatsoever is prohibited without the written consent of UM having been first had and obtained;
(6) I am fully aware that if in the course of making this Work I have infringed any copyright whether intentionally or otherwise, I may be subject to legal action or any other action as may be determined by UM.

Candidate's Signature Date: 27.7.2021

Subscribed and solemnly declared before,

Witness's Signature Date: 27 July 2021

Name:

Designation:

THERMOCHEMICAL CONVERSION OF *CHLORELLA* SPP. INTO BIOCHAR AND ITS POTENTIAL ENVIRONMENTAL APPLICATIONS

ABSTRACT

Microalgae are the first photosynthetic life forms of primitive earth and were able to fix atmospheric carbon dioxide (CO_2) with the help of sunlight, thus creating a major step in the evolution of terrestrial plants. Microalgae are receiving increased attention recently based on their applicability in biomass production and implications on carbon capture. The microalgal biomass can be converted to several green products such as biochar and bioethanol via thermochemical conversion for environmental utilization. Biochar can be produced through thermochemical processes such as conventional pyrolysis and wet torrefaction. Thus, this study aims to study the production of microalgal biochar and its by-product using thermochemical conversion as a green technology in approach for environmental utilization. The feasibility of microalgal biochar production by conventional pyrolysis as well as simultaneous production of biochar and bioethanol using advanced wet torrefaction are investigated. Then, the characterization of microalgal biochar produced is studied for potential utilization as alternative coal fuel. Finally, the additional application of microalgal biochar on the adsorption of dye pollutants for wastewater treatment is also analyzed. Microalgae *Chlorella vulgaris* FSP-E with maximum biomass productivity of 0.87 g L^{-1} day^{-1} showed a biochar yield of 26.9% accomplished by conventional slow pyrolysis. *C. vulgaris* FSP-E biochar showed an alkaline pH value with H/C and O/C atomic ratios that are beneficial for carbon sequestration and soil application. The higher heating value of 23.42 MJ/kg of microalgal biochar also possesses its value as alternative coal. Microalgal biochar consisted of large aggregates with irregular porosity showed potential characteristics in the adsorption study. Besides, the simultaneous production of biochar and bioethanol can also be carried out through wet torrefaction. Microwave-assisted acid hydrolysis pretreatment by wet

torrefaction was employed on two indigenous microalgae, *Chlorella vulgaris* ESP-31 and *Chlorella* sp. GD with different biomass compositions. The highest biochar yields of 54.5% and 74.6% can be obtained from *C. vulgaris* ESP-31 and *Chlorella* sp. GD, respectively under the wet torrefaction condition with an improvement in the properties for fuel. Wet torrefaction showed the high char yield with potential alternative fuel properties by using lower energy expense compared to the conventional slow pyrolysis. The high total reducing sugar concentration obtained in the liquid hydrolysate after the acid hydrolysis pretreatment was able to achieve the highest ethanol yield of 0.0761 g ethanol/ g microalgae. In addition, the microalgal biochar showed additional feasible adsorption performances on methylene blue and Congo red dye uptake with optimization on parameters such as adsorbent dosage, pH, initial concentration and time for future wastewater treatment utilization. Thermochemical conversion of biomass to biochar from microalgae using both conventional slow pyrolysis and wet torrefaction showed a feasible green conversion technology for environmental utilization. With the co-production of high total reducing sugar in the liquid hydrolysate that can be utilized for bioethanol production and solid biochar as another value-added product. In summary, acid hydrolysis pretreatment using wet torrefaction can be one of the environmentally sustainable conversion technologies towards the future application of renewable energy production.

Keywords: Microalgae; biochar; bioethanol; pyrolysis; wet torrefaction; environmental sustainability.

PENUKARAN *CHLORELLA* SPP. KE BIOCHAR MELALUI TERMOKIMIA DAN POTENSINYA UNTUK APLIKASI PERSEKITARAN

ABSTRAK

Mikroalga adalah kehidupan pertama dalam bentuk fotosintesis di bumi yang dapat mengurangkan karbon dioksida (CO_2) atmosfera dengan bantuan cahaya matahari dan mewujudkan suatu langkah utama terhadap evolusi tumbuhan daratan. Mikroalga menerima perhatian yang tinggi berdasarkan penggunaannya dalam pengeluaran biomass dan implikasi dalam tangkapan karbon. Biojisim mikroalga boleh ditukar kepada beberapa bioproduk hijau seperti biochar dan bioetanol melalui penukaran termokimia untuk kegunaan alam sekitar. Biochar boleh dihasilkan melalui proses termokimia seperti proses pirolisis konvensional dan proses torrefaction basah. Dengan itu, kajian ini bertujuan untuk mengkaji pengeluaran biochar dan produk sampingannya daripada mikroalga menggunakan penukaran termokimia sebagai teknologi hijau untuk kegunaan and aplikasi alam sekitar. Penglaksanaan pengeluaran biochar mikroalga dari proses pirolisis konvensional telah ditentukan dan diikuti dengan pengeluaran serentak biochar dan bioetanol menggunakan proses torrefaction basah yang baru. Pencirian biochar mikroalga dari kedua-dua proses telah dikaji untuk penggunaan potensi masa depan sebagai bahan api alternatif. Di samping itu, penggunaan tambahan biochar mikroalga atas penjerapan bahan pencemar pewarna untuk rawatan air sisa juga dikaji. Mikroalga *Chlorella vulgaris* FSP-E dengan produktiviti biojisim maksimum 0.87 g L^{-1} $hari^{-1}$ menunjukkan hasil biochar sebanyak 26.9% yang dicapai oleh proses pirolisis perlahan konvensional. Biochar *C. vulgaris* FSP-E menunjukkan nilai pH alkali dengan nisbah atom H/C dan O/C yang bermanfaat untuk penyerapan karbon dan penggunaan aplikasi tanah. Potensi aplikasi biochar mikroalga sebagai arang batu alternatif juga telah ditunjukkan dengan nilai pemanasan 23.42 MJ/kg yang tinggi. Biochar mikroalga terdiri daripada agregat besar dengan porositi yang tidak teratur menunjukkan ciri-ciri yang

berpotensi untuk kajian penjerapan. Pengeluaran serentak biochar dan bioetanol juga boleh dilakukan melalui proses torrefaction basah sebagai teknologi hijau masa depan untuk memenuhi krisis permintaan tenaga dunia. Prarawatan asid hidrolisis yang dibekalkan dengan ketuhar gelombang mikro telah digunakan atas *Chlorella vulgaris* ESP-31 dan *Chlorella* sp. GD dengan komposisi biojisim yang berlainan. Kadar penghasilan biochar tertinggi sebanyak 54.5% dan 74.6% boleh didapati daripada *C. vulgaris* ESP-31 dan *Chlorella* sp. GD, masing-masing di bawah proses torrefaction basah dengan peningkatan sifat sebagai bahan bakar. Torrefaction basah menunjukkan hasil biochar yang tinggi dengan sifat potensi bahan bakar melalui suhu rendah dan masa pendek berbanding dengan pirolisis konvensional. Kadar pengerolehan jumlah kepekatan gula yang tinggi dalam hidrolisat cecair selepas parawatan asid hidrolisis dapat mencapai hasil pengeluran etanol tertinggi sebanyak 0.0761 g etanol/ g mikroalga. Di samping itu, biochar mikroalga menunjukkan prestasi penjerapan yang optimum terhadap pengambilan pewarna metilena biru dan kongo merah dengan pengoptimuman parameter seperti dos penjerap, pH, kepekatan permulaan dan masa bagi penggunaan aplikasi rawatan air buangan akan datang. Pertukaran termokimia biojisim kepada biochar dari mikroalga menggunakan proses pirolisis lambat konvensional dan proses torrefaction basah menunjukkan teknologi penukaran hijau yang sesuai untuk penggunaan alam sekitar selanjutnya. Dengan pengeluaran serentak jumlah gula dalam hidrolisat cecair yang boleh digunakan untuk pengeluaran bioetanol dan biochar pepejal sebagai produk dengan nilai tambahan, prarawatan asid hidrolisis yang menggunakan proses torrefaction basah boleh dijadikan sebagai salah satu teknologi penukaran alam sekitar yang mampan ke arah masa depan terhadap aplikasi pengeluaran tenaga boleh diperbaharui bagi pemeliharaan alam sekitar.

Kata kunci: Mikroalga, biochar, bioetanol, pirolisis, torrefaction basah.

ACKNOWLEDGEMENTS

First, I would like to express my sincere gratitude to all of my supervisors and co-supervisor: Prof. Dr. Ling Tau Chuan, Dr. Ong Hwai Chyuan and Prof. Chen Wei-Hsin from National Cheng Kung University for their support, guidance and motivation throughout my whole research journey. Furthermore, I would also like to appreciate Associate Prof. Dr. Ir. Show Pau Loke for his kind advice and assistance throughout the whole PhD journey.

I would also like to thank the Bioseparation Research Group University of Nottingham Malaysia and related members: Chung Hong, Wai Yan, Shireen, Kit Wayne, Revathy, Isabelle, Gwen and the rest of the group members for their kind motivation and guidance in my research. I would also like to appreciate the helpful Yen Yee and Associate Prof. Dr. Suchithra Thangalazhy Gopakumar for their kind assistance with the laboratory facilities and guidance in the research field.

I would also like to thank the Genfuel Research Group National Cheng Kung University (NCKU), Taiwan and related members: Peggy, Mini, Yi-Xian, Kevin, Yu-Ying, Yi-Kai senior, Sun senior, Jun Feng, Matteo, Alan, Steven, Michael, Yu-Zhi and other unmentioned lab group members, including NCKU Chemical Engineering Prof. Jo-Shu Chang's lab members for their kind assistance and support in the lab facilities during my research journey in Tainan, Taiwan.

Also, I would like to thank the Taiwan Tai Sugar Research Cooperation and related members: Prof. Sheen Herng-Kuang, Ms Ng and Alice Nian-Ci for their kind assistance and support in the lab facilities. I would like to express my gratitude to Prof. Sheen who shared his research knowledge and guided me in my research journey in Taiwan.

I would also like to thank the UM Biofuel Lab members: Shiou Xuan, Brandon, Jass, Dr. Lee Xin Jiat, Cristal, Hoora, Yong Yang, Elaine, Gaowei and other related lab

members for their kind assistance for lab and research discussion throughout the whole PhD journey.

Last but not least, I would like to thank my family members, my loved one and all of my friends for their strong supports during my whole PhD journey. Thank you so much to everyone.

TABLE OF CONTENTS

LIST OF FIGURES

LIST OF TABLES

LIST OF SYMBOLS AND ABBREVIATIONS

%	: Percentage
<	: Less than
±	: Plus-minus sign
µL	: Microliter
µm	: Micrometer
A	: Ampere
°C	: Degree Celsius
CAS	: Chemical Abstracts Service
cm	: Centimeter
cm^{-1}	: Wavenumber unit
cmol/kg	: Centimole per kilogram
CR	: Congo red
DNS	: 3,5-dinitrosalicylic acid
E- or E+	: Exponent scientific notation
g	: Gram
Gt	: Gigatonne
h	: Hour
HHV	: Higher heating value
K/s	: Rate constant unit
L	: Liter
M	: Molarity
m^2/g	: Square meters of surface per gram of solid
MB	: Methylene blue
mg/g	: Milligram per gram

MHz : Megahertz

min : Minutes

MJ/kg : Mega joule per kilogram

mL : Milliliter

mm : Millimeter

mol% : Mole percentage

n : Samples number

nm : Nanometer

p : P-value or probability value

ppm : Parts per million

psi : Pounds per square inch

r : Correlation coefficient

R^2 : Coefficient of determination

rpm : Revolutions per minute

s : Second

sp. : Unspecified species (singular)

spp. : Unspecified species (plural)

W : Watt

w/w : Weight for weight

wt% : Percentage by weight

wt/wt : Weight percent per weight percent

LIST OF APPENDICES

CHAPTER 1: INTRODUCTION

This chapter provides the outline of the background study and problem statement of the research with importance and relevance of the study field. The scope of research with the aim and objectives will be outlined too.

1.1 Background

In this civilized and developed era with technologies, the world is reaching an unbalanced status where energy depletion starts to occur. Due to the increasing globalization of the world economy, energy demand is widely increased from all over the world. This phenomenon is associated with the growth of environmental issues such as reducing the supply of fossil fuels and increasing greenhouse gas emissions that lead to global warming issues (Daly, 1994; García-Martos et al., 2013; Liu et al., 2013). Therefore, the development of alternative green energy and sustainable renewable biofuels is gaining more research attention and the application of energy derived from biomass can be one of the sustainable opportunities to meet the growing worldwide energy demand (Berndes et al., 2003; Gonzalez-Salazar et al., 2014; Jacobson, 2009; Präger et al., 2019). Renewable energy such as biomass is receiving more attention on its applicability for sustainable supply to the environment (Al-Hamamre et al., 2017). When biomass serves as a source for energy production, the microalgal biomass is considered as a promising feedstock on its wide distribution and rapid growth (Chen et al., 2015; Roberts et al., 2015). Microalgae can be cultivated easily indoor or outdoor at a large scale with basic sources such as sunlight and carbon dioxide for bioenergy production. Growing microalgal biomass is a distinctive way in which carbon sequestration of atmospheric carbon dioxide can occur to minimize the greenhouse gases effect on the Earth's atmosphere (Gronnow et al., 2013). Biochar production from microalgae can be utilized in agriculture as a fertilizer for crop productivity while carrying out carbon

storage underground for a long time which helps in the mitigation of global climate change. A potential improvement on conversion of biomass to biochar through thermochemical processes such as pyrolysis, hydrothermal carbonization and torrefaction is commendable for further utilizing the microalgal biomass after extraction of lipids and carbohydrates or proteins for biofuel such as bioethanol production.

1.2 Problem statement

Generally, there is still a lack of literature study on the conversion of microalgal biomass to biochar production. Malaysia is still lacking study and application of biochar on agriculture while other countries such as Taiwan have been into the biochar research and are promoting its beneficial use for the agriculture industry. The conversion of microalgal biomass to biochar is a new approach to green technology. Upgrading the conventional conversion technology, especially in pyrolysis for biochar production can be beneficial for the optimization of this technology in future implementation. The limited literature on this conventional conversion technology makes it necessary that further research is much needed to explore the technology and obtain higher biochar yields and more value-added by-products from various feedstocks (Khoo et al., 2013). In addition, there is previous literature focusing on wet torrefaction using biomass feedstocks such as lignocellulosic biomass and macroalgae (Chen et al., 2015; Chen et al., 2011; Chen et al., 2012, 2012; Teh et al., 2017), however, there is limited literature of pretreatment on microalgal biomass towards co-production of biochar and bioethanol. A microalgal biorefinery approach where wastewater can be used as a nutrient source for the production of microalgal biomass with energy-rich components like lipids/carbohydrates for biofuel such as bioethanol production and the subsequent conversion of the remaining biomass to biochar through thermochemical processes is a strategy that will greatly utilize the potential of microalgae as a renewable third-generation biofuel feedstock.

1.3 Scope of research

This research is focused on environmental science and management on green technology of conversion of microalgae to value-added bio-products. The topic of research is about the conversion of microalgal biomass to biofuel namely biochar and bioethanol and its application for alternative green fuel. The research is focused on the optimization of biochar production from microalgae for suitable quality and properties of biochar. The research also focused on developing a potential optimum treatment method such as wet torrefaction that can be adopted to produce microalgal biochar and bioethanol that are suitable for application such as bio-adsorbent and alternative fuel. The application of microalgal biochar as bio-adsorbent for wastewater treatment is also discussed with the approach of microalgal biorefinery towards environmental sustainability where the microalgae from the wastewater treatment process can be utilized for further application in the wastewater treatment cycle.

1.4 Research objectives

The research aims to study the production of microalgal biochar and its by-product using thermochemical conversion as a green technology in approach to environmental utilization and application. The objectives of this research are as follows:

1. To determine the feasibility of biomass and biochar production from microalgae *Chlorella* sp. using conventional pyrolysis.
2. To study the simultaneous production of biochar and hydrolysate by-products from microalgae *Chlorella* spp. using wet torrefaction with microwave-assisted acid hydrolysis pretreatment.
3. To investigate the microalgal bioethanol production from acid pretreated hydrolysate produced under wet torrefaction.
4. To investigate the utilization of microalgal biochar on adsorption of dye pollutants for wastewater treatment.

1.5 Importance and relevance of the study

The research shows the importance of the study of environmental science and management through the application of green technology in biofuel and value-added products conversion by a renewable source of microalgae. The utilization of biomass waste occurred in the production of more value-added bio-products such as biochar, bio-oil and bioethanol. As one of the innovative green products, biochar is receiving research attention based on its potential for developing negative carbon emission technologies towards mitigation of climate change (Mulabagal et al., 2017). Conversion of biomass to biochar plays an important role in carbon sequestration as an alternative approach for biomass energy with CO_2 capture and storage where CO_2 emissions could be reduced with the production of carbon-negative biofuel. Other than utilizing biochar as an

alternative fuel source in bioenergy conversion, it is also applicable in water treatment technology as a bio-adsorbent (Amin et al., 2016; Tan et al., 2017). This has increased the role of biochar in nutrient-reuse technologies and added more value to its commercial application in the near future for sustainable development. In addition, bioethanol is one of the recent important green fuel products due to its combined application with the current fuel product in the market for vehicles and engines combustion (Demirbas, 2011; Turkcan, 2018). Generally, bioethanol can be produced from sugary and starchy-rich feedstock such as sugarcane and maize (Chen et al., 2011). However, due to the food conflict, microalgae can be considered as another attractive feedstock in perspective of its availability for bioethanol production (Gan et al., 2018). The co-production of bioethanol and value-added biochar from microalgal biomass can be one of the environmentally sustainable conversion technologies in near future for the application of energy production in approach to microalgal biorefinery towards a sustainable environment. Furthermore, the utilization of microalgae residue from the wastewater treatment process for value-added applications such as adsorbent can be a green approach towards a sustainable and biorefinery concept in the wastewater treatment process.

CHAPTER 2: LITERATURE REVIEW

This chapter discusses the literature review on microalgae and biofuels namely biochar and bioethanol with the algal biomass as a renewable source towards biofuel and biochar production. The conventional and recent thermochemical conversion processes used for algal biochar production are also discussed in this chapter.

2.1 Microalgae

Microalgae are unicellular photosynthetic microorganisms, usually in the size range of 1-400 μm and invisible to the naked eye (Bharathiraja et al., 2015; Demirbas, 2010; Oncel, 2013; Suganya et al., 2016; Ullah et al., 2015; Vassilev et al., 2016). They are the first photosynthetic life forms on primitive earth and able to fix the atmospheric carbon dioxide (CO_2) with the help of sunlight, thus creating a major step in the evolution of terrestrial plants. Microalgae can be photosynthetic or non-photosynthetic and in view of their metabolic mode, they can be divided into photoautotrophic, heterotrophic, mixotrophic and photoheterotrophic based on their energy and carbon source requirements (Bharathiraja et al., 2015; Brennan et al., 2010; Sambusiti et al., 2015). The nutritional requirements for microalgal cultivation are simple: an energy source which is primarily sunlight, organic or inorganic carbon source, certain essential micro and macronutrients, vitamins and optimal conditions of temperature and pH. Microalgae can be cultivated artificially within open systems like ponds and closed photobioreactors in freshwater, seawater and wastewater other than their natural environments (Chen et al., 2011; Christenson et al., 2011; Eriksen, 2008). Microalgae can help mitigate large amounts of CO_2 emissions as about half of the dry weight of microalgal biomass is carbon. Certain microalgae are tolerant to the high amounts of CO_2 present in flue gas and therefore haves been a part of carbon capture technology. They have very high carbon fixing or photosynthetic efficiency compared to terrestrial plants and with their short life

cycle that lasts a few days, they also have high biomass productivity. These attributes of microalgae contribute greatly to the reduction of greenhouse gases (GHG) emissions and simultaneous provision of a renewable feedstock for biofuels (Abbasi et al., 2010; Demirbas, 2010; Gai et al., 2015; Slade et al., 2013; Ziolkowska et al., 2014). Microalgae are currently regarded as third-generation feedstock for biofuel production. With their ability to accumulate very high amounts of lipids or carbohydrates and the absence of lignin that helps in simple pretreatment methods, microalgal biomass has been used for the production of a variety of biofuels like biodiesel, bioethanol, biohydrogen and biobutanol (Brennan et al., 2010; Chen et al., 2011; Dong et al., 2015; Gouveia et al., 2009; Slade et al., 2013). Apart from serving as a feedstock for biofuel production, microalgae can also produce a number of pharmacologically and nutritionally important fine chemicals like pigments and fatty acids and simultaneous production of biofuel feedstock and fine chemicals in a microalgal biorefinery can greatly improve the economics of the process (Aziz, 2015; Bharathiraja et al., 2015; Pacheco et al., 2015).

Wastewaters are rich in organic and inorganic nutrients, and with their high chemical oxygen demand (COD) and biological oxygen demand (BOD), they pose a threat to environmental safety if untreated. A variety of nutrients or pollutants can be found in industrial wastewater such as nitrogen, phosphate, organic carbons, volatile fatty acids, pharmaceutical compounds, heavy metals, and dyes (Rashid et al., 2013; Wang et al., 2016). Using wastewater as a source of nutrients can greatly reduce the production costs of microalgae. The growth of microalgae in wastewater provides microalgal biomass and simultaneous bioremediation of wastewater. Thus, microalgae are most commonly used in wastewater treatment and biomass production (Kiran et al., 2014; Wang et al., 2016). Microalgae are potential raw materials in renewable energy and can be converted into biofuels and other bio-products (Demirbas, 2010; Ghayal et al., 2013; Gouveia et al., 2009; Wu et al., 2017). Conversion of microalgal biomass to any valuable biofuel product

can take place in a number of ways: (i) thermochemical processes that can convert the whole biomass into a range of products like biogas and bio-oil, which includes pyrolysis, gasification, hydrothermal liquefaction and torrefaction, (ii) chemical processes like transesterification that can convert the microalgal lipids to biodiesel, and finally (iii) biochemical methods like fermentation for production of bioethanol, biobutanol, biohydrogen and anaerobic digestion for methane production (Chen et al., 2015). In all these processes, microalgal biomass is pretreated in an appropriate manner and fed into the process. Conversion of microalgal biomass has increasingly been performed via thermochemical processes, as some processes, such as hydrothermal liquefaction and hydrothermal carbonization, can intake microalgal biomass with a water content of up to 40%. An important by-product derived from these processes is called biochar, which can be used as a fertilizer.

2.2 Biochar

Biochar is carbon-rich charcoal of any kind of biomass, produced by thermal decomposition of the organic feedstock under limited oxygen (O_2) supply at a relatively low temperature (Ahmad et al., 2013; Alhashimi et al., 2017; Chang et al., 2015; Joseph et al., 2009). It can be simply defined as charcoal that can be used in agriculture to improve soil function and reduce emissions from the biomass caused by natural degradation to CO_2 (Wang et al., 2012). Biochar is produced through torrefaction or pyrolysis process like most of the charcoal or under gasification (Anderson et al., 2013; Chaiwong et al., 2013; Chen et al., 2015; Chen et al., 2014; Chen et al., 2016; Garcia-Perez et al., 2010; Goyal et al., 2008; Libra et al., 2011). Biochar produced from different feedstocks varies widely in their composition. Microalgae-based biochar consisted of large aggregates with the size range of 10-100 μm with a 1-μm irregular porosity. These features are different from biochar produced from lignocellulosic biomass in terms of the

structure after pyrolysis (Bach et al., 2017; Joseph et al., 2009; Torri et al., 2011). Other than utilizing biochar as process fuel in bioenergy conversion, it acts as a long-term sink for atmospheric carbon dioxide in the carbon sequestration process. Carbon dioxide emissions could be reduced up to 84% and it is highly possible to produce a carbon-negative biofuel through biochar sequestration (Lehmann, 2007). In addition to the reduction of GHG emissions and carbon sequestration, biochar can improve soil fertility for higher crop production. It has been demonstrated that biochar amendment can improve the water holding capacity and nutrient status of many soils (Hossain et al., 2010; Joseph et al., 2009). Biochar also helps in the uptake or removal of polycyclic aromatic hydrocarbons (PAHs) and toxic elements in the soil for better crop productivity (Brennan et al., 2014). Probably because of their capacity as an adsorbent, biochar can adsorb and remove certain toxic substances from soil, enhancing the activity of soil biota (Sarkar et al., 2015). Biochar production from algal feedstock has a lower carbon content surface area and cation exchange capacity compared to lignocellulose biochar. It has higher pH which can balance acidified soils and tends to have a higher content of nutrients including minerals such as nitrogen, ash and inorganic elements (Chaiwong et al., 2013; Oasmaa et al., 2001). These featured characteristics are beneficial for soil amendment in agriculture for crop productivity and other soil applications (Koide, 2017; Kołtowski et al., 2017; Sun et al., 2017). Other than that, biochar is also applicable to wastewater treatment. Biochar can be used as an adsorbent to remove pollutants such as dyes and heavy metals from industrial wastewater after appropriate pre-treatment (Agarwal et al., 2015; Cho et al., 2016; Liu et al., 2012; Liu et al., 2009; Mandal et al., 2017; Niazi et al., 2016). Biochar production can be considered as one of the potential value-added strategies with microalgae cultivation in wastewater treatment based on the multiple utilities in the context of bio-refinery (Demirbas, 2008; Sarkar et al., 2015).

2.3 Bioethanol

Bioethanol is one of the recent important green fuel products due to its combined application with the current fuel product in the market for vehicles and engines combustion (Demirbas, 2011; Turkcan, 2018). Generally, bioethanol can be produced from sugary and starchy-rich feedstock such as sugarcane and maize (Chen et al., 2011). Other than that, microalgae can be considered as another attractive feedstock in perspective of its availability for bioethanol production (Gan et al., 2018). Bioethanol is expected to be the most widely used biofuel around the world from the conversion of rich-starch biomass sources (John et al., 2011). Microalgal biomass with no food conflict issues is a potentially suitable candidate for the production of bioethanol (Phwan et al., 2018). Bioethanol showed its importance as an alternative fuel to blend with current petroleum liquid fuel in the market for application in transportation vehicles and engines combustion (Demirbas, 2011; Turkcan, 2018). Other than that, the application of bioethanol can be seen in power co-generation systems, fuel cells, electric power generation and the chemical industry as raw chemical and enhancers (Champagne, 2007; Petrou et al., 2009). With the recognition of bioethanol as a sustainable green fuel (Sirajunnisa et al., 2016), global production is in rapid growth and expected to achieve a breakthrough production by the year 2020 (Bibi et al., 2017). Hence, the advancement of the pretreatment methods and technologies can be looked into to meet the rapid growth in bioethanol production (Phwan et al., 2018). Previous studies related to the pretreatment methods on microalgae for bioethanol production are shown in Table 2.1.

Table 2.1: Previous studies related to the pretreatment methods on microalgae for bioethanol production.

Microalgae	Pretreatment/ Saccharification	Ethanol production yield	References
Chlamydomonas mexicana	Sonication and enzymatic	9.64-10.50 g/L	(El-Dalatony et al., 2016)
Chlamydomonas reinhardtii UTEX 90	Enzymatic	235 mg ethanol/ g algae	(Choi et al., 2010)
Chlorella sp.	Chemical (HCl and $MgCl_2$)	22.60 g/L	(Zhou et al., 2011)
Chlorella sp. KR-1	Enzymatic and chemical (HCl)	0.16 g ethanol/ g residual biomass	(Lee et al., 2015)
Chlorella vulgaris	Chemical (H_2SO_4)	0.40 g ethanol/ g algae	(Lee et al., 2011)
Chlorella vulgaris FSP-E	Chemical (H_2SO_4)	11.66 g/L	(Ho et al., 2013)
Chlorococcum infusionum	Chemical (NaOH)	0.26 g ethanol/ g algae	(Harun et al., 2011)
Chlorococcum sp.	Supercritical fluid	3.83 g/L	(Harun et al., 2010)
Dunaliella sp.	Autoclave and chemical (H_2SO_4)	0.91 ± 0.05 g/L	(Karatay et al., 2016)
Scenedesmus abundans PKUAC 12	Chemical (H_2SO_4) and enzymatic	0.103 g ethanol/ g biomass	(Guo et al., 2013)
Scenedesmus bijugatus	Autoclave and chemical (H_2SO_4)	0.158 g ethanol/ g residual biomass	(Ashokkumar et al., 2015)
Scenedesmus obliquus CNW-N	Chemical (H_2SO_4)	8.55 g/L	(Ho et al., 2013)
Scenedesmus sp.	Combined mechanical and chemical	0.0791-0.0856 g ethanol/ g biomass	(Sivaramakrishnan et al., 2018)
Schizocytrium sp.	Hydrothermal and enzymatic	11.80 g/L	(Kim et al., 2012)

2.4 Algal biomass as the source for producing biofuels and biochar

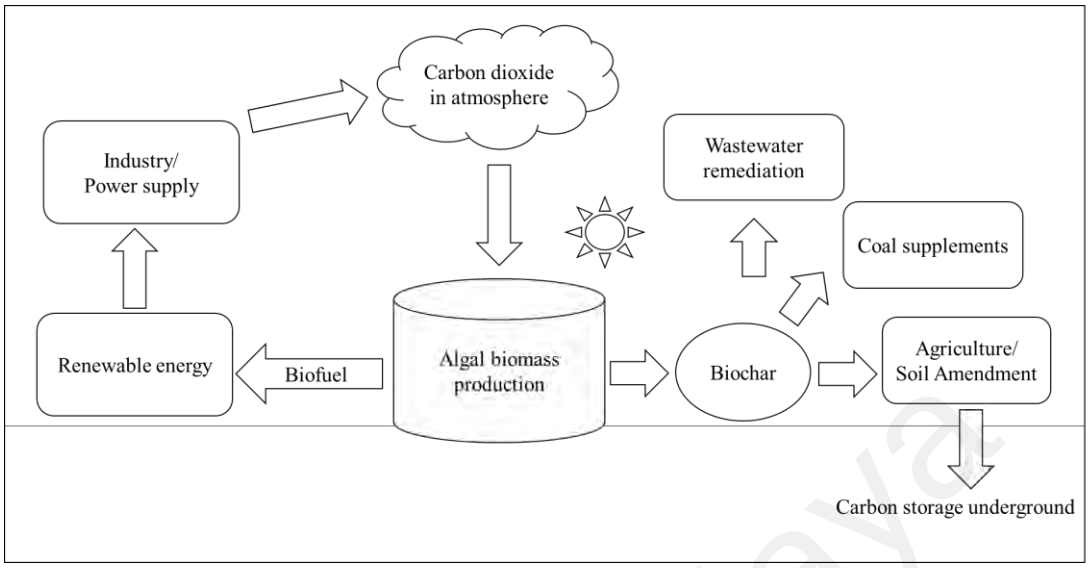

Figure 2.1: Algal biomass production for renewable energy production and carbon sequestration.

The schematic view of algal biomass production in renewable energy and carbon sequestration is shown in Figure 2.1. With the ability in nutrients uptake, algae possess a high growth rate and environmentally tolerant characteristic to rapidly dominate in high nutrients environment. The high nutrient content of algae properties makes it a suitable feedstock in biochar production for use in soil amendment and implementation for long-term carbon sequestration. Algal biochar derived from the remediation of wastewater could provide a notable benefit in the future by utilizing biomass for carbon-negative energy generation and application to the environment (Bird et al., 2011). The high nutrient content of algal biomass makes it a disadvantage in pyrolysis product distribution where the more bio-oil product can be obtained. However, extraction of lipids can be done for bio-oil production and the residue can be used in biochar production in the context of biorefinery (Wang et al., 2013). Algae have been known as one of the promising sustainable energy feedstocks for the future without the dependence on fossil fuels and their growth can efficiently reduce emissions of greenhouse gases. Microalgae are a popular choice for biofuel production due to the ease of cultivation in large amounts in various environments

(Vassilev et al., 2016). All types of biofuels (i.e., solid, liquid and gas biofuels) can be generated from microalgae using several conversion methods such as direct combustion, chemical conversion, biochemical conversion and thermochemical conversion. In addition to the success of algal technology in fuel production, other value-added co-products such as biochar can be produced simultaneously from algal feedstock for a biorefinery concept (Foley et al., 2011; Rashid et al., 2013).

Biochar is gaining more attention on its long-term advantage in carbon sequestration and application in agriculture for soil amendment (Ennis et al., 2012). Biochar technology involved CO_2 uptake through photosynthesis. The captured carbon undergoes conversion processes such as pyrolysis to produce biochar with the characteristic of long-term carbon storage through soil amendment (Sohi et al., 2009). Biochar production differs from other biomass energy production systems as this technology is carbon-negative. The International Biochar Initiative (2008) estimated that biochar production has the potential of mitigation of climate change by providing 3.67 Gt CO_2 per year using only biomass wastes. Biochar is the potential to sequester up to 12% of greenhouse gases from anthropogenic sources in ecologically and economically sustainable systems (Ennis et al., 2012). Implementation of biochar's ability in mitigation of climate change at the global scale is recognized (Molina et al., 2009).

As a strategy to store captured carbon for a long time on impact to greenhouse gas accumulation, biomass is converted into biochar that has more than 90% carbon (Heilmann et al., 2010). Biochar derived from microalgae is nutrient-rich (especially nitrogen-rich) so is well-suited to serve as a fertilizer in agricultural soil (Torri et al., 2011). With all the advantages of algal biochar, converting algal biomass into biochar can be economically feasible for algal production enterprises (Bryant et al., 2012). However, to date, there is still very limited literature regarding algal biochar and its utilization. This

may markedly hinder the future development and application of algae-based biochar (Shukla et al., 2017), suggesting the need for a comprehensive literature review in this promising area.

2.5 Thermochemical conversion

Microalgal biomass is harvested and can be converted into biochar. Microalgal biomass required some pre-treatment for better char yield and quality. Biochar is generally produced through thermochemical conversions such as pyrolysis, hydrothermal carbonization, and torrefaction. The conventional way of biochar production is through slow pyrolysis which generates high char yield. There are other recent developments of biochar production using processes such as microwave-assisted pyrolysis, hydrothermal carbonization or torrefaction. Microwave pyrolysis is one of the efficient thermochemical processes in the production of biochar, bio-oil and syngas that has been successfully applied to plant residues, wood and sewage sludge (Lei et al., 2011). The advantages of microwave pyrolysis are such high products yield, reduction of harmful chemicals in bio-oil, energy, and cost-saving. Hydrothermal carbonization produced a final carbonaceous material which is also denoted as hydrochar. Torrefaction is a pre-treatment method to produce carbon-rich solid products (Chen et al., 2015; Kumar et al., 2017). Future investigation on the recently developed biochar production processes such as torrefaction or hydrothermal carbonization and the optimization of nutrients extracted microalgal residue can be carried out for microalgal biochar production.

2.5.1 Conventional pyrolysis

Pyrolysis is the heating of biomass with the absence of oxygen or air at a given rate typically at a temperature range of around 300-700 ℃ (Chen et al., 2015). The products obtained from pyrolysis are determined by several factors, in particular, the temperature and heating rate (Basu, 2010). Biochar yield increases with decreasing pyrolysis

temperature at a higher residence time with a preferable low heating rate. Other than that, feedstock properties such as moisture content and particle size also affect the yield of biochar from pyrolysis (Tripathi et al., 2016). Slow pyrolysis which is known as a conventional process in charcoal production could yield the maximum amount of biochar from biomass compared to other processes, such as fast pyrolysis and gasification (Chaiwong et al., 2012; Mohan et al., 2014). Up to 50% of the carbon from biomass may be stored in the stable biochar through pyrolysis (Bird et al., 2011). Biomass undergoes a slow pyrolysis process with a vapour residence time from several minutes to hours for char production (Du, 2013). Vapours are restrained and reacted with solid-phase extensively for more char yield at the end of the process (Mohan et al., 2014). Slow pyrolysis is, in general, carried at low heating rates of 0.1-1 K/s with a residence time of around 450-550 s. Pre-pyrolysis happens at the beginning, followed by solid decomposition corresponding to the high rate pyrolysis process to form pyrolysis products. Decomposition of the char finally occurs at a very low rate and carbon-rich biochar is formed (Suganya et al., 2016). Most of the traditional slow pyrolysis used fixed bed reactors where heating is provided by heated surface but there are studies that looked into alternative heating methods such as microwave heating (Du, 2013; Wan et al., 2009).

2.5.2 Microwave-assisted pyrolysis

Microwave-assisted pyrolysis is one of the most efficient thermochemical processes in the production of biochar, bio-oil and syngas and it has been successfully applied to plant residues, such as wood and sewage sludge (Lei et al., 2011). Some of the advantages of microwave pyrolysis are high products yield, reduction of harmful chemicals in bio-oil, energy, and cost-saving. Microwave technology uses electromagnetic waves to cause the oscillation of material molecules and to produce heat. The technical advantages of microwave-assisted pyrolysis over conventional pyrolysis are (1) uniform microwave

heating that is applicable on larger biomass particles, (2) production of higher heating value syngas that can be used for in-situ electricity for microwave generation, (3) cleaner products due to no agitation and fluidization in the process, and (4) microwave heating is a mature technology with scale-up feasibility (Du, 2013). Figure 2.2 depicts the conventional slow pyrolysis and microwave-assisted pyrolysis used for biochar production. There are numerous studies on the pyrolysis of lignocellulosic biomass but reports on the production of algal biochar via microwave heating are limited (Wan et al., 2009). Biochar that undergoes further chemical or thermal processing after production can be transformed into activated carbon (Spokas et al., 2011). However, a study shows the decrease of functional groups in biochar due to the release of volatiles during pyrolysis making it a challenge as an effective adsorbent (Wang et al., 2015). Microwave-assisted pyrolysis can be used in future scale-up production from algal products into biochar for applications such as soil fertilizer based on its economic production process.

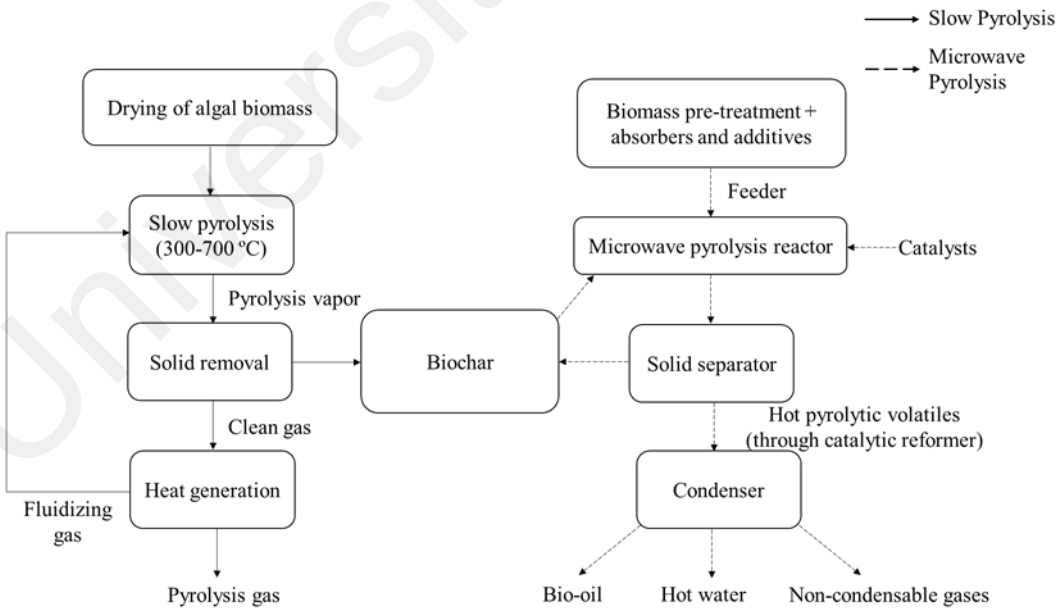

Figure 2.2: Conventional slow pyrolysis and microwave-assisted pyrolysis in biochar production.

2.5.3 Torrefaction

Torrefaction is a thermochemical conversion process that is performed under atmospheric pressure at a temperature between 200-300 ℃ under an inert condition in the absence of oxygen (Chen et al., 2014, 2015). The process partly decomposes biomass and produces a solid product (called torrefied biomass or char) with high carbon content. Torrefaction is used for biofuel production from microalgae and its prime purpose is to produce biochar (Bach et al., 2017). Torrefaction is an emerging thermal biomass pre-treatment process able to remove volatiles through different decomposition reactions to reduce major limitations of biomass, upgrade biomass quality and alter the combustion behaviour (Nhuchhen et al., 2014). By altering the combustion behavior, fuel flexibility is enhanced by making a wide range of fuels efficiently applicable in a co-firing power plant. Torrefaction of microalgal biomass grown by using flue gas from the thermal power plant can be made suitable for co-firing in a pulverized coal power (Wu et al., 2012). The thermal pre-treatment of torrefaction can be divided into dry and wet torrefaction, where wet torrefaction is also known as hydrothermal torrefaction or hydrothermal carbonization (Chen et al., 2015; Yan et al., 2009). A comparison of the characteristics of dry and wet torrefaction is shown in Table 2.2. The major advantage of wet torrefaction over dry torrefaction is its ability to produce energy-dense products within a short residence time due to the high heat transfer rate in the aqueous media (Coronella et al., 2012; Hoekman et al., 2013). In wet torrefaction, microalgae are treated under hot compressed water, producing a solid product that has high calorific value, better hydrophobicity, and lower ash content (Bach et al., 2017). Torrefaction produced biochar with high calorific value or higher heating value can be used as an alternative feedstock for clean energy production than fossil fuel. The study of combined biochar and torrefied biomass using kernel shell for fuel production showed the average pyrolysis and torrefaction system efficiency of 59.7% and make it a potential alternative for small-scale

mills application (Salgado et al., 2020). The hydrophobicity of biochar based on the surface functional groups and the lower ash content are important to determine its effectiveness in the application of adsorption as an adsorbent in pollutants uptake from soil and water. The study by Bach et al. (2017) showed that, after wet torrefaction, at least 61.5% of energy in the microalgal biomass is retained. The calorific value intensified up to 21% and there is a decrease in the ash content of the microalgae. Torrefaction is usually carried out at a low temperature and short residence time under low heating rate to give a higher yield of solid product (Deng et al., 2009; Nhuchhen et al., 2014). Wu et al. (2012) reported that the solid yield decreased when the torrefaction temperature is increased. The effect of residence time on the mass yield of torrefied biomass at 300 ℃ shows the mass yield decreased with an increase in the residence time. The study concluded that temperature influenced the mass yield more than residence time. Chen et al. (2014) showed the isothermal and non-isothermal torrefaction characteristics and kinetics of a microalga *Scenedesmus obliquus* CNW-N. Microalgae are classified based on the torrefaction temperature, light, mild and severe torrefaction from the maximum decomposition rate and weight loss. Non-isothermal torrefaction required intense pretreatment than the isothermal torrefaction. Pretreatment severity is intensified by the increasing of heating rate in non-isothermal torrefaction. Uemura et al. (2015) reported the yields of solid, liquid and gas for a series of torrefaction temperature on a macroalga *Laminaria japonica*. The solid yield decreased when the torrefaction temperature was increased. The decrease in solid yield may be attributed to the decomposition of two major components, alginate and mannitol in *L. japonica.* However, both the liquid and gas yields increased when the temperature was increased i*n* conjunction with a decrease of solid yield with torrefaction temperature. Bach et al. (2017) mentioned that the solid yield decreased with an increase in temperature and residence time. The solid yield decreased from 61.68 to 52.58% when the temperature was increased from 160 to 180 °C. The solid

yield decreased from 62.92 to 51.84% when the residence time increased from 5 to 30 min. Chen et al. (2016) showed that the solid yield of 51.3-93.9% in the torrefied microalgae residue at the temperature ranged from 200-300 ℃ with a residence time of 15-60 min. Previous study also shows the solid yield of 50.8-95.7% in microalgae *Chlamydomonas* sp. JSC4 residue after torrefaction at temperature 200-300 ℃ for 15-60 min. It is recommended that torrefaction of microalgae residue should be carried out at an optimum temperature of 250 ℃ or below for less weight loss and higher energy densification (Mwangi et al., 2015). The impact of torrefaction upon biomass properties has been extensively investigated in the last decade. However, there is limited literature on the study of algal biochar from torrefaction process. As torrefied algal biomass is a high quality and environmental friendly solid product that may offer considerable opportunities for worldwide greenhouse gas mitigation, future research on this area is suggested.

Table 2.2: Comparison of the characteristics of dry and wet torrefaction.

Characteristics	Torrefaction	
	Dry	Wet (Hydrothermal)
Temperature	200-300 ℃	180-260 ℃
Media	Inert nitrogen gas	Hot compressed water
Pressure	Atmospheric pressure	200-700 psi
Residence time	80 min	5 min
Cooling process	Flowing nitrogen; indirect water cooling	Immerse into ice bath rapidly
Additional processes	-	Filtration and evaporation
Energy density	Lower	Higher

2.5.4 Hydrothermal carbonization

Hydrothermal carbonization (HTC) is a new thermochemical technique that has gained more attention in recent years due to its environmental friendly and cost-effectiveness (Erlach et al., 2012; Xiao et al., 2012). HTC is a distinctive process that involves the conversion of carbohydrate components of biomass into carbon-rich solids in water where biochar is produced at lower temperatures (180-260 °C) and elevated water or steam pressures (Libra et al., 2011; Titirici et al., 2012). The process takes place in water under self-generated pressures of less than 10 bar with water as solvent (Titirici et al., 2012). This process can be suitable for concentrating carbon of wet biomass where no drying is required prior to reaction, making it a potential alternative for the treatment of some waste streams (Brownsort, 2009). Char produced from hydrothermal carbonization is called hydrochar (Libra et al., 2011). HTC produces a higher product in a shorter period of time and requires lower energy expense than the conventional carbonization process (Tekin et al., 2014). The advantages of the HTC process include (1) required only low carbonization temperature, (2) can be synthesized in the aqueous phase, (3) inexpensive process, (4) renewable materials can be used as sources such as biomass and for the use of value-added chemicals, such as nanoparticles in the structure (Kubo, 2013). Char product obtained from HTC has the following properties: uniform spherical particles; controlled porosity; functional surfaces (eg: -OH, -C=O, -COOH); easily controlled surface chemistry and electronic properties; and can bind CO_2 from the plant precursor if the carbon is negative (Titirici et al., 2012).

In a hydrothermal process, biomass can be converted into valuable products such as biochar, bio-oil and gaseous products by manipulating process variables such as temperature, time of reaction, feedstock, the presence of catalysts and pressure (Tekin et al., 2014). Temperature is the most influential variable in the HTC process followed by

residence time and types of feedstock (Nizamuddin et al., 2017). Lower temperature tends to give a higher yield of solid product compared to higher temperatures by affecting its physical and chemical characteristics. At a higher temperature, the carbon content is higher whereas the hydrogen and oxygen content is lower. This results in a formation of biochar with greater higher heating value (HHV). Char produced from HTC of microalgae has a unique composition and with bituminous coal quality (Heilmann et al., 2010). Process conditions were under a lower temperature of 200 ℃ with 0.5 h of reaction time for effective carbonization and production of algal char. The brief reaction time in the batch process suggested the development of a continuous process for HTC processing of algae. There are no specific catalytic agents that significantly enhanced the carbonization process and/or increase the yield of biochar. The most conceivable alternative pathway proposed in the study was carbonization via a dehydration route. As there is very limited literature on algal char production from the HTC process, it would be an interesting topic for future studies. HTC process offers the advantages of lowering the production cost and shortening the time needed for the production of biochar. This can be achieved by utilizing algal biomass residue and converting it into a more valuable biofuel and other products. HTC represents a feasible alternative way to potential wet biomass in biochar production by omitting the drying process.

2.6 Characterization of algal biochar

Biochar obtained by slow pyrolysis from a *Chlorella*-based algal residue was characterized for its chemical composition (Chang et al., 2015). The biochar produced has high nitrogen content as well as other inorganic elements such as phosphorus, iron, calcium, potassium and magnesium. The biochar yield and contents varied at different temperatures. The biochar yield increased from 56.3% at 300 °C to a maximal value of 66.2% at 500 °C, then slightly declined to around 65% at 700 °C. The hydrogen and

nitrogen contents decreased with increasing temperature. Because of its high nitrogen and mineral content, this biochar can be used as a fertilizer. Ferreira et al. (2015) observed that char production occurred at temperatures between 450-600 °C for raw and defatted microalgae. It was also revealed that the activation energies for pyrolysis of original and defatted microalgae were about the same and for the same process, the changes in the composition of the biomass influenced the final products. Defatted *C. vulgaris* biomass was subjected to fast pyrolysis in a fluidized bed reactor at 500 °C (Wang et al., 2013). A biochar yield of 31% compared to the bio-oil yield of 53% and gas yield of 10% is reported. Energy recovery of algal biomass in bio-oil and biochar is 94%. The biochar produced shows high inorganic content (potassium, nitrogen and phosphorus) which is suitable to provide nutrients for crops. Torri et al. (2011) showed the potential conversion of *Chlamydomonas reinhardtii* biomass harvested after hydrogen production into nitrogen-rich biochar, biodiesel and bio-oil. Pyrolysis was carried out in a fixed bed reactor at 350 °C to obtain biochar that is the largest fraction in terms of mass, 44±1% w/w dry-biomass. *Scenedesmus dimorphus* biomass was investigated for the effect of different temperatures of pyrolysis and the product profile obtained (Bordoloi et al., 2016). The results showed that there are major differences among the biochar produces at different pyrolysis temperatures. The study also showed that high ash content is due to the presence of exogenous material that could not be removed from the raw algal biomass. Biochar produced at a lower temperature can be easily mineralized by microorganisms compared to biochar produced at a higher temperature (Bordoloi et al., 2016). Slow pyrolysis at 400 °C with 30 min retention time yield 35% of char and fast pyrolysis at 500 °C with 10-20 s retention time yield 20% char (Hallenbeck et al., 2016). The product yield depends upon various operating parameters but generally low temperature and high residence time favor the char production (Xiao et al., 2010). This shows that temperature is one of the key factors in optimizing the pyrolysis process of biochar production.

On the other hand, pyrolysis of microalgal biomass for biofuels production is gaining more attention but detailed degradation mechanism and kinetics of the process have not been fully explored yet. Thereby, a comprehensive study on pyrolysis kinetics of microalgal biomass was performed (Bach et al., 2017). Other than pyrolysis, there are few recent experimental investigations on the use of hydrothermal treatment for generating energy products from microalgae but still, much research needs to be devoted to this area (Barreiro et al., 2013). Uchimiya et al. (2011) suggested that biochar produced from hydrothermal processing may be a more suitable biosorbent than that produced by pyrolysis. Upgrading conventional conversion techniques will be beneficial for other applications of biochar. Li et al. (2016) reviewed microwave pyrolysis in biochar production from woody biomass, herbaceous biomass and sewage sludge. It was reported that the highest biochar yield was more than 60 wt%. The optimization of yield and quality of biochar strongly depends on feedstock properties, reactor types, and operating parameters (Li et al., 2016). A catalyst derived from biochar was used in the transesterification of microalgal oil for the production of biodiesel (Dong et al., 2015). The biochar was produced by Auger pyrolysis of Douglas fir at 600 °C followed by sulfonation. The biochar-derived catalyst was found more efficient than the commercial catalyst Amberlyst-15 for the pre-esterification of microalgal oils. The application of biochar catalysts can be helpful in reducing environmental impact by decreasing the amount of corrosive acid in waste streams (Dong et al., 2015). Grierson et al. (2013) showed that the application of biochar using microalgal biomass as a feedstock on large scale for bio-energy and carbon storage (bio-CCS) will require considerable advances in cultivation technology, must harness waste nutrients from aligned industries and adopt alternate drying methods. Besides, there is an implementation of biochar production process from small wastewater treatment sewage sludge such as by Pyrochar (Draper, 2016). Table 2.3 summarizes previous studies on properties of biochar produced under

various conditions. Each of the biochar properties indicates the suitability of biochar for applications such as wastewater treatment or fertilizer and soil amendment in agricultural use.

Table 2.3: Summary of previous studies on properties of biochar produced under various conditions.

Biomass source	pH	Proximate analysis (wt%)			Ultimate analysis (wt%)					BET Surface area (m^2/g)	Cation-exchange capacity (cmol/kg)	References
		Volatile matter	Ash content	Fixed carbon	C	H	N	O	Higher heating value (MJ/kg)			
Desmodesmus communis	-	22	36.8	41	51	3	7	14	-	-	-	(Conti et al., 2016)
Arthrospira platensis (Spirulina)	-	28	29.5	42	51	2.5	7.7	18	-	-	-	(Conti et al., 2016)
Spirulina sp.	-	-	47.8		45.3	1.24	2.6	-	-	-	-	(Chaiwong et al., 2013)
Chlamydomonas reinhardtii	-	-	45	-	40	1.4	5.3	9.3	13	-	-	(Torri et al., 2011)
Scenedesmus dimorphus	7.2-8.3	3.3-17	39.6-44.2	43.4-52.4	46.8-53.6	7.9-8.5	5.6-6.5	31.4-39.5	19.0	1.7-123	-	(Bordoloi et al., 2016)
Blue-green microalgae + iron	-	-	-	-	60.3-75.3	-	3.6-4.9	15.4-29.7	-	38.3-128.3	-	(Peng et al., 2014)
Corn straw	10.0	-	16.7	-	58.0	2.7	2.3	21.5	-	14.7	23.8	(Xu et al., 2016)
Napier grass	8.9-11.1	-	20.1-25.1	-	50.2-51.3	1.8-4.1	2.4-2.9	3.9-10.0	18.8-22.8	11.0-26.1	-	(Yadav et al., 2016)

Table 2.3, continued.

Paulownia elongate tree	9.4	-	4.08	-	88.1	1.23	0.17	6.4	-	310	27.4	(Vaughn et al., 2017)
Mulberry wood	10.2-11.1	-	7.52-9.82	-	67.9-80.1	1.63-4.53	1.58-2.16	16.6-25.2	-	16.6-58.0	19.0-23.3	(Zama et al., 2017)
Douglas fir and White fir	7.1-7.3	-	2.7-3.1	-	65.7-83.9	-	0.21-0.36	-	-	2.82-156	10.7-13.2	(Mukome et al., 2013)
Softwood + algal digestate	6.8	-	6.4	-	58.1	4.16	0.41	31.7	-	2	67	(Mukome et al., 2013)
Softwood (pine)	7.9	-	17	-	71.2	2.88	0.91	11.6	-	4.9	3.2	(Mukome et al., 2013)
Hardwood (oak)	9.5	-	2.8	-	88.0	2.55	0.44	14.8	-	153.1	14.9	(Mukome et al., 2013)
Hardwood (cottonwood)	9.5	-	4.2	-	82.5	1.64	0.49	5.6	-	301.6	16.5	(Mukome et al., 2013)
Buckwheat husk	9.1-10.0	-	4.0-33.1	-	70.1-83.9	1.8-4.4	0.89-0.99	13.3-24.4	-	10.7-17.8	10.1-11.7	(Zama et al., 2017)

CHAPTER 3: MATERIALS AND METHODS

This chapter discusses the methodology of the research on conversion of microalgal biomass to biochar and bioethanol towards green technology application. The first part discusses the cultivation of microalgae and biochar production through pyrolysis follows by the co-production of biochar and bioethanol using wet torrefaction with microwave-assisted acid hydrolysis pretreatment. The final part presents the adsorption study of microalgal biochar on dye pollutants uptake for application.

3.1 Methodology of study

The flow chart of research activities is shown in Figure 3.1. The research covered the cultivation of microalgae towards biomass production for further conversion to biochar. The study of growth curve and biomass productivity of the selected microalgae species were investigated. The microalgal biochar production using conventional pyrolysis was carried out followed by the recently developed conversion process. The co-production of biochar and bioethanol was performed using wet torrefaction or known as hydrothermal carbonization. Finally, the application of microalgal biochar on adsorption of dye pollutants uptake was carried out prior to the completion of the research project.

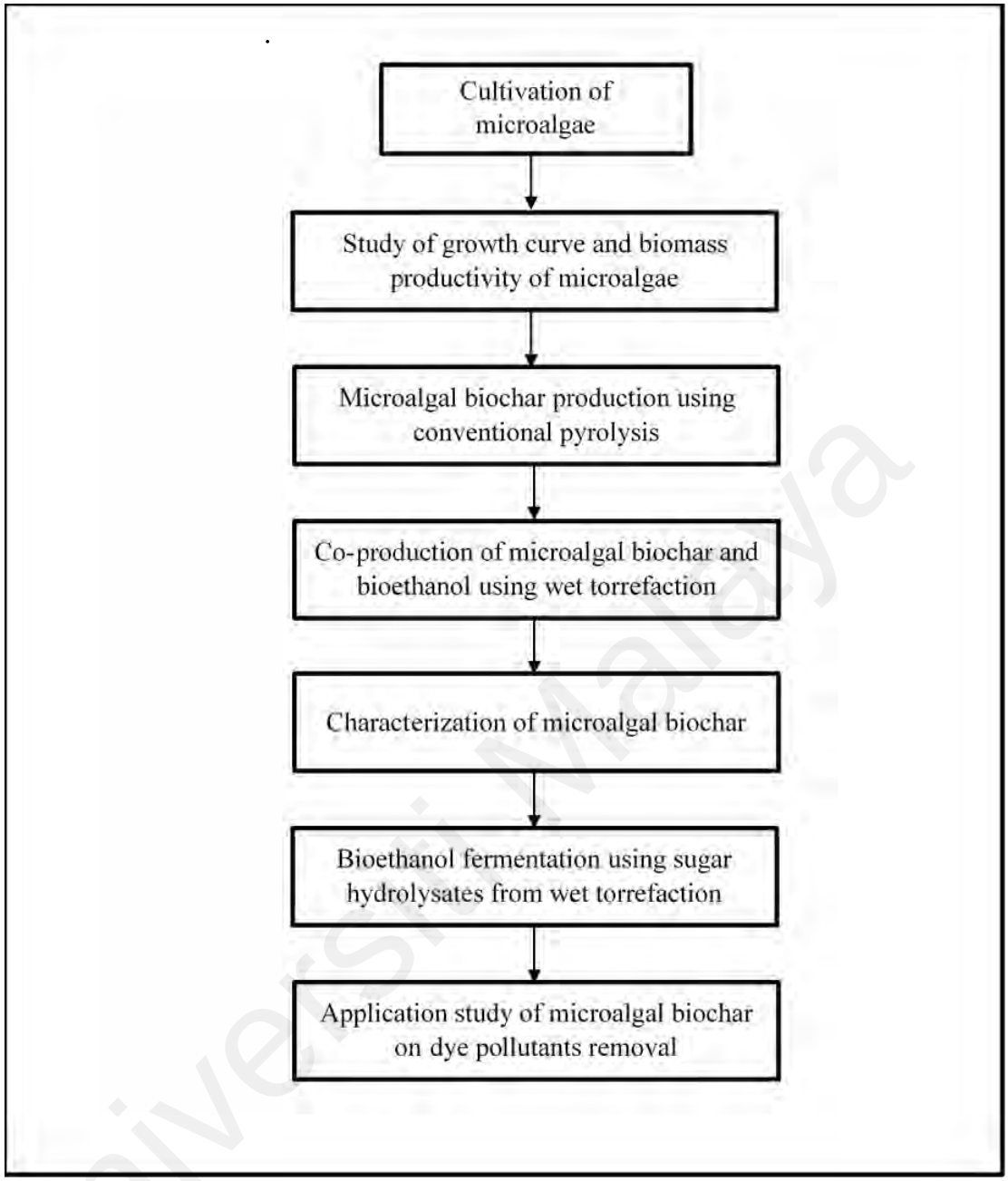

Figure 3.1: Flow chart of research methodology.

3.2 Cultivation of microalgae and biochar production through pyrolysis

3.2.1 Cultivation of *Chlorella* sp.

An indigenous microalgae *Chlorella vulgaris* FSP-E strain was obtained from Research Center for Energy Technology and Strategy, National Cheng Kung University, Tainan, Taiwan (Chen et al., 2013; Chen et al., 2015). A modified concentration of basal medium was used as the culture medium. The microalgal strain was pre-cultured and transfer into a batch photobioreactor (PBR) (Ho et al., 2013), with an optimized inoculum size of 0.06 g L^{-1} within pH 6-7. The cultivation will be carried out in PBR of the size of 1L at 26 ± 1 ℃ with an agitation rate of 300 rpm. The sole carbon source of 2.5, 5.0 and 7.5% CO_2 were supplied continuously to the microalgae culture during cultivation. The microalgal biomass concentration in the PBR was determined regularly with 12 h sampling interval time by measuring optical density at a wavelength of 680.8 nm using UV-Vis spectrophotometer (Model UV-1800, Shimadzu) until reaching exponential growth stage where dried cell mass at the constant maximum productivity. The microalgal biomass was harvested using centrifugation at 6000 rpm for 5 min and then was washed using distilled water three times. The microalgal biomass was oven-dried at 70 ℃ overnight prior to use.

3.2.2 Pyrolysis on microalgal biochar production

Pyrolysis was carried out by heating the reactor to the temperature of 500 ℃ with a holding time of 30 min in a fixed-bed stainless steel tubular reactor (Thangalazhy-Gopakumar et al., 2012), using a split-able mini tube furnace (Berkeley Scientific, USA). A continuous nitrogen gas flow of 100 mL min^{-1} was provided throughout the pyrolysis process. Around 5 g of microalgal biomass was loaded into the reactor to obtain biochar, bio-oil and gases products. Bio-oil was obtained through condensation of volatile products in ice-cooled flasks. The experiments were repeated three times with an average

standard deviation within 5.0 wt% for biochar, bio-oil and gases. Weight of biochar and bio-oil was obtained as the weight percentage of biomass whereas gas yield was obtained by total weight percentage difference of biochar and bio-oil. Thermogravimetric analysis (TGA) was carried out under nitrogen conditions at a heating rate of 15 °C min^{-1} at the temperature range of 30 to 925 °C to study the thermal decomposition behaviour of microalgal biomass and biochar under pyrolysis.

3.2.3 Characterization of microalgal biochar

The proximate analysis which includes the determination of moisture content, volatile matter, fixed carbon and ash content of samples was carried out using TGA (Perkin Elmer, USA) based on ASTM D7582-15 (Lee et al., 2017). Ultimate analysis which includes the determination of carbon (C), hydrogen (H), nitrogen (N), oxygen (O) and sulphur (S) within the samples was carried out using an elemental analyzer (LECO CHN628S, UK). The content of O was obtained by difference from C, H, N and ash content. The higher heating value (HHV) of samples was determined using a bomb calorimeter (Parr 6100, USA). All the analysis was carried out in duplicate for the average value. The pH values were obtained in triplicate using a ratio of 1.0 g of biochar in 20 mL deionized water for 1.5 hours. Fourier transform infrared spectroscopy (FTIR) was used to identify the functional groups on the surface of samples. The FTIR spectrum of the disc was recorded at wavenumber within the range of 400 to 4000 cm^{-1} with a resolution of 8 cm^{-1}. The surface morphology of microalgal biomass and biochar were examined using a scanning electron microscope (SEM, Quanta 400F, USA). Characterization of the physical and chemical properties of microalgal biochar is of great importance in determining their potential applications as a bio-adsorbent or alternative fuel.

3.3 Co-production of biochar and reducing sugar from microalgae using wet torrefaction with microwave-assisted acid hydrolysis pretreatment

3.3.1 Raw materials and chemicals

Two indigenous raw microalgae, namely, *Chlorella vulgaris* ESP-31 and *Chlorella* sp. GD were obtained from Research Center for Energy Technology and Strategy, National Cheng Kung University, Tainan, Taiwan, and National Chiao Tung University, Hsinchu, Taiwan, respectively (Kuo et al., 2015). Two kinds of *Chlorella* spp. with different carbohydrates composition were employed to examine the microalgae performance in the co-production of bioethanol and biochar. *Chlorella vulgaris* ESP-31 represents microalgal biomass with high carbohydrates composition that may be suitable for further biofuel/ bioethanol production; while *Chlorella* sp. GD represents the microalgal biomass with low carbohydrates content cultivated from the process of the wastewater treatment plant for additional application of biochar in approach to microalgae biorefinery. The biomass was ground and sieved and then kept in a clean air-tight sample container before further pretreatment reaction. Concentrated sulfuric acid (CAS: 7664-93-9; Merck) was purchased, and the concentrations of 0.1 M and 0.2 M diluted sulfuric acid were prepared for acid hydrolysis using wet torrefaction.

3.3.2 Experimental apparatus and procedure

The schematic diagram of the experimental setup used for acid hydrolysis using pretreatment wet torrefaction is shown in Figure 3.2. A modified household microwave (Tatung TMO-23MC, 2450 MHz, maximum power = 800 W) was used for the pretreatment torrefaction at several operating conditions of temperature (160, 170 °C) and reaction time (5, 10 min) with a fixed current output of 10 A (Bach et al., 2017; Chen et al., 2012). In each of the pretreatment, a mixture of 20 g microalgal biomass with 100 mL of diluted sulfuric acid (0.1, 0.2 M) and pure deionized water (DI water) as blank, was

prepared and poured into the reactor. The reactor was purged with N_2 for 10 min to ensure the absence of oxygen in the reactor before the reaction. The temperature and pressure of the reactor were monitored throughout the reaction to ensure a constant experiment condition. After the reaction, the mixture was centrifuged to separate the solid and liquid products using a centrifuge (HITACHI High-speed Micro Centrifuge CF15RN himac) operating at 15,000 rpm for 15 min at 10 ℃. After the separation, the solid product (biochar) was dried at 105 ℃ for 24 h and kept in a closed bottle while the liquid product (hydrolysate) was stored at below -4 ℃ until further measurement. Two independent experiments with average technical replicates were done for each of the experimental conditions to show good reproducibility with a standard deviation within ± 5%.

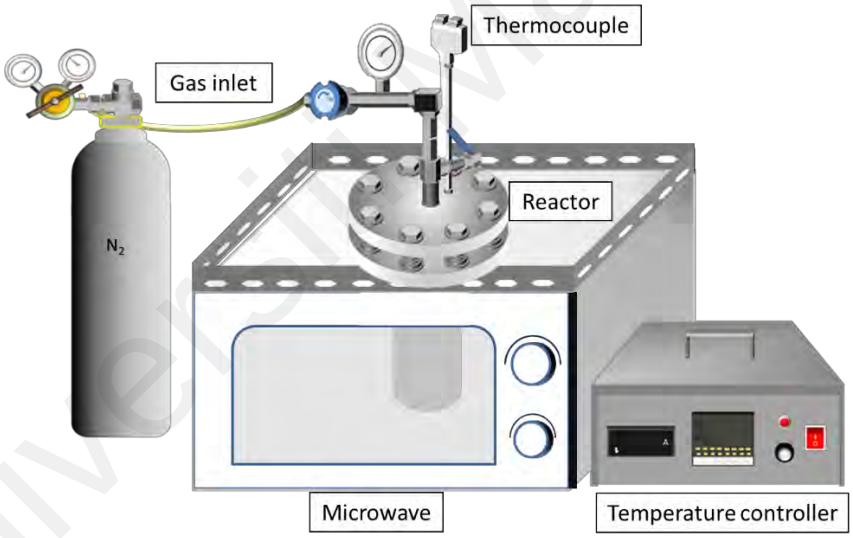

Figure 3.2: The schematic diagram of the experimental setup for acid hydrolysis using pretreatment wet torrefaction.

3.3.3 Characterization of microalgal biomass and biochar

The compositions of both microalgae species including the components of carbohydrates, proteins, and lipids were determined by modified quantitative saccharification (QS) method, elemental analyzer, and direct transesterification method,

respectively, as described in a previous report (Ho et al., 2013). The basic properties of the microalgae and biochar such as proximate analysis, elemental analysis, and higher heating value (HHV) were carried out according to the standard procedure of the American Society for Testing and Materials (ASTM) (Standard, 2007, 2009, 2013). Proximate analysis, including the measurements of moisture, volatile matter, and ash contents, was determined using a thermogravimetric analyzer (TGA; Perkin Elmer Diamond TG/DTA) according to ASTM D7582-15 (Lee et al., 2017). The elemental analysis was performed using an elemental analyzer (Perkin Elmer 2400 Series II CHNS/O Analyzer) to obtain the weight percentages of elements C, H, and N in both microalgal biomass and biochar, and the weight percentage of O was calculated by difference, that is, O = 100-C-H-N.

A bomb calorimeter (IKA C6000) was used to measure the HHV of biomass before and after the torrefaction. TGA (SDT Q600 TGA, TA Instruments) was carried out in an inert nitrogen gas condition at a heating rate of 20 °C min^{-1} from 50 to 925 °C to study the thermal decomposition behavior of microalgal biomass under wet torrefaction. The biochar yield ($Y_{biochar}$), energy enhancement factor (*EEF*) from HHV, and energy yield (Y_E) were calculated using the following equations, respectively (Bach et al., 2017).

$$\mathrm{Y_{biochar}}(\%) = \frac{\mathrm{m_{biochar}}}{\mathrm{m_{raw}}} \times 100 \tag{3.1}$$

$$\mathrm{EEF} = \frac{\mathrm{HHV_{biochar}}}{\mathrm{HHV_{raw}}} \tag{3.2}$$

$$\mathrm{Y_E}(\%) = \mathrm{Y_{biochar}} \times \mathrm{EEF} \tag{3.3}$$

In these equations, the weights of biochar and the raw microalgae were denoted as $m_{biochar}$ and m_{raw}, respectively, and HHV of the biochar and raw biomass were denoted as $HHV_{biochar}$ and HHV_{raw}, respectively.

Furthermore, Fourier transforms infrared spectroscopy (FT-IR; Perkin Elmer Spectrum 100) was used to identify the functional groups on the surfaces of microalgal biomass and biochar. The FT-IR spectrum of the disk was recorded at a wavenumber range of 650-4000 cm^{-1} with 4 cm^{-1} resolution. Other than that, the surface morphology of the microalgal biomass before and after the pretreatment was investigated using a scanning electron microscope (SEM, HITACHI S-3000N).

3.3.4 Determination of total reducing sugar

The hydrolysate obtained after the acid hydrolysis from microalgal biomass was analyzed using the 3,5-dinitrosalicylic acid (DNS) method to determine the concentration of total reducing sugar (Miller, 1959). Glucose was used to prepare the standard curve for calibration with a regression equation of $R^2 = 0.9975$. The reducing sugar solution was diluted with distilled water up to 1 mL in a test tube, and 1 mL of DNS solution was added to the samples and boiled at 90 °C for 5 min. UV-vis spectrophotometer (Biomate 3S, Thermo Scientific) was used to measure the absorbance of the samples at a wavelength of 540 nm. Two independent experiments with average technical replicates were done for each of the experimental conditions to show good reproducibility with a standard deviation within ± 5%.

3.3.5 Statistical analysis of data

The experiments were conducted with two independent experiment replicates. The significant differences between the mean of samples *C. vulgaris* ESP-31 and *Chlorella* sp. GD were subject to a t-test with $p < 0.05$. Subsequently, the correlation between the solid biochar and liquid hydrolysate product yields was determined using Pearson correlation with r value as the population correlation coefficient. All analyses were carried out using the statistical software IBM SPSS Statistics.

3.4 Bioethanol production from acid pre-treatment hydrolysate of microalgae through separate hydrolysis and fermentation

3.4.1 Experimental materials

The dried microalgal biomass of *Chlorella* sp. GD and *Chlorella vulgaris* ESP-31 species were provided as described in the previous Section 3.3.1. The diluted acids used for the pretreatment wet torrefaction were from the dilution of concentrated sulfuric acid (H_2SO_4, CAS: 7664-93-9, Merck) to 0.1 and 0.2 M. The microorganism species used for the fermentation process was *Saccharomyces cerevisiae* (*S. cerevisiae*) Type II yeast from Sigma-Aldrich. The yeast extract (Difco™ YM Broth), bacterial peptone (Friendemann Schmidt), potato dextrose agar (Friendemann Schmidt), potassium dihydrogen phosphate (Panreac, E.U.), and ammonium chloride (Shimakyu's Pure Chemicals) were used for the fermentation process. Standard 3,5-dinitrosalicylic acid (CAS: 609-99-4; Alfa Aesar), potassium sodium tartrate (CAS: 304-59-6; Choneye Pure Chemicals) and sodium hydroxide (CAS: 1310-73-2; Merck) were adopted for the analysis of total reducing sugar concentration. Standard D(+)-glucose (Merck), D(+)-galactose (Merck), 5-hydroxymethyl-2-furaldehyde (5-HMF, 97% Alfa Aesar), and ethanol (CAS: 64-17-5, 99.9% HPLC grade Duksan Pure Chemicals) were employed in the high-performance liquid chromatography (HPLC) analysis as the calibration standard chemicals. Methanol (CAS: 67-56-1, 99.9% HPLC grade Duksan Pure Chemicals) was diluted with deionized water (DI water) to serve as the HPLC mobile phase.

3.4.2 Separate hydrolysis and fermentation (SHF) for bioethanol production

3.4.2.1 Acid pretreatment wet torrefaction for hydrolysate

The acid pretreatment was carried out using wet torrefaction to obtain the solid biochar and liquid microalgal hydrolysate for further bioethanol production in this study. Figure 3.3 shows the general sketch of the apparatus for acid pretreatment using microwave-

assisted wet torrefaction for bioethanol production. A household microwave with a 2,450 MHz frequency and a maximum power of 800 W was modified for experimental use as described in Section 3.3.2. The experiment was carried out with few operating parameters (160 ℃, 10 min; 170 ℃, 10 min; 170 ℃, 5 min) with 0, 0.1, and 0.2 M diluted H_2SO_4 acid concentrations at fixed 10 A of current output. For each of the acid pretreatment, around 20 g of dried microalgal biomass was mixed and poured into the reactor with a solution of 100 mL diluted H_2SO_4 or pure deionized water (DI water). Before the reaction, N_2 gas was purged through the reactor for 10 min to make sure the inert atmosphere inside the reactor. A solid-liquid mixture was obtained after the pretreatment and centrifugation was used to collect the solid biochar and liquid hydrolysate. The liquid hydrolysate was kept in a tightly closed bottle at below -4 ℃ for further analysis and fermentation procedure.

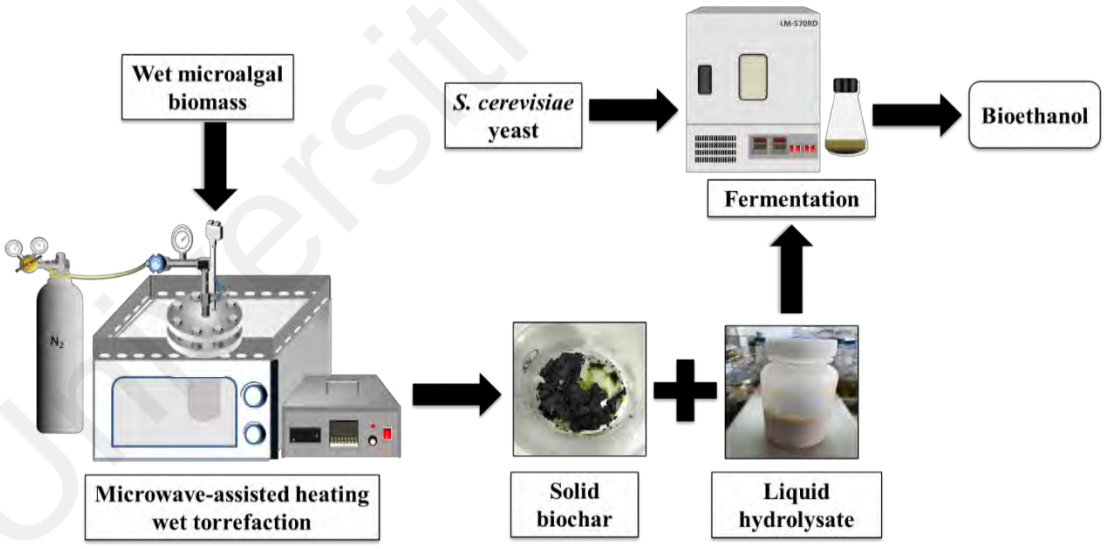

Figure 3.3: General sketch of the experimental setup for acid hydrolysis using microwave-assisted wet torrefaction for bioethanol production.

3.4.2.2 Yeast culture media preparation

The activation of yeast was carried out by adding 5 g of dry yeast *S. cerevisiae* powder into 50 mL of warm distilled in a beaker. The mixture solution was incubated at 32 ℃ for 6 h in an incubator before being inoculated in the culture agar medium. The yeast culture agar media was prepared by adding 4 g yeast extract, 8 g bacterial peptone, 8 g glucose, and 24 g agar in 400 mL of distilled water (Sebayang et al., 2017). The solution was autoclaved at 121 ℃ for 30 min before transferring to Petri dishes in the UV laminar flow chamber. Streak plating of the *S. cerevisiae* yeast was carried out for two cycles to obtain a pure yeast culture and the Petri dishes were incubated in an incubator at 37 ℃ for 48 h before being further used in fermentation for bioethanol production.

3.4.2.3 Fermentation of microalgal hydrolysate

The fermentation process was carried out in 150 mL flasks containing 50 mL hydrolysate with 0.5 g yeast extract, 0.2 g potassium dihydrogen phosphate (KH_2PO_4), and 0.1 g ammonium chloride (NH_4Cl) as fermentation nutrients (Sebayang et al., 2017). The solutions were adjusted to pH 4.6 and cold sterilized using UV light before being inoculated with 1.5 g/L *S. cerevisiae* yeast (3 mL of 6% w/w) and purged with nitrogen gas for the optimum anaerobic fermentation condition (Adnan et al., 2014; Khoja et al., 2015). The fermentation was carried out at a controlled room temperature of around 29 ℃ in dark conditions at the non-agitation state (Ueno et al., 1998). The samples were collected at an 8 h interval for 120 h to determine the total reducing sugar concentration and bioethanol concentration throughout the fermentation process. A fermentation time of 120 h is selected based on the ethanol production where it will be reaching a maximum production with the depletion of reducing sugar available in the hydrolysate (Chang et al., 2018). Duplication of the batch fermentation was carried out to obtain average experimental data with a standard deviation ≤ 5.

3.4.3 Total reducing sugar concentration

The standard method of 3,5-dinitrosalicyclic acid (DNS) was used to measure the total reducing sugar concentrations in the hydrolysate before and after fermentation (Miller, 1959). The calibration curve was prepared using glucose as a standard with $R^2 = 0.9961$ within the test ranges. About 1 mL of sample was diluted with DI water and added with 1 mL of DNS solution in the test tube before boiling at 90 ℃ for 5 min. The absorbance of the sample was detected using a UV-vis spectrophotometer (Biomate 3S, Thermo Scientific) at a wavelength of 540 nm for the determination of total reducing sugar concentration.

3.4.4 High-performance liquid chromatography (HPLC)

A high-performance liquid chromatography (HPLC) system (Perkin Elmer Series 200 Pump, Degassex™ Model DG-4400) equipped with refractive index detector (RI TESTHIGH 2000-F), and Ca column (SUPELGOGEL Ca 30 cm × 7.8 mm column) was used to determine the glucose and galactose contents in the hydrolysate after wet torrefaction. A sample volume of 20 µL was injected into the system with a column heater (TESTHIGH column heater Model 2001) to maintain the temperature at 90 ℃ and a flow rate of 0.2 mL/min with deionized water (DI water) as the mobile phase. The calibration curves by regression equations with $R^2 = 0.9968$ and $R^2 = 0.9951$ were obtained for glucose and galactose standards, respectively, within the test ranges for analysis.

For the determination of 5-HMF after fermentation, the HPLC system equipped with UV/Vis Detector (Hitachi UV Detector L-2400), autosampler (Hitachi Autosampler L-2200), system pump (Hitachi Pump L-2130), and LC-8 column (SUPELCOSIL™ LC-8 15 cm × 4.6 mm column) with column heater (SUPER CO-150) was used. The sample detection was carried out at a flow rate of 0.3 mL/min with methanol: DI water = 20: 80 as the mobile phase, under a controlled column temperature of 35 ℃ at a wavelength of

250 nm (Teh et al., 2017). A calibration curve by a regression equation with $R^2 = 0.9965$ was obtained for the 5-HMF standard within the test ranges for analysis.

For the ethanol determination, the HPLC system (Waters 2695 Separations Module with Waters Temperature Control Module II) equipped with refractive index detector (Waters 2414 Refractive Index Detector) and C-18 column (SUPELCO C-18 RP) were used with the system condition of 70 °C at a flow rate of 0.1 mL/min and 0.008 N H_2SO_4 as the mobile phase. Calibration was carried out by a regression equation with $R^2 = 0.9998$ within the test ranges. The experimental ethanol yield was calculated as expressed in Eqs. (1) and (2) (Ho et al., 2013). The ethanol productivity was also determined based on Eq. (3) (Gronchi et al., 2019). The theoretical ethanol yield was estimated by stoichiometry calculation as a baseline reference to the experimental data, and the experimental conversion probability was determined as expressed in Eq. (4) (Gombert et al., 2015; Markou et al., 2013).

$$\text{Ethanol yield (g ethanol/g microalgae)} = \frac{\text{Concentration of ethanol in fermentation solution (g/L)}}{\text{Concentration of initial microalgal biomass solution (g/L)}} \tag{3.4}$$

$$\text{Ethanol yield in percentage (\%)} = \text{Ethanol (g ethanol/ g microalgae)} \times 100 \tag{3.5}$$

$$\text{Ethanol productivity (g/L/h)} = \frac{\text{Experimental ethanol concentration (g/L)}}{\text{Fermentation time of 120 h}} \tag{3.6}$$

$$\text{Experimental conversion probability (\%)} = \frac{\text{Experimental ethanol concentration (g/L)}}{\text{Theoretical ethanol concentration (g/L)}} \times 100 \tag{3.7}$$

3.4.5 Statistical analysis of data

Two independent experiment replicates were employed in the study. IBM SPSS Statistics was used as the software for statistical data analyses. The statistical t-test with p-value ($p < 0.05$) was used to determine the significant differences between the mean samples of the two microalgae groups ($n = 18$). In addition, the population correlation coefficient between the total reducing sugar and 5-HMF in microalgal hydrolysates ($n = 18$) was determined as r-value using Pearson correlation.

3.5 Adsorption of microalgal biochar on dye pollutants uptake

3.5.1 Microalgal biochar adsorbent preparation and characterization

Wet-torrefied microalgal biochar (*Chlorella* sp. GD) was obtained from the wet torrefaction process under a temperature of 160-170 ℃ with a holding time of 5-10 min using a modified household microwave as described in Section 3.3.2. The collected biochars were crushed using pestle and mortar and sieved through a test sieve (Endecotts, ISO3310-1, 200SIW.500) with a mesh size of 500 μm before being stored in a desiccator for further experimental use. The surface morphology of the wet-torrefied microalgal biochar adsorbent was observed using a field emission scanning electron microscope (FESEM, Zeiss Auriga). Brunauer-Emmett-Teller (BET) surface analyzer (Micromeritics TriStar II 3020) was used to examine the specific surface area, pore-volume, and pore size distribution of the wet-torrefied microalgal hydrochar under N_2 gas adsorption. To determine the point of zero charge (pH_{pzc}) of the microalgal adsorbent, around 45mL of 0.1 M potassium nitrate (KNO_3) were prepared in the 100 mL conical flask. A series of the solution with initial pH (pH_0) ranged from pH 2 to 11 were prepared by adding acid and base solution of 0.1 M nitric acid (HNO_3) and 0.1 M potassium hydroxide (KOH), respectively. The solutions were then top up to 50 mL of KNO_3. Around 0.05 g adsorbent was then added to the flask and shaken for 24 h at 30 ℃. The final pH (pH_f) was recorded

thereafter. Finally, the point of intersection between the plot and x-axis which is known as PZC was obtained by plotting the graph between the difference of initial and final pH (ΔpH) against the initial pH.

3.5.2 Dyes adsorbate preparation

Methylene blue (MB; R&M Chemicals, CAS: 61-73-4, $C_{16}H_{18}ClN_3S \cdot xH_2O$, 319.86 g/mol) and Congo red (CR; Sigma-Aldrich, CAS: 573-58-0, $C_{32}H_{22}N_6Na_2O_6S_2$, 696.66 g/mol) were used as the dye adsorbates for the batch adsorption study. Distilled water was employed for the dyes solution preparation throughout the study. The stock solutions of MB and CR dyes with a concentration of 1000 ppm were prepared by dissolving 1 g of the dye powder into 1 L of distilled water in the volumetric flask. The desired concentrations of the dye adsorbates were prepared by dilution with distilled water. Acid and base solutions of 0.1 M of hydrochloric acid (HCl) and 0.1 M of sodium hydroxide (NaOH) were used for the adjustment of pH solution to the desired pH value. A calibrated pH meter (Mettler Toledo) was used for pH determination.

3.5.3 Batch adsorption studies

The adsorption experiments of MB and CR were carried in a batch study using the adsorbent of wet-torrefied microalgal hydrochar. The batch adsorption experiments were conducted using a water bath shaker (Memmert) under a constant agitation rate of 150 rpm at 30 ℃ with 50 mL of fixed working volume in conical flasks. To determine the effect of adsorbent dosage in adsorption, the amount of adsorbent mass (0.1, 1, 2, 3, and 5 g/L) was prepared at a fixed 50 ppm initial concentration under natural pH solution. The mixtures were shaken until reaching an equilibrium state to obtain the final dye concentration. The effect of pH was determined at varying initial pH from 2 to 10 under an initial concentration of 50 ppm with the adsorbent dosage of 5 g/L at an equilibrium state. The effects of initial concentration for MB and CR dyes were determined at the

concentration ranging from 5 to 360 ppm and 10 to 550 ppm, respectively, using the optimum adsorbent dosage and pH condition until equilibrium. For the determination of the contact time effect towards the kinetic study, the samples were collected at each of the pre-defined time intervals under optimum conditions to analyze the dye concentration.

For all the determination of dye concentration, around 3 mL of samples were pipetted and centrifuged at 10,000 rpm for 5 min using a centrifuge (Centrifuge Labogene Scanspeed Mini) for separation of liquid and solid products. The aliquots were then used to determine the final absorbance of the solution using a UV-Vis spectrophotometer (Analytik Jena SPEKOL 1500) at the wavelength of 665 nm and 497 nm for MB and CR dyes, respectively. Calibration curves were determined between the concentration and absorbance value to obtain the final concentration. Triplication of the batch adsorption study was carried out to obtain the average experimental data. In addition, control tests without the adsorbent which is similar to the operating condition of batch adsorption study were conducted simultaneously to investigate the possible deprivation factors of the dyes such as sorption onto the glassware, degradation, and volatilization throughout the experiment.

3.5.4 Experimental data and model fitting

The following equations were employed to calculate the removal percentage and adsorption capacity (Q_e, mg/g) of MB and CR dyes (Lee et al., 2016):

$$\text{Removal percentage } (\%) = \frac{C_0 - C_e}{C_0} \times 100\% \tag{3.8}$$

$$\text{Adsorption capacity, } Q_e \text{ (mg/g)} = \frac{(C_0 - C_e)V}{W} \tag{3.9}$$

where C_0 is denoted as the initial concentration of dye adsorbate (ppm or mg/L), C_e is denoted as the equilibrium concentration (ppm or mg/L), V is denoted as the total volume of adsorbate solution (L) and W is denoted as the amount of adsorbent (g).

Three commonly used types of isotherm models (Langmuir, Freundlich, and Temkin) were used to study and predict the adsorption performance at equilibrium (Li et al., 2016). To study the favourability of the adsorption process, the dimensionless constant separation factor (R_L) was determined with elucidation on the essential features of the Langmuir model based on the influence of isotherm shape (Meroufel et al., 2013). The adsorption process can be said to be favorable if $0 < R_L < 1$ while unfavorable if $R_L > 1$, furthermore it is regarded as linear and irreversible if R_L equals 1 and 0, respectively (Hall et al., 1966). The kinetics of the adsorption was determined using few commonly used kinetic models namely pseudo-first-order, pseudo-second-order, and Elovich by fitting the equilibrium adsorption capacity over time (t). The intraparticle diffusion model was employed to evaluate the rate-determining steps for dye adsorption based on the Q_t vs $t^{0.5}$ plot (Lee et al., 2016). Indication of the rate controlled by intra-particle diffusion can be determined when there is a linear plot passing through the origin. Furthermore, the adsorption rate can be indicated to be limited by two or more steps if a non-linear plot or linear plot not passing through the origin is observed (Weber et al., 1963). In addition, the Boyd plot of B_t against t based on the Boyd kinetic model was employed to predict the actual slow step in the adsorption process (Nethaji et al., 2013).

Table 3.1 shows the adsorption equilibrium isotherm and kinetic models with the equations and model parameters employed in this study. The model parameters of the adsorption equilibrium isotherm and kinetic models were evaluated using non-linear curve fit by software Origin 8. The value of the coefficient of determination (R^2) was obtained to determine the goodness-of-fit of the models with the experimental data.

Table 3.1: Adsorption equilibrium isotherm, kinetic and mechanism models.

Model	Equation	Reference
Isotherm		
Langmuir	$Q_e = \frac{Q_m K_L C_e}{1 + K_L C_e}$	(Langmuir, 1918)
Separator factor	$R_L = \frac{1}{1 + K_L C'_0}$	(Hall et al., 1966)
Freundlich	$Q_e = K_F C_e^{(1/n)}$	(Freundlich, 1906)
Temkin	$Q_e = \frac{RT}{B} \log A C_e$	(Temkin, 1940)
Kinetic and mechanism		
Pseudo-first-order	$Q_t = Q_e\left(1 - e^{-k_1 t}\right)$	(Lagergren, 1898)
Pseudo-second-order	$Q_t \frac{k_2 t Q_e^2}{1 + k_2 t Q_e}$	(Ho et al., 1998)
Elovich	$Q_t = \frac{1}{\beta}\ln(\alpha\beta) + \frac{1}{\beta}\ln t$	(Roginsky et al., 1934)
Intraparticle diffusion	$Q_t = k_p t^{0.5} + C_i$	(Weber et al., 1963)
Boyd	$B_t = -0.4977 - \ln(1 - \frac{Q_t}{Q_e})$	(Boyd et al., 1947)

Nomenclature:
Q_m (mg/g) – Langmuir maximum adsorption capacity,
K_L (L/mg) – Langmuir adsorption constant,
C'_0 (mg/L) – highest initial concentration,
K_F ((mg/g)(L/mg)$^{1/n}$) – Freundlich constant,
n – Freundlich exponent,
R (J/(mol K)) - gas constant,
T (K) – temperature,
B (J/mol) – Temkin constant,
A (L/mg) – maximum binding constant,
k_1 (1/h) - pseudo-first-order rate constant,
k_2 (g/(mg h))- pseudo-second-order rate constant,
β (g/mg) – Elovich constant,
α (mg/(g h))- initial adsorption rate,
k_p (mg/(g h$^{0.5}$)) - intraparticle diffusion rate constant,
C_i (mg/g) - intercept of intraparticle diffusion plot,
B_t - Boyd kinetic mathematical function

CHAPTER 4: RESULTS AND DISCUSSION

This chapter presents the research findings to date on the research of microalgal biomass to biochar and bioethanol. Biochar production from microalgae cultivation through pyrolysis as a sustainable carbon sequestration and biorefinery approach are discussed. Simultaneous production of biochar and reducing sugar from microalgae using wet torrefaction with microwave-assisted acid hydrolysis pretreatment follows with the bioethanol production from the pre-treated microalgal hydrolysate are discussed too. Finally, the adsorptive removal of dye pollutants using the microalgal biochar is discussed.

4.1 Biochar production from microalgae cultivation through pyrolysis as a sustainable carbon sequestration and biorefinery approach

4.1.1 Biomass productivity of microalgae

Microalgae have received more research attention as the third generation biofuels due to their high CO_2 fixation efficiency and sustainable high energy production (Hirano et al., 1997; Ho et al., 2011; Silitonga et al., 2017). Selection of microalgae strains with high biomass productivity and energy content is one of the crucial significance towards the commercial applications of microalgae in industry, therefore indigenous microalga *Chlorella vulgaris* FSP-E as one of the high biomass productivity microalgae species with maximum productivity up to 699 mg L^{-1} day^{-1} was selected in this study as the representative to determine the feasibility of *Chlorella* sp. for biomass and biochar production using the conventional process (Chen et al., 2016; Chen et al., 2015). Microalgae cultivation is highly related to several factors such as nutrients, temperature, inoculum size, pH, aeration rate, light intensity and CO_2 supply (Eloka-Eboka et al., 2017). For the study of CO_2 sequestration towards clean technology in microalgae

cultivation, different concentrations (2.5, 5.0 and 7.5%) of CO_2 were used in the study for optimal biomass productivity.

The data of cultivation of microalgae *Chlorella vulgaris* FSP-E with different CO_2 concentration supplies was shown in Table 4.1. Cultivation using 2.5% CO_2 concentration supply showed the highest maximum biomass concentration and productivity which are 8.35 g L^{-1} and 0.87 g L^{-1} day^{-1} respectively. Cultivation using 7.5% CO_2 concentration supply showed the second-highest of maximum biomass concentration and productivity which are 7.63 g L^{-1} and 0.65 g L^{-1} day^{-1} in 13 cultivation days. Cultivation using 5.0% CO_2 concentration supply showed maximum biomass concentration (7.56 g L^{-1}) at day 17 with average and maximum biomass productivity of 0.31 g L^{-1} day^{-1} and 0.46 g L^{-1} day^{-1} respectively. Cultivation of *C. vulgaris* FSP-E using 2.5% CO_2 supply gives the highest biomass productivity (0.58 g L^{-1} day^{-1}) in cultivation time of 14 days. Therefore, it is suggested that the optimum CO_2 concentration for the growth of *C. vulgaris* FSP-E is 2.5% which gives the highest biomass productivity in a shorter cultivation time.

Table 4.1: Biomass productivity on the cultivation of microalgae *Chlorella vulgaris* FSP-E at different carbon dioxide gas concentrations.[1]

Carbon dioxide concentration (%)	Cultivation time[2] (days)	Maximum biomass concentration (g L^{-1})	Average biomass productivity (g L^{-1} day^{-1})	Maximum biomass productivity (g L^{-1} day^{-1})
2.5	14	8.35	0.58 ± 0.27	0.87
5.0	17	7.56	0.31 ± 0.13	0.46
7.5	13	7.63	0.47 ± 0.23	0.65

[1] All the data are the mean of two independent experimental data sets.
[2] The cultivation time required to reach the exponential growth stage.

4.1.2 Thermogravimetric analysis of microalgal biomass

The thermal decomposition behaviour of *Chlorella vulgaris* FSP-E under pyrolysis was investigated using a thermogravimetric analyzer (TG) to measure the amount and percentage change in the weight of microalgal biomass as a function of temperature. The amount and rate of change in microalgal biomass due to decomposition, oxidation or dehydration were derived as TGA plot and its derivative with respect to temperature was derived as DTG plot (Chaiwong et al., 2012). The temperature peak observed from the DTG plot determines the activation of the thermochemical process. The reaction can easily occur when the peak of DTG is shown at a low temperature. The height of the DTG plot determines the capability of the volatilisation reaction to release a volatile matter of the sample throughout the pyrolysis process (Chaiwong et al., 2013).

The pyrolytic characteristics of *C. vulgaris* FSP-E at a temperature between 30 ℃ to 925 ℃ were determined by TGA and presented in Figure 4.1. The TG plot showed three stages of dehydration, devolatilization and solid decomposition occurred during the pyrolysis process. The first stage of weight loss occurred up to around 225 ℃ due to the dehydration of moisture content in the sample, followed by the next stage of devolatilization from 225 ℃ to 525 ℃ due to the loss of volatile components. The final stage was solid decomposition from around 525 ℃ to 925 ℃ with minimal weight loss at a slower rate. The peak in the DTG plot for *C. vulgaris* FSP-E occurred at around 325 ℃ indicates that the highest volatile matter was released and give the highest yield of bio-oil. The remaining solid residue at 925 ℃ is 19.7% and this showed the high biochar production at the end of pyrolysis.

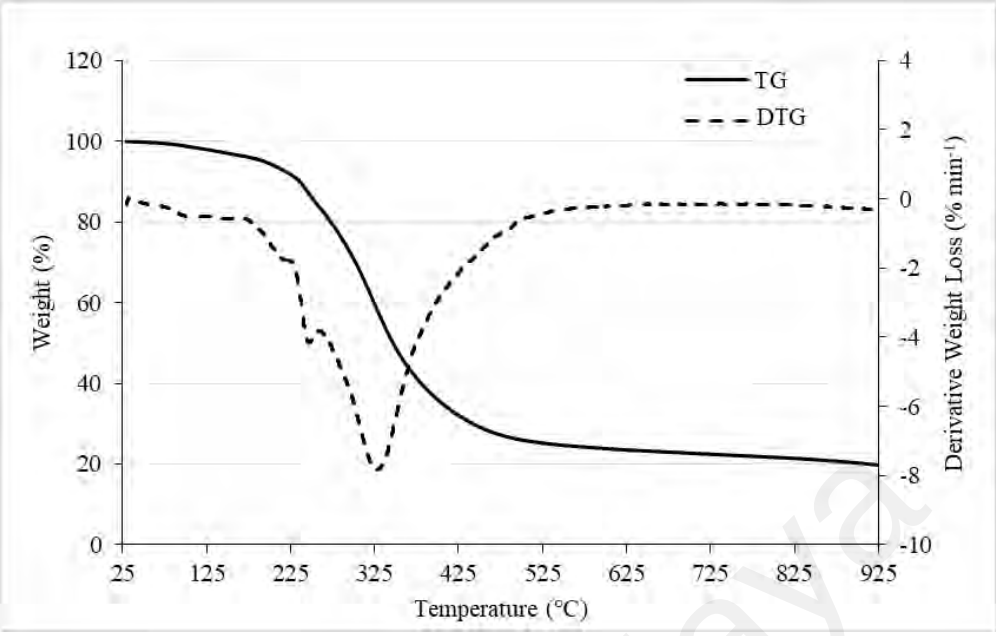

Figure 4.1: TG and DTG plots of *Chlorella vulgaris* FSP-E pyrolysis at a heating rate of 15 °C min^{-1}.

4.1.3 Yield of microalgal biochar

The product yield from pyrolysis is strongly related to the parameters such as temperature, heating rate and residence time (Hodgson et al., 2016). Therefore, pyrolysis was performed at 500 °C with a slow heating rate at high residence time for optimum high char yield (Chaiwong et al., 2012; Chang et al., 2015). The average biochar, bio-oil and gas yield from the pyrolysis of microalgal biomass were shown in Table 4.2. The highest biochar yield from *C. vulgaris* FSP-E that can be obtained throughout the experiment is 38.4 wt% whereas the lowest yield is 21.55 wt%. The biochar yield range is in good agreement with the previous study of biochar production from microalgae by slow pyrolysis with a yield of around 28-31% (Chaiwong et al., 2012). Pyrolysis conditions and parameters greatly affect the microalgal biochar yield, therefore this makes an interesting future approach to carry out optimization on pyrolysis of *C. vulgaris* FSP-E based on parameters such as temperature, residence time, heating rate and other related factors to obtain higher microalgal biochar yield for commercial application (Jindo et al.,

2014; Yu et al., 2017). Furthermore, other recent developed methods such as hydrothermal carbonization and torrefaction may be applicable on the microalgal biochar production to investigate a more energy saving and environmental friendly process based on clean technology policy (Wilk et al., 2017; Yu et al., 2017).

Table 4.2: Overall pyrolysis product distribution from *Chlorella vulgaris* FSP-E biomass.[1]

Product Distribution	Biochar	Bio-oil	Gases
Average yield (wt%)	26.9 ± 4.09	29.5 ± 0.59	43.6± 3.77

[1] All the data are the mean of three independent experimental data sets.

4.1.4 Proximate and ultimate analysis

The chemical properties include proximate and ultimate analysis of dried *C. vulgaris* FSP-E biomass and biochar were presented in Table 4.3. According to Table 4.3, it is evident that microalgal biochar has a more alkaline pH value. The biochar alkalinity is important for the stabilization of heavy metals in soil, making microalgal biochar viable for soil amendment application in agriculture (Zhang et al., 2013). From the proximate analysis, volatile matter content in microalgal biochar was reduced while fixed carbon and ash content were increased after pyrolysis. The ash content of microalgal biochar increased due to the removal of volatiles and the accumulation of inorganic content in biomass. The decrease of volatile matter fraction of combustible carbon makes microalgal biochar suitable to be used in coal-fueled boilers without a significant conversion process (Tag et al., 2016).

From the ultimate analysis, the C content in microalgal biochar increased to 61.32 wt% and this fits the requirement for it to be considered as biochar according to The European Biochar Certificate (EBC, 2012). The finding is similar to one of the previous studies on biochar derived from *Chlorella vulgaris* with a C content of 62.0 wt% (Wang et al., 2013).

The microalgal biochar in this study also possesses higher C content compared to the biochars derived from other popular microalgae such as *Spirulina* sp. and *Chlamydomonas* sp. with the C content of 45.23 wt% and 40.0 wt%, respectively (Chaiwong et al., 2012; Torri et al., 2011). The H, O and S content were decreased while N content almost remained the same. The N and S contents of biochar vary and are dependant on the feedstock properties and pyrolysis temperature. For biomass with low S content, it is a major advantage in energy conversion where CO_2 emission can be reduced during the process (Basu, 2010). The H/C and O/C atomic ratios were decreased to 0.69 and 0.15 respectively in microalgal biochar compared to the dried microalgal biomass. This associate with the dehydrogenation and demethanation reactions that occurred during pyrolysis. With the H/C and O/C atomic ratios as an indicator for biochar stability, it is suggested that low H/C and O/C atomic ratios (H/C ratio < 0.6; O/C ratio < 0.4) in microalgal biochar will be effective for carbon sequestration in soil application (Ippolito et al., 2012). With the high C/N and mineral contents, microalgal biomass is also a suitable feedstock for biochar production which could be environmentally beneficial to carbon sequestration and soil fertility (Chaiwong et al., 2013). The higher heating value (HHV) of coal is normally found to be between 25 to 35 MJ/kg (Chen et al., 2015), and the HHV of other microalgal biochars based on previous literature is in the range of 7.56-23.0 MJ/kg (Yu et al., 2017). In this study, the HHV obtained in microalgal biochar (23.42 MJ/kg) shown that it approaches a similar calorific value as coal and is potentially to be used as an alternative source in coal energy production.

Table 4.3: Properties, proximate and ultimate analysis of dried *Chlorella vulgaris* FSP-E biomass and its respective biochar.

Properties	Dried biomass	Biochar
pH	6.2	8.1
Proximate analysis (dry basis, wt%)		
Moisture content	2.76	3.81
Volatile matter	80.62	17.40
Fixed carbon	14.50	65.34
Ash content	2.17	13.45
Ultimate analysis (dry basis, wt%)		
C	49.58	61.32
H	7.09	3.55
N	9.83	9.76
O	31.33	11.92
S	0.76	0.02
H/C (mol%)	1.70	0.69
O/C (mol%)	0.47	0.15
C/N (-,wt/wt)	5.04	6.28
Higher heating value (HHV) (MJ/kg)	21.64	23.42

4.1.5 Functional group

The FTIR spectra of *Chlorella vulgaris* FSP-E and its derived biochar showed a number of peaks that indicate the chemical functional groups in the structure of samples before and after the pyrolysis process. The peak wavenumbers from the FTIR spectra in Figure 4.2 have been identified and summarized in Table 4.4 based on the functional groups together with literature data. Overall, the FTIR spectra of both microalgal biomass and biochar have a similar trend line but the respective biochar showed fewer peak wavenumbers. This indicates that the pyrolysis process had some effect on the structure and functional group composition in microalgae. Some peaks in the microalgal biochar spectra had disappeared and new peaks appeared compared to microalgal biomass due to

the release of volatiles and breaking of chemical bonds during pyrolysis reaction (Zheng et al., 2017). This is consistent with the decrease of volatile matter in the proximate analysis of microalgal biochar. The high temperature of pyrolysis reaction led to the destruction of C≡C, C═O, C─O and N─H functional groups in microalgal biochar. However, new functional groups of aromatic C─H and alkene C═C were found in the structure. This result is similar as reported by El-Hendawy (2006) on the formation of the polyaromatic structure after the carbonization of biomass. The functional group of carboxylic O─H remained in the microalgal biochar even after the pyrolysis reaction. The existence of O-containing functional groups and the high O/C atomic ratio (0.15) in microalgal biochar indicates the possible application in adsorption study (Wei et al., 2017; Zhou et al., 2015). This can be an applicable biorefinery approach of microalgal biochar as a value-added bio-adsorbent product from the energy production of microalgae together with the reduction of carbon footprint in the environment.

Table 4.4: Chemical functional group in *Chlorella vulgaris* FSP-E biomass and its respective biochar based on FTIR spectra.

Class	Functional group	Wavelength range (cm^{-1})		
		Reference[b]	Microalgal biomass	Microalgal biochar
Carboxylic acids	O─H stretch (s)[a]	3300-2500	3276	3215
Alkanes	C─H stretch(s)	3000-2850	2928	-
Alkynes	C≡C stretch (w)	2140-2100	2110	-
Allenes	C═C═C stretch (m)	2000-1900	1986	1983
Aldehydes and Ketones	C═O stretch(s)	1730-1720	1730	-
Amides	N─H out of plane	1640-1600	1634	-
Alkanes	CH_2, CH_3 deformation	1470-1350	1450	1411

Table 4.4, continued.

Alkyl aryl ether	C─O stretch (s)	1275-1200	1238	-
		1075-1020	1042	1065
Aromatics	C─H out of plane(m)	885-870	-	874
Alkenes	C═C plane (s)	730-665	-	713

[a] s-strong, m-medium and w-weak

[b] Based on (Coates, 2006)

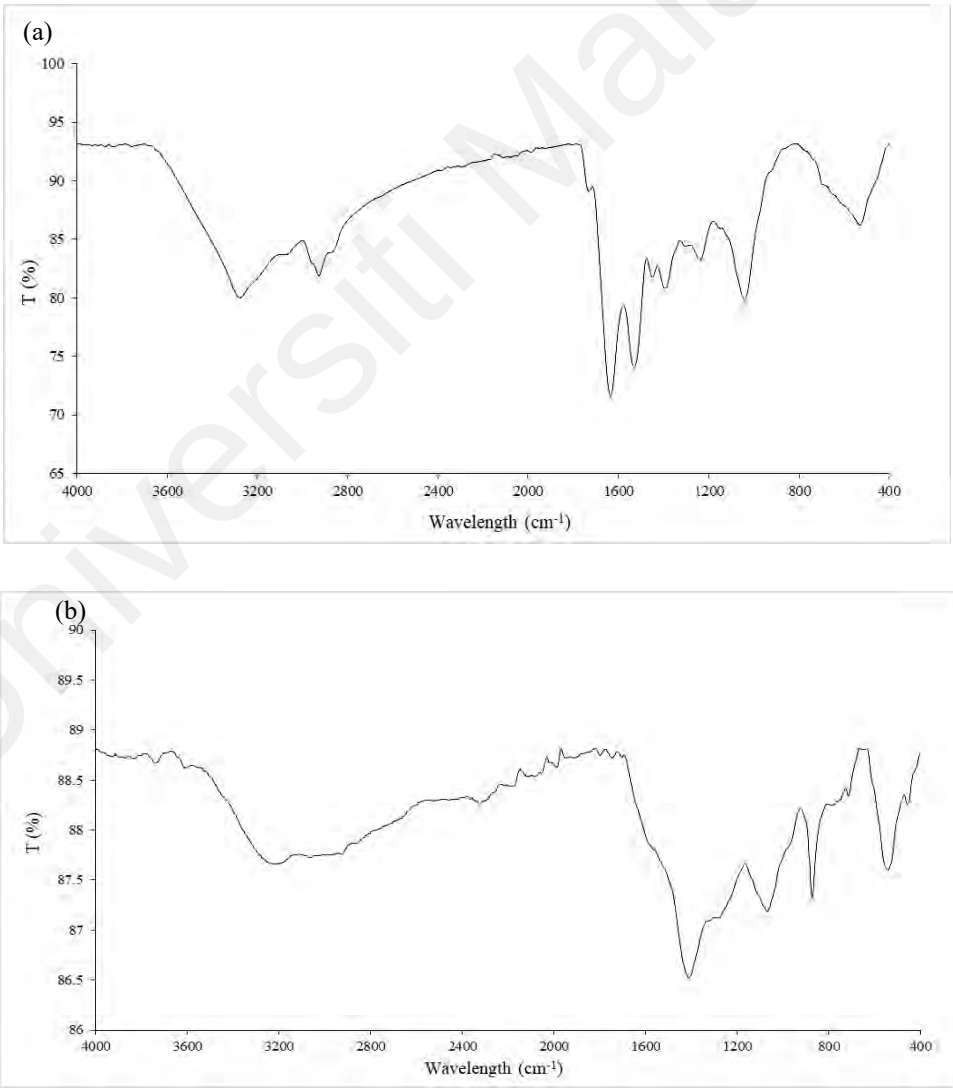

Figure 4.2: FTIR spectra for *Chlorella vulgaris* FSP-E biomass (a) and its respective biochar (b).

4.1.6 SEM observation

The surface morphology of microalgal biomass and biochars were observed by scanning electron microscopy (SEM) at magnifications ranging from 800-25000 times. The data were shown in Figure 4.3. As compared to original microalgal biomass with rough and globular agglomerate structure surface, microalgal biochar showed fragmented and porous structure after the pyrolysis process. Some loopholes were formed on the biochar compared to original agglomerated microalgal cells. The fragmented and porous structure should be caused by rigorous reaction during pyrolysis process (Chang et al., 2015). The irregular porous structure formed may contain an active binding site that can potentially utilize in the application as a bio-adsorbent. Further investigation on microalgal biochar for adsorption of pollutants in soil and water can be carried out on a microalgal biorefinery approach to produce the value-added and eco-friendly product.

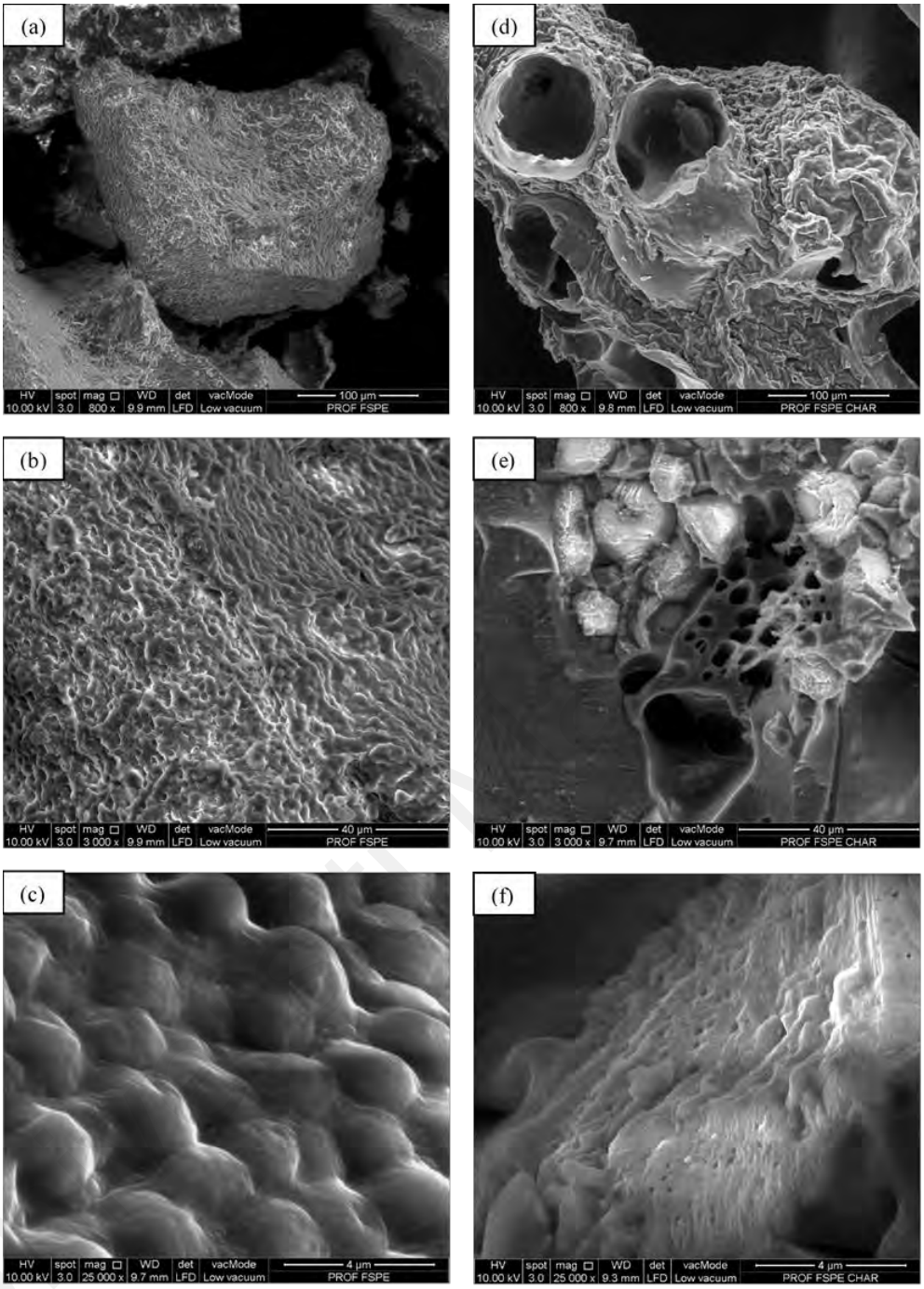

Figure 4.3: SEM images for *Chlorella vulgaris* FSP-E biomass (a,b,c) and its respective biochar (d,e,f) at different magnifications (800-25000×).

4.2 Simultaneous production of biochar and reducing sugar from microalgae using wet torrefaction with microwave-assisted acid hydrolysis pretreatment

4.2.1 Biomass composition of raw microalgae materials

Composition analysis was carried out to determine the biomass composition of raw microalgae *Chlorella vulgaris* ESP-31 and *Chlorella* sp. GD is shown in Table 4.5. It is found that raw *C. vulgaris* ESP-31 consists of a high carbohydrate content (57.5%), which accounts for the largest composition in the microalgae biomass. In contrast, raw *Chlorella* sp. GD is composed of low carbohydrate content (8.64%) while the protein content (59.75%) taking up the biggest portion in the microalgae biomass. The carbohydrate component in raw microalgae consists of sugar components such as glucose is important to determine the best viability of microalgae species under acid hydrolysis treatment for total reducing sugar recovery, in an approach for future application in microalgal bioethanol production (Ho et al., 2013). Both the microalgae *C. vulgaris* ESP-31 and *Chlorella* sp. GD showed good adaptation and well growth performance in wastewater medium (Chen et al., 2018; Kuo et al., 2015), where the biomass can be utilized to produce value-added energy products such biochar and bioethanol after acid hydrolysis wet torrefaction pretreatment (Bach et al., 2017; Phwan et al., 2018). From the composition analysis, an assumption can be made where microalga *C. vulgaris* ESP-31 with high carbohydrate will be a good potential candidate for bioethanol production compared to *Chlorella* sp. GD is based on the abundance of sugar components.

Table 4.5: Biomass composition of raw microalgae species.

Microalgae species	Components (%)				Proximate analysis (dry basis, wt%)				Ultimate analysis (dry basis, wt%)			
	Carbo-hydrates	Protein	Lipid	Others	Moisture content	Volatile matter	Fixed carbon	Ash content	C	H	N	O
Chlorella vulgaris ESP-31	57.50	18.30	15.38	8.82	4.88	85.59	2.76	6.77	47.98	7.85	3.04	41.13
Chlorella sp. GD	8.64	59.75	7.86	23.75	4.86	73.89	17.53	3.72	49.83	7.65	10.32	32.20

4.2.2 Solid yield

The solid yields of the microalgae (*C. vulgaris* ESP-31 and *Chlorella* sp. GD) at several wet torrefaction operating temperatures and holding times under various acid concentrations (0, 0.1 and 0.2 M) are shown in Figure 4.4. For *C. vulgaris* ESP-31, the highest solid yields of 54.5%, 31.0%, and 23.9% are obtained at the acid concentrations of 0, 0.1 M, and 0.2 M, respectively; while for *Chlorella* sp. GD, the highest solid yields of 74.6%, 68.9%, and 51.2% are obtained under the concentrations of 0, 0.1 M, and 0.2 M, respectively. Microalgae *Chlorella* sp. GD gives an overall higher solid yield range as compared to *C. vulgaris* ESP-31 ($p < 0.05$). This is due to the differences in the raw biomass composition as shown in Table 4.5. With the higher carbohydrates content of 57.5% in *C. vulgaris* ESP-31, the microalga has a low resistance towards hydrolysis and hence it is more reactive during the process to give more reducing sugar in the liquid hydrolysate and associate with low solid yield compared to *Chlorella* sp. GD with a lower carbohydrates content of 8.64% (Bach et al., 2017; Bougrier et al., 2008; Wilson et al., 2009). Overall, the biochar yield shows a decreasing trend when the acid medium for reaction increases from blank pure water to 0.1 M and 0.2 M diluted sulphuric acid for both microalgal biomass (Figure 4.4). Furthermore, the solid yield is lower at a higher temperature of 170 °C and a prolonged holding time of 10 min. This shows that, when the acid hydrolysis reaction is more vigorous, more energy from the biomass is distributed to the liquid hydrolysate product and this will be discussed further under Section 4.2.8. As a comparison with other studies on acid hydrolysis wet torrefaction using lignocellulosic biomass and macroalgae (Chen et al., 2012; Teh et al., 2017), microalgae have a relatively lower solid yield as compared to the lignocellulosic biomass and macroalgae. Other than the differences in carbohydrates component of raw biomass, this may be also attributed to the cellular structure and smaller particle form of microalgae where hydrolysis reaction is more reactive during wet torrefaction compared to raw

biomass from lignocellulosic feedstock and macroalgae (Bach et al., 2017; Harun et al., 2014). The *Chlorella* spp. undergoes acid hydrolysis wet torrefaction possess a relatively higher biochar yield (23.9-74.6%) compared to the one obtained from studies of Yuan et al. (2015) and Wang et al. (2013) on fixed-bed pyrolysis (19.3–43.46%), and fluidized-bed fast pyrolysis (31.0%), respectively, where acid hydrolysis wet torrefaction may be an effective thermochemical conversion approach for the co-production of microalgal biochar.

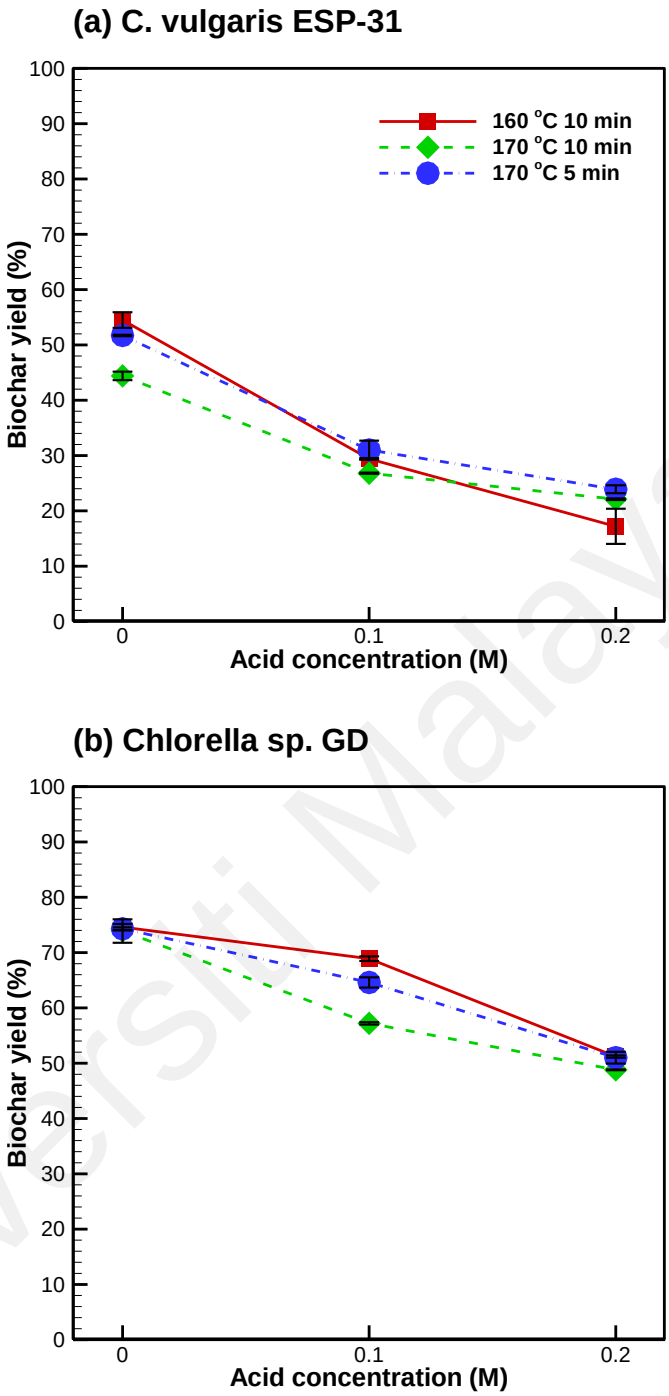

Figure 4.4: Biochar yield of (a) *C. vulgaris* ESP-31 and (b) *Chlorella* sp. GD biomass under several torrefaction conditions.[1]

[1] All the points are the mean of two independent experimental data sets and error bars indicate the standard deviation.

4.2.3 Proximate and ultimate analyses

The proximate and ultimate analyses of biochar *C. vulgaris* ESP-31 and *Chlorella* sp. GD after wet torrefaction are shown in Table 4.6. The proximate analysis shows an overall decrease trend in the moisture content of raw microalgae biomass (*C. vulgaris* ESP-31: 4.88 wt%; *Chlorella* sp. GD: 4.86 wt%) compared to biochars after wet torrefaction (*C. vulgaris* ESP-31: 0.72-3.58 wt%; *Chlorella* sp. GD: 1.27-5.27 wt%). The decrease in moisture content promotes long-term storage and handling of samples after the thermal pretreatment process (Teh et al., 2017). The biochars obtained after acid hydrolysis shows an increase in the volatile matter content (*C. vulgaris* ESP-31: 85.51-90.41 wt%; *Chlorella* sp. GD: 71.56-81.98 wt%) as compared to the torrefaction process in a pure water medium (*C. vulgaris* ESP-31: 76.99-78.67 wt%; *Chlorella* sp. GD: 71.36-74.65 wt%) under the same operating temperature and holding time. The observation is similar to previous literature (Chen et al., 2012; Teh et al., 2017) which shows the reaction of acid towards the conversion of polysaccharides of raw microalgal biomass into hydrocarbon with a shorter chain. The composition of fixed carbon content is obtained from the differences of moisture, volatile matter, and ash contents (Chen et al., 2012), therefore showing relatively low fixed carbon content in the biochars after the acid hydrolysis based on the higher volatile matter contents. Furthermore, microalgal biochars obtained after the pretreatment show a lower ash content (*C. vulgaris* ESP-31: 2.66-5.83 wt%; *Chlorella* sp. GD: 2.69-6.43 wt%) compared to macroalgal biochar (12.60 wt%) (Teh et al., 2017), and this indicates microalgae feedstock possesses better properties for fuel application after the wet torrefaction. In addition, the wet torrefied microalgal biochar also showed a lower ash content compared to the study by Wang et al. (2013) on microalgal biochar produced from fast pyrolysis with ash content of 20%, which further indicates the approachable alternative fuel application of wet torrefied microalgal biochar.

Based on the ultimate analysis, the C contents of the raw microalgae (*C. vulgaris* ESP-31: 47.98 wt%; *Chlorella* sp. GD: 49.83 wt%) increase after the torrefaction process in the microalgal biochars (*C. vulgaris* ESP-31: 54.72-68.71 wt%; *Chlorella* sp. GD: 52.79-58.81 wt%). The C contents obtained for both microalgal biochars are in the range of biochar requirement according to the European Biochar Certificate (EBC 2012). The H content in both microalgal biochars increases after the acid hydrolysis wet torrefaction may be due to the dehydration reaction catalyzed by acid or the free-radical decarboxylation of carboxyl group throughout the acid pretreatment (Denisov et al., 2013). The finding is also supported by the increase of functional groups as observed by FT-IR in Section 4.2.6. However, there is a decreasing trend in the O content of microalgal biochars, whereas the N content remains about the same as compared to raw microalgal biomass for the two species. Microalgal biomass with higher N content as compared to macroalgae (Teh et al., 2017; Yu et al., 2017) consists of more nutrients that are suitable for soil application and crop production (Wang et al., 2013). For the efficiency of combustion in coal fuel application, solid fuel with low H/C and O/C ratios is recommended (Liu et al., 2013). As a correlation, the atomic composition of the raw microalgal biomass and biochars after the torrefaction process is determined and presented in a van Krevelen diagram, as shown in Figure 4.5. Overall, there is an improvement in the fuel properties of microalgal biochars obtained after acid hydrolysis wet torrefaction which determines the effects of the thermal process towards the reduction of C─H and O─C bonds with lower energy and addition of C─C bond with higher energy (Liu et al., 2013). However, there is an exceptional observation for the microalgal biochars produced at 160 °C under the acid condition, especially for *C. vulgaris* ESP-31 which makes the biochar less applicable for solid fuel application compared to microalgal biochar produced by wet torrefaction in pure water medium (Bach et al., 2017).

Table 4.6: Proximate and ultimate analysis of biochar *C. vulgaris* ESP-31 and *Chlorella* sp. GD after wet torrefaction.[1]

Microalgae biochar	Torrefaction condition	H_2SO_4 (M)	Proximate analysis (*dry basis, wt%*)				Ultimate analysis (*dry basis, wt%*)			
			Moisture content	Volatile matter	Fixed carbon	Ash content	C	H	N	O
C. vulgaris ESP-31	160 °C, 10 min	DI water (blank)	1.61 ± 0.09	78.67 ± 4.84	13.90 ± 3.67	5.83 ± 1.27	54.72 ± 1.60	8.83 ± 0.23	3.60 ± 0.06	32.85 ± 0.51
		0.1 M H_2SO_4	3.58 ± 1.91	85.51 ± 2.71	5.60 ± 4.78	5.32 ± 0.93	63.37 ± 3.80	13.31 ± 3.67	4.50 ± 1.00	18.82 ± 2.02
		0.2 M H_2SO_4	1.34 ± 0.41	90.34 ± 4.91	4.94 ± 6.31	3.39 ± 1.00	65.67 ± 2.98	13.29 ± 3.59	3.49 ± 1.59	17.56 ± 3.20
	170 °C, 10 min	DI water (blank)	1.76 ± 0.52	77.88 ± 0.85	15.64 ± 0.09	4.72 ± 1.47	57.40 ± 0.69	8.85 ± 0.40	3.79 ± 0.13	29.96 ± 0.24
		0.1 M H_2SO_4	1.75 ± 0.41	85.60 ± 3.89	7.75 ± 1.37	4.91 ± 2.93	67.62 ± 0.87	10.30 ± 0.48	3.50 ± 0.01	18.58 ± 1.58
		0.2 M H_2SO_4	1.48 ± 0.01	90.41 ± 2.50	5.44 ± 1.48	2.66 ± 1.03	68.71 ± 1.02	10.48 ± 0.19	2.82 ± 0.04	17.99 ± 0.14
	170 °C, 5 min	DI water (blank)	1.81 ± 0.50	76.99 ± 2.03	15.65 ± 2.33	5.55 ± 0.80	55.43 ± 1.76	8.80 ± 0.00	3.76 ± 0.50	32.01 ± 3.06
		0.1 M H_2SO_4	0.72 ± 0.18	88.71 ± 9.06	7.15 ± 6.80	3.43 ± 2.07	63.23 ± 0.45	10.10 ± 0.21	3.76 ± 0.44	22.92 ± 1.86
		0.2 M H_2SO_4	1.32 ± 0.24	89.69 ± 0.97	5.23 ± 0.88	3.77 ± 0.16	67.16 ± 0.54	10.32 ± 0.00	2.80 ± 0.15	19.72 ± 0.24

[1] All the data are the mean of two independent experimental data sets.

Table 4.6, continued

Chlorella sp. GD	160 °C, 10 min	DI water (blank)	4.78 ± 0.82	71.63 ± 0.26	18.00 ± 0.15	5.61 ± 1.22	53.72 ± 0.31	7.92 ± 0.09	10.77 ± 0.18	27.59 ± 0.82
		0.1 M H_2SO_4	4.31 ± 0.42	73.52 ± 3.44	20.17 ± 0.35	2.00 ± 2.67	52.79 ± 1.75	8.17 ± 0.32	9.77 ± 0.30	29.28 ± 0.29
		0.2 M H_2SO_4	2.57 ± 0.02	73.53 ± 0.64	17.49 ± 0.27	6.43 ± 0.36	56.66 ± 0.56	8.29 ± 0.14	8.86 ± 0.05	26.18 ± 0.83
	170 °C, 10 min	DI water (blank)	2.98 ± 0.02	74.65 ± 8.13	16.09 ± 8.05	6.28 ± 0.06	54.09 ± 0.12	8.00 ± 0.08	10.49 ± 0.10	27.42 ± 0.11
		0.1 M H_2SO_4	1.44 ± 0.78	81.98 ± 3.89	11.97 ± 4.68	4.62 ± 0.01	56.46 ± 2.98	8.15 ± 0.21	9.29 ± 0.93	26.09 ± 2.25
		0.2 M H_2SO_4	1.27 ± 0.02	80.76 ± 5.73	13.30 ± 6.43	4.68 ± 0.69	58.51 ± 0.13	8.43 ± 0.10	8.72 ± 0.08	24.34 ± 0.80
	170 °C, 5 min	DI water (blank)	5.27 ± 0.64	71.36 ± 0.57	17.89 ± 0.19	5.50 ± 0.12	54.84 ± 0.64	8.09 ± 0.24	10.91 ± 0.05	26.17 ± 1.05
		0.1 M H_2SO_4	4.37 ± 0.12	71.56 ± 0.42	21.39 ± 0.33	2.69 ± 0.64	53.88 ± 0.55	8.09 ± 0.11	9.97 ± 0.05	28.05 ± 1.03
		0.2 M H_2SO_4	2.96 ± 0.33	73.08 ± 0.31	18.73 ± 0.38	5.23 ± 1.03	55.17 ± 1.58	8.26 ± 0.21	8.65 ± 0.36	27.92 ± 1.12

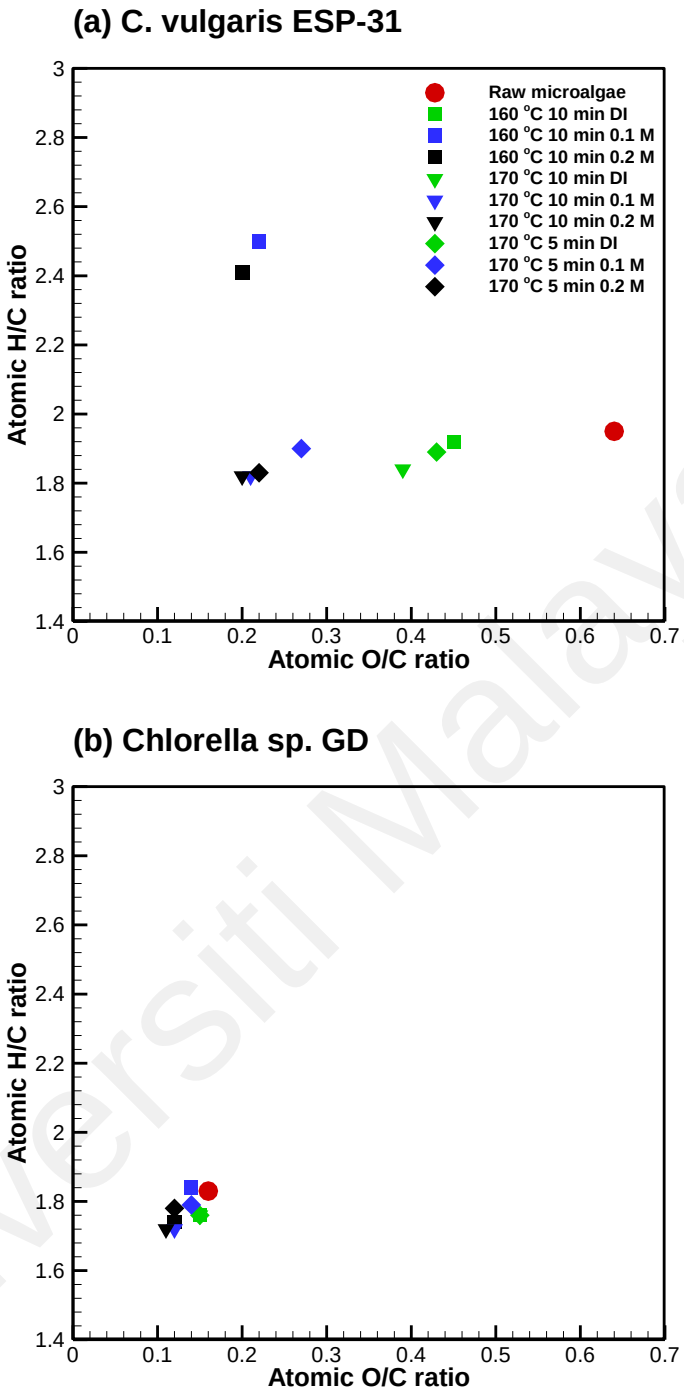

Figure 4.5: The van Krevelen diagram of (a) *C. vulgaris* ESP-31 and (b) *Chlorella* sp. GD, and their respective biochars after torrefaction under various operating conditions.[1]

[1] All the points are the mean of two independent experimental data sets.

4.2.4 Higher heating value and energy enhancement

The higher heating value (HHV) and energy yield of the torrefied solid product are two essential properties to indicate a wet torrefaction process. The HHV for both microalgae species under each of the operating conditions (temperature and holding time: 160 ℃, 10 min; 170 ℃, 10 min; 170 ℃, 5 min; with acid concentrations of 0, 0.1 and 0.2 M) are presented in Table 4.7. The enhancement factor of HHV and energy yield of the solid product produced under each of the operating conditions, which are calculated based on Eq. (3.2) and Eq. (3.3), respectively, are plotted in Figure 4.6 and Figure 4.7, respectively. The torrefied biomass obtained after acid hydrolysis treatment shows a higher HHV range (*C. vulgaris* ESP-31: 23.56-32.35 MJ/kg; *Chlorella* sp. GD: 21.77-24.47 MJ/kg) compared to the raw biomass for both microalgae species (*C. vulgaris* ESP-31: 19.23 MJ/kg; *Chlorella* sp. GD: 21.26 MJ/kg). As for fuel-burning with C content acts as an exothermic role while O acts as an endothermic role, the higher C and lower O properties from ultimate analysis as shown in Table 4.6 explains the increase of HHV in torrefied biomass (Chen et al., 2011). As a correlation, the weight loss of biomass with the ratio of total energy between torrefied and raw biomass led to the increase of the enhancement factor after acid hydrolysis wet torrefaction as presented in Figure 4.6. The HHV of *C. vulgaris* ESP-31 increases from 19.23 MJ/kg to the highest 31.23 MJ/kg, whereas the HHV of *Chlorella* sp. GD increases from 21.26 MJ/kg to the highest 25.32 MJ/kg after acid hydrolysis torrefaction condition. As a result, the HHVs of microalga *C. vulgaris* ESP-31 obtained from the study are relatively higher compared to microalga *Chlorella* sp. GD ($p < 0.05$). As a correlation with the ultimate analysis as presented in Table 4.6, HHV increases with the increase of C and H contents. *C. vulgaris* ESP-31 biochars exhibit higher C and H contents than *Chlorella* sp. GD after acid hydrolysis wet torrefaction and thus produce higher HHV. This is consistent with the knowledge that higher C and H contents will lead to the higher energy content of the product (Sheng et

al., 2005). As compared to macroalga species (*Eucheuma denticulatum*) with HHV value of around 16.03 to 18.07 MJ/kg after acid hydrolysis torrefaction (Teh et al., 2017), microalgae exhibit a higher HHV value which makes it potential as an alternative solid fuel. Furthermore, the *Chlorella* spp. microalgal biochar after acid hydrolysis wet torrefaction also presented better HHV performance compared to the microalgal biochar produced from pyrolysis with HHV of 23.0 MJ/kg (Wang et al., 2013), where this can be one of the approachable thermochemical conversion methods for the co-production of microalgal biochar for alternative fuel application. For the solid product obtained after acid hydrolysis torrefaction at 0.1 and 0.2 M of diluted sulphuric acid, the results show a decreasing trend in the energy yield compared to wet torrefaction without acid treatment. This is relative to the energy distribution to the liquid hydrolysate with increasing of total reducing sugar contents after torrefaction as further discussed in Section 4.2.8.

Table 4.7: Higher heating value (HHV) of (a) *C. vulgaris* ESP-31 and (b) *Chlorella* sp. GD after torrefaction under various operating conditions.[1]

Sample(s)	Torrefaction condition(s)	Hydrolysis medium	HHV (MJ/kg)	
			C. vulgaris ESP-31	*Chlorella* sp. GD
Raw microalgae	-	-	19.23 ± 0.06	21.26 ± 0.18
Torrefied biochar	160 °C, 10 min	DI water (blank)	23.56 ± 0.05	21.77 ± 0.31
		0.1 M H_2SO_4	25.15 ± 1.36	22.23 ± 0.10
		0.2 M H_2SO_4	30.56 ± 1.94	23.17 ± 0.13
	170 °C, 10 min	DI water (blank)	25.52 ± 0.30	23.15 ± 0.21
		0.1 M H_2SO_4	30.23 ± 0.17	24.47 ± 0.44
		0.2 M H_2SO_4	32.35 ± 0.26	25.32 ± 0.13
	170 °C, 5 min	DI water (blank)	23.82 ± 0.31	22.05 ± 0.17
		0.1 M H_2SO_4	28.92 ± 0.51	22.93 ± 0.37
		0.2 M H_2SO_4	31.23 ± 0.90	23.58 ± 0.17

[1] All the data are the mean of two independent experimental data sets.

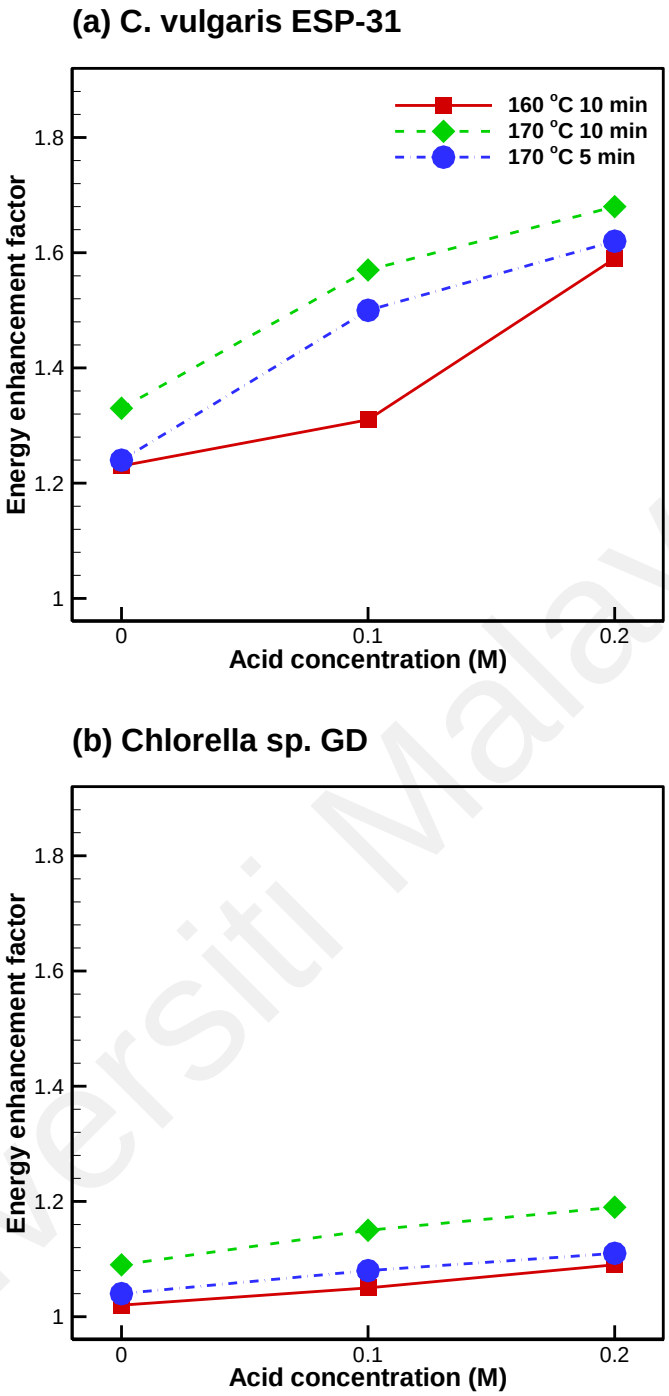

Figure 4.6: Energy enhancement factor of (a) *C. vulgaris* ESP-31 and (b) *Chlorella* sp. GD after torrefaction under various operating conditions.

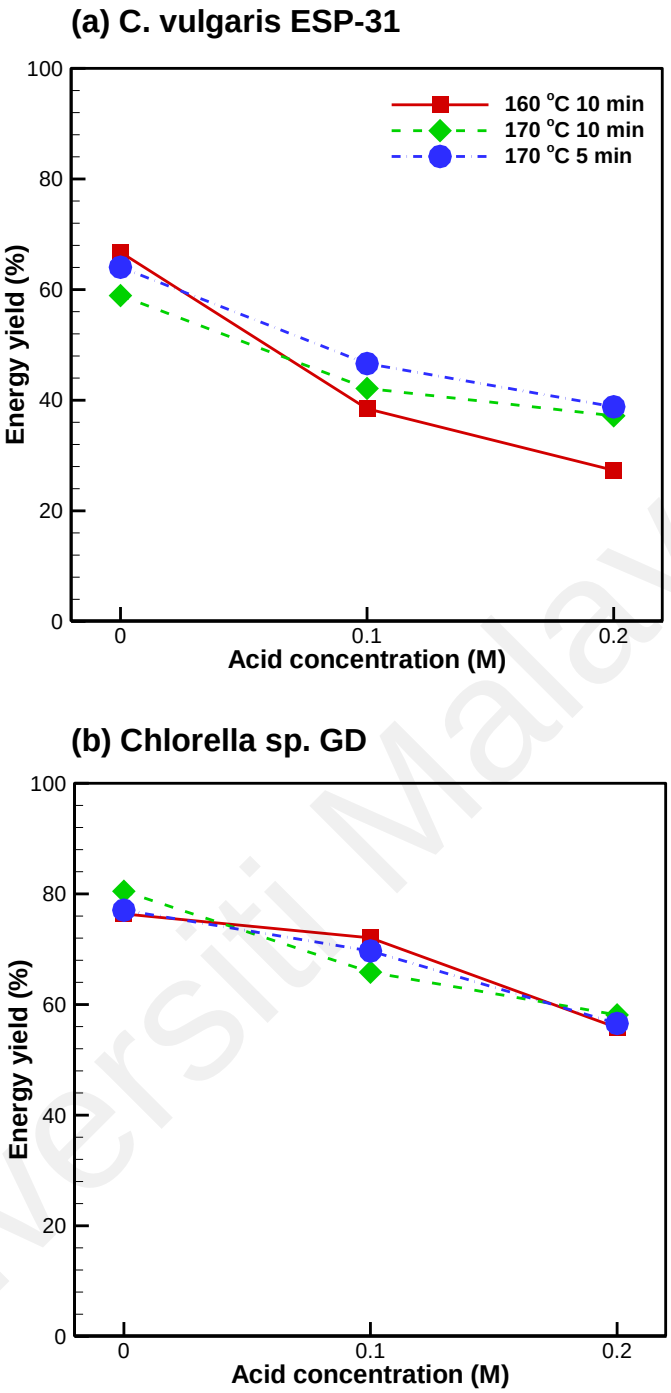

Figure 4.7: The energy yield of (a) *C. vulgaris* ESP-31 and (b) *Chlorella* sp. GD after torrefaction under various operating conditions.

4.2.5 Thermogravimetric analysis

Thermogravimetric analysis is employed to study the behavior of microalgae *C. vulgaris* ESP-31 and *Chlorella* sp. GD and their respective biochar before and after acid hydrolysis wet torrefaction. The derivative thermogravimetric (DTG) plot of the raw microalgae biomass and the biochars produced under each of the operating condition were shown in Figure 4.8 to determine the volatilization reaction occurred in the samples (Chaiwong et al., 2013). According to the DTG curves, dehydration occurs at the beginning at the temperature around 105 ℃. After that, the first stage reaction occurs between 105 and 300 ℃ which indicates the devolatilization and oxidative reactions of carbohydrates and protein components (Chen et al., 2014). The second stage reaction occurs at the temperature range of 300-450 ℃ which indicates the devolatilization and combustion of lipids components, follows with the third stage reaction of the effect on the combustion of char produced at higher temperatures (Bach et al., 2017; Chen et al., 2014). As observed in Figure 4.8, the peak temperatures of *C. vulgaris* ESP-31 biochar obtained after wet torrefaction in the first stage reaction are lower compared to the raw biomass, and vice versa for microalga *Chlorella* sp. GD biochar. This is due to the lower carbohydrate contents in torrefied *C. vulgaris* ESP-31 compared to the raw biomass, where the rich carbohydrate compounds have been transformed to produce total reducing sugar in the liquid hydrolysate under acid hydrolysis medium, making it an approach to bioethanol production (Ho et al., 2013). For *Chlorella sp.* GD biochar, the contrast trend as compared to *C. vulgaris* ESP-31 can be related to the higher solid yield and lower total reducing content in the hydrolysate as presented in Figure 4.4 and Figure 4.11, respectively. This may be due to the consequences of the low carbohydrate composition in the raw *Chlorella* sp. GD biomass, as presented in Table 4.5. For the reaction occurring at the temperature of around 800 ℃, this can be assumed on the decomposition of inorganic substances as similar to the study of macroalgae after acid hydrolysis

torrefaction (Teh et al., 2017). Overall, the weight loss occurs in the first stage reaction in terms of the decomposition of carbohydrates and proteins increase with acid concentration, however showing no significant differences in the increased intensity of wet torrefaction operating conditions of temperature and holding time. This can be assumed that acid concentration plays a significant role compared to temperature and holding time in the pretreatment to produce total reducing sugar under wet torrefaction for microalgal bioethanol production.

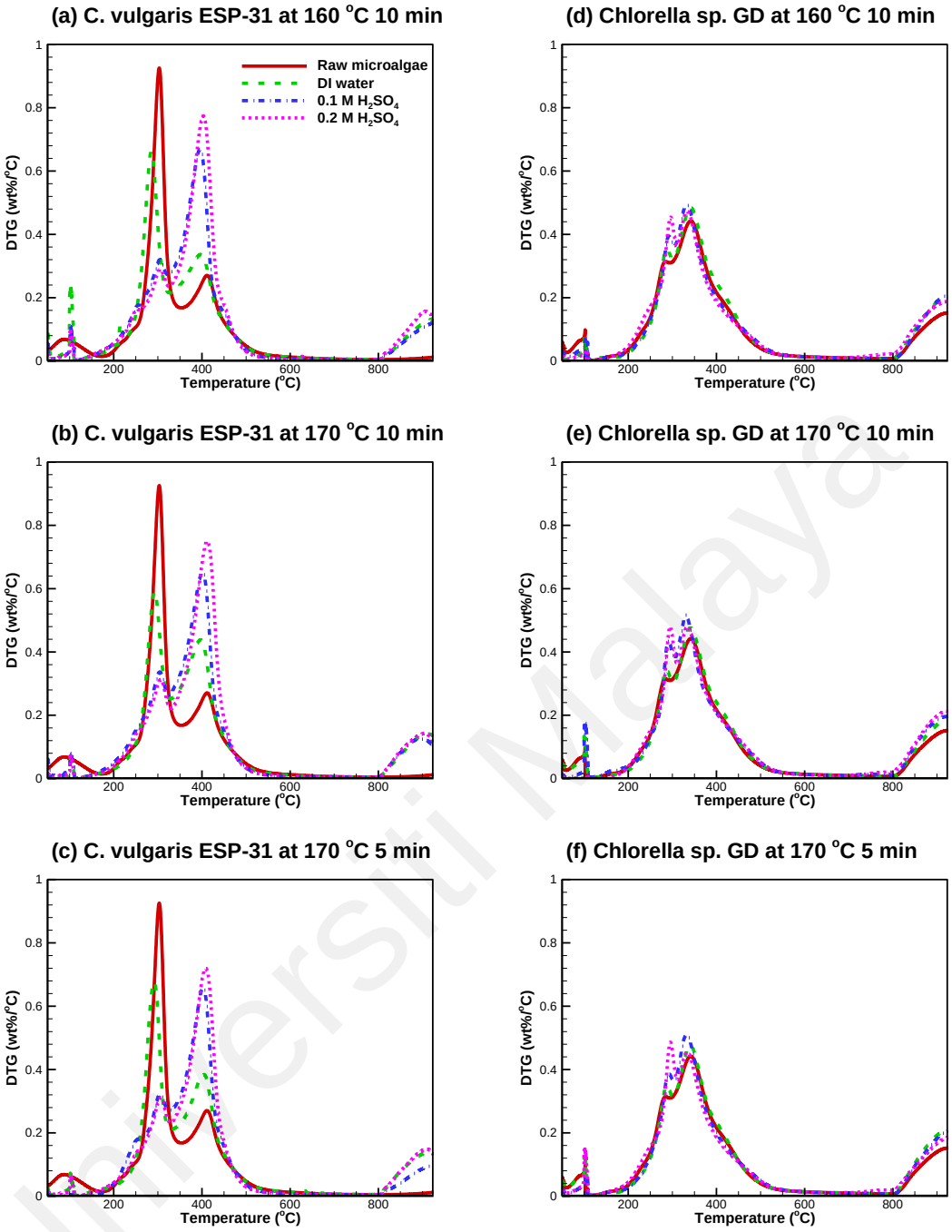

Figure 4.8: DTG curves for microalgae *C. vulgaris* ESP-31 and *Chlorella* sp. GD and the respective biochars produced in acid medium of 0, 0.1 and 0.2 M concentration under operating condition 160 °C with 10 min holding time (a,d), 170 °C with 10 min holding time (b,e) and 170 °C with 5 min holding time (c,f), respectively.

4.2.6 Fourier transform infrared (FT-IR) analysis

FT-IR can be used to examine the chemical composition and functional group contents of microalgal biomass, and the bond assignment of the chemical functional group relative to the biomass component in FT-IR spectra is shown in Table 4.8. A comparison of FT-IR spectra for *C. vulgaris* ESP-31 and *Chlorella* sp. GD raw microalgal biomass is presented in Figure 4.9. According to the FT-IR spectra obtained from both microalgae species derived biochars after wet torrefaction in the wavenumber range of 650-4000 cm^{-1}, the intensity peak at around 3270 cm^{-1} shows the presence of O-H hydroxyl groups in the biochars. There is an increase of the O-H hydroxyl functional group after wet torrefaction in the medium of 0.1 and 0.2 M of diluted sulphuric acid as compared to the raw biomass. This might be due to the acid pretreatment that causes apparent modification to the biochars contained with higher structural O content and increased alcohol character (Lawrinenko et al., 2015). The peak occurred at wavenumber 2800-3000 cm^{-1} determines the C─H stretching vibration from the lipid, whereas the peaks at around 1600-1400 cm^{-1} determine the C═O stretching vibration and N─H amide from protein. There is an increase in the peak intensities for microalgae *C. vulgaris* ESP-31 after wet torrefaction acid treatment compared to the raw biomass, which reflects the increase of the relative content of protein and lipid, derived by the consuming of carbohydrates. This observation is similar to the previous study done by Bach et al. (2017). It is also evident that there is an increase of carboxylic groups after wet torrefaction acid pretreatment which might increase the active sites and enhance the sorption capacity for biochars on soil and water application (Rajapaksha et al., 2016). However, there are no significant peak changes in the protein and lipid content of microalgae *Chlorella* sp. GD after wet torrefaction acid treatment might be due to the initial low composition of the carbohydrate content in the biomass.

Table 4.8: Bond assignment of chemical functional groups in microalgae in FT-IR spectra.

Wavenumber (cm^{-1})	Bond assignment
3600-3000	O─H hydroxyl group
2957, 2920, 2872, 2852	─CH_2 and ─CH_3 from fatty acids
1620, 1520	C═O and N─H of amide associated with protein
1455	─CH_3 and ─CH_2 of lipids and proteins
1160, 1086, 1050, 1036	C─O of carbohydrates

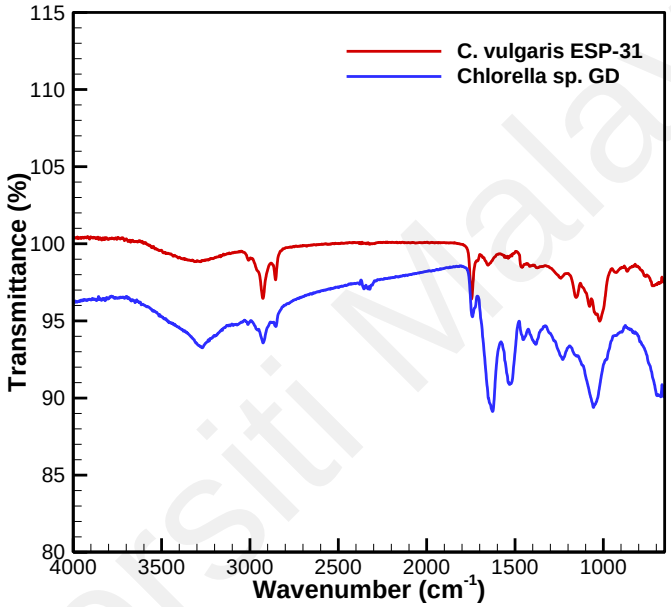

Figure 4.9: FT-IR spectra of *C. vulgaris* ESP-31 and *Chlorella* sp. GD raw microalgal biomass.

4.2.7 Scanning electron microscopy (SEM) observation

The scanning electron microscopy (SEM) images of the raw microalgae *C. vulgaris* ESP-31 and *Chlorella* sp. GD and their respective biochars after acid hydrolysis wet torrefaction are shown in Figure 4.10. For the two raw microalgae, a rough and globular agglomerate cellular structure is observed with the absence of cracks on the surfaces, as presented in Figure 4.10a and Figure 4.10c for microalgae *C. vulgaris* ESP-31 and *Chlorella* sp. GD, respectively. Undergoing the acid hydrolysis reaction with the acid

concentrations of 0.1 M and 0.2 M, the biochars exhibit a fragmented and porous structure after the wet torrefaction, as seen in Figure 4.10b and Figure 4.10d for microalgal biochars *C. vulgaris* ESP-31 and *Chlorella* sp. GD, respectively. As compared to the raw biomass, some tiny cracks and loopholes can be observed on the surfaces of biomass with the exertion of temperature and acid medium for the reaction. The porous structure can be due to the heat and acid reaction during wet torrefaction. With the noticeable porous structure on the surfaces of microalgal biochars, some active binding sites may occur which makes it potential for further application as bio-adsorbent in soil and water application (Gan et al., 2018; Yu et al., 2018; Zheng et al., 2017).

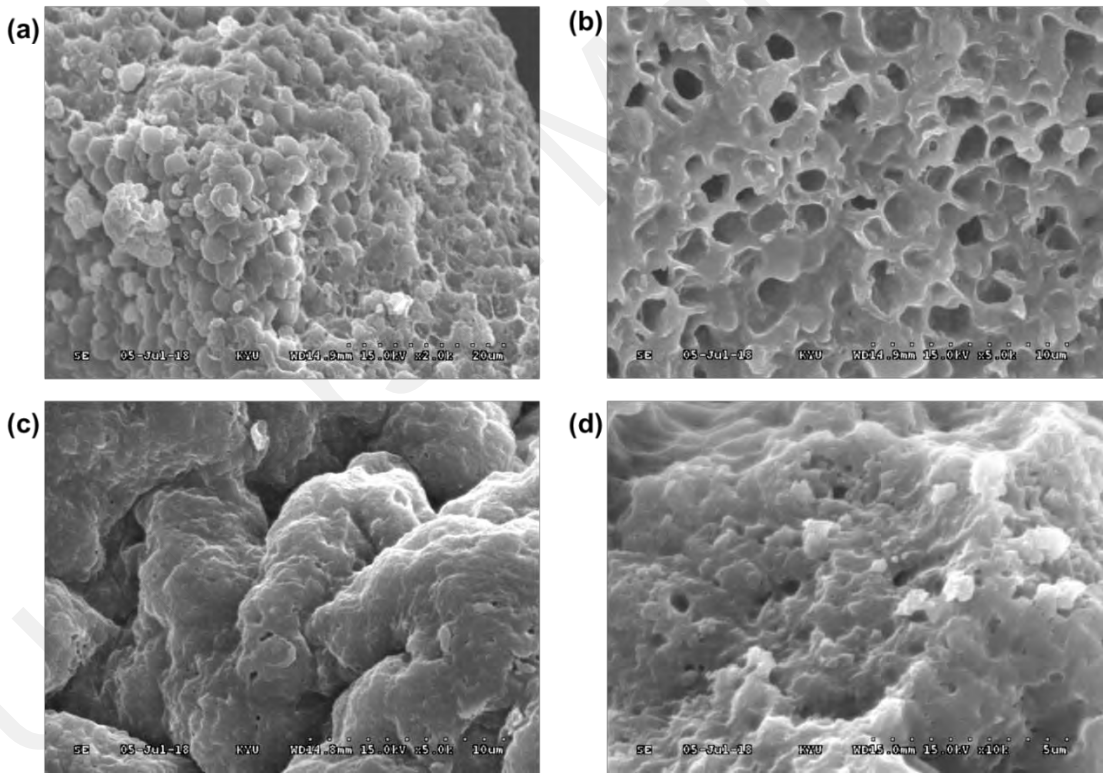

Figure 4.10: SEM images for microalgae (a) *C. vulgaris* ESP-31 raw biomass and (b) its respective biochar, (c) *Chlorella* sp. GD raw biomass and (d) its respective biochar after acid hydrolysis wet torrefaction at different magnifications (×2000 to ×10,000).

4.2.8 Hydrolysates

Simultaneous production of microalgal biochar and reducing sugar contained hydrolysate for fermentation of bioethanol can be achieved through wet torrefaction treatment. For further application in bioethanol production, the total reducing sugar content in the liquid hydrolysate after wet torrefaction is one of the important factors. In this study, diluted acid is used as the medium for acid hydrolysis pretreatment due to the possible occurrence of excessive degradation of substrates which will lead to the reduction of total reducing sugar yield (Paudel et al., 2017; Phwan et al., 2018). The total reducing sugar concentration in hydrolysates produced from pretreatment of microalga *C. vulgaris* ESP-31 (7.31-98.11 g/L) shows a higher yield ($p < 0.05$) compared to *Chlorella* sp. GD (1.08-12.08 g/L), as shown in Figure 4.11. As related to the high carbohydrates content in *C. vulgaris* ESP-31 that leads to a more reactive hydrolysis process towards the biomass, the hydrolysate also contains a high total reducing sugar after the treatment (Markou et al., 2013). Overall, the total reducing sugar concentration shows an increasing trend with increasing acid medium concentration from blank pure water to 0.1 M and 0.2 M of diluted sulphuric acid. In addition, the total reducing sugar concentration also increases with an increase of torrefaction intensity at temperature 170 °C and a prolonged holding time of 10 min. The relatively higher total reducing sugar content of *C. vulgaris* ESP-31 (7.31-98.11 g/L) showed a negative correlation ($r = -0.908$) with the relatively lower solid yield of *C. vulgaris* ESP-31 (17.2-54.5 wt%). In addition, the lower total reducing sugar content of *Chlorella* sp. GD (1.08-12.08 g/L) also showed a similar correlation ($r = -0.851$) with the higher solid yield of *Chlorella* sp. GD (48.8-74.6 wt%). This shows that an overall product energy distribution occurs according to the treatment reaction where the final solid and liquid product yields are correlated with each other. As a comparison to the previous literature on macroalgae (Teh et al., 2017), the total reducing sugar concentration of microalgae *C. vulgaris* ESP-31 obtained after the

acid hydrolysis wet torrefaction is higher compared to macroalgae (5.49-51.47 g/L), thus making microalgae with high carbohydrate content as one of the suitable feedstock for further bioethanol production. The produced hydrolysate with a high content of reducing sugars could be utilized for optimization on bioethanol production. Therefore, this study presents a conversion technology which may be applicable in the future to produce a value-added by-product and high-value biofuel.

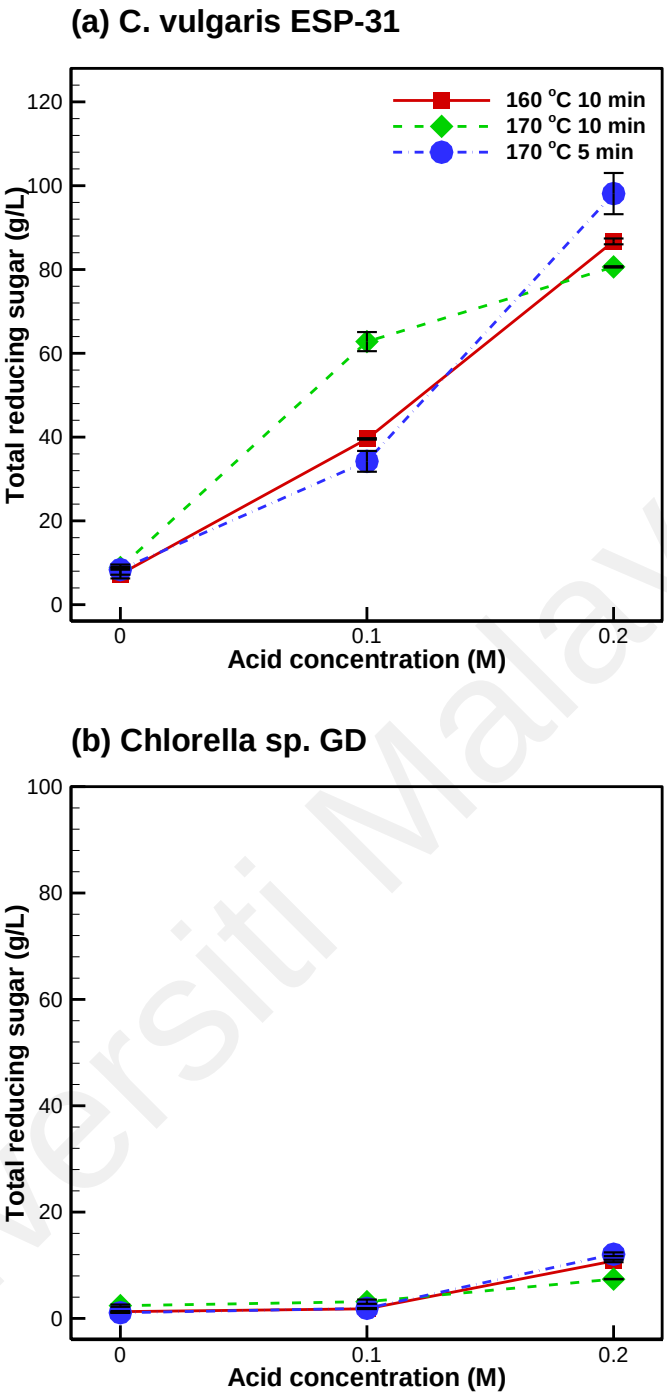

Figure 4.11: Total reducing sugar concentration of (a) *C. vulgaris* ESP-31 and (b) *Chlorella* sp. GD hydrolysate after acid hydrolysis under several operating conditions.[1]

[1] All the points are the mean of two independent experimental data sets and error bars indicate the standard deviation.

4.3 Bioethanol production from acid pre-treated microalgal hydrolysate using wet torrefaction

4.3.1 Components of microalgal biomass

The raw *Chlorella vulgaris* ESP-31 consisted of a large portion of carbohydrate content (57.50%) with components of protein (18.30%), lipid (15.38%), and other remaining components (8.82%). However, a large portion of protein content (59.75%) with components of carbohydrate (8.64%), lipid (7.86%), and other remaining components (23.75%) were found in the raw *Chlorella* sp. GD. Compared to other studies (Illman et al., 2000; Mata et al., 2010), microalga *C. vulgaris* ESP-31 showed a slightly high carbohydrate component where this is in good agreement with one of the previous studies (Ho et al., 2013), stating the carbohydrate-rich microalgae biomass may produce more reducing sugar after pretreatment and thus suitable as a feedstock for fermentation of bioethanol production. A comparison of the best viability of the two microalgae species based on their raw composition components can be determined towards the co-production of value-added energy products on biochar and bioethanol.

4.3.2 Effect of acid wet torrefaction on hydrolysates reducing sugar content

Microwave-assisted heating wet torrefaction was employed to carry out the acid hydrolysis pretreatment on the microalgal biomass to produce liquid hydrolysates and solid biochar concurrently. The microalgal hydrolysates with different total reducing sugar contents were obtained under various wet torrefaction operating conditions and shown in Table 4.9. Acid concentration is one of the significant pretreatment parameters for higher reducing sugar concentration in hydrolysate for further bioethanol production. Diluted sulphuric acid (H_2SO_4) was used in the acid hydrolysis reaction due to the extra H^+ ion for a more acidic medium which could lead to higher network disruption in the compounds with intra- and inter-chain hydrogen bonds while enhancing the hydrolysis efficiency (Abd-Rahim et al., 2014; Teh et al., 2017).

The result obtained was compatible with the assumption where the higher the acid concentration, the higher the concentration of total reducing sugar. The total reducing sugar and glucose concentration in microalgal *C. vulgaris* ESP-31 hydrolysate increased from 7.31 to 98.11 g/L and 3.302 to 81.27 g/L, respectively, when the acid concentration increased from 0 to 0.2 M under each of the wet torrefaction operating conditions. A similar trend could be seen in microalgal *Chlorella* sp. GD hydrolysate where the total reducing sugar increased from 1.08 to 18.29 g/L, and the glucose and galactose concentrations increased from 0.064 to 3.248 g/L and from 0.077 to 5.812 g/L, respectively, with the increase of the acid concentration from 0 to 0.2 M under each of the operating conditions.

The high concentration of glucose and low concentration of galactose in the microalgal hydrolysate of *C. vulgaris* ESP-31 after pretreatment showed a viable option for bioethanol production where the conversion of ethanol was depending on the fermentation of these fermentable sugars (Kadhum et al., 2019). Compared to the previous study on macroalgal hydrolysate with a range of 0.42-3.94 g/L (Teh et al., 2017), microalgal hydrolysate presented a higher glucose content ranging from 0.064 to 81.27 g/L, as shown in Table 4.9. It could be attributed to the recovery of reducing sugar from microalgal biomass under acid pretreatment using wet torrefaction was higher compared to macroalgae due to the smaller particle sizes and making it a suitable candidate for bioethanol production.

Table 4.9: Total reducing sugar concentration in microalgal hydrolysates after acid pretreatment under various wet torrefaction operating conditions.[1]

Torrefaction condition	Pretreatment medium	*C. vulgaris* ESP-31			*Chlorella* sp. GD		
		Total reducing sugar (g/L)	Glucose (g/L)	Galactose (g/L)	Total reducing sugar (g/L)	Glucose (g/L)	Galactose (g/L)
160 °C,	DI water	7.31	3.302	n.d.[2]	1.28	0.064	0.162
10 min	0.1 M H_2SO_4	39.57	6.190	0.072	1.81	1.041	0.195
	0.2 M H_2SO_4	86.71	81.27	n.d.	10.81	1.286	1.627
170 °C,	DI water	8.37	4.274	n.d.	1.08	0.067	0.077
5 min	0.1 M H_2SO_4	34.22	4.078	n.d.	1.91	0.089	0.115
	0.2 M H_2SO_4	98.11	80.40	n.d.	12.08	0.689	1.077
170 °C,	DI water	8.86	4.665	n.d.	2.41	0.095	0.081
10 min	0.1 M H_2SO_4	62.79	25.93	n.d.	3.16	1.737	0.908
	0.2 M H_2SO_4	80.62	56.64	n.d.	18.29	3.248	5.821

[1] All the points are the mean of two independent experimental data sets.
[2] n.d.: not detected.

4.3.3 Reducing sugar by-products after acid wet torrefaction

Other than reducing sugar, reducing sugar by-products such as 5-HMF can be obtained along with microwave-assisted heating wet torrefaction using dilute acids (Lee et al., 2020). The concentration of 5-HMF in microalgal hydrolysates after acid pretreatment under several wet torrefaction operating conditions is shown in Figure 4.12. The concentration of 5-HMF in *C. vulgaris* ESP-31 hydrolysate (2.41-11.63 g/L) was generally higher with $p < 0.05$ in comparison with *Chlorella* sp. GD hydrolysate (2.13-5.12 g/L) after torrefaction pretreatment. This might be due to the correlation ($r = 0.876$) between 5-HMF and the reducing sugar concentration as discussed in Section 4.3.2, where reducing sugar could be degraded into 5-HMF by-product during the torrefaction pretreatment. As the acid concentration increased from 0 to 0.2 M, 5-HMF showed an increasing trend under each of the wet torrefaction operating conditions. This can be explained by the higher the severity of acid hydrolysis wet torrefaction, the greater the degradation of reducing sugar in the formation of 5-HMF by-product (Zhang et al., 2017). In contrast to Figure 4.12b, the 5-HMF concentration in *Chlorella* sp. GD hydrolysate did not show an increasing trend with the increase of acid concentration to 0.2 M under the operating temperature of 170 °C with holding times of 5 min and 10 min. This can be assumed that further degradation of 5-HMF into other organic acids such as levulinic acid and formic acid might occur at the operating conditions with an acid concentration of 0.2 M or higher (Almeida et al., 2009; Jeong et al., 2012; Mutripah et al., 2014).

As a comparison to the previous study (Teh et al., 2017), the 5-HMF concentration obtained in the microalgal hydrolysate was higher (2.13-11.63 g/L) than that obtained in macroalgal hydrolysate (0.09-0.40 g/L). This will be a disadvantage where 5-HMF is a toxic inhibitor in the fermentation process for bioethanol production (Anburajan et al., 2018; Prasad et al., 2018). Leave aside the shortcoming in bioethanol production, 5-HMF is receiving significant attention and recognition as the top-priority chemical derived from

biomass through the chemical conversion of carbohydrates (Rout et al., 2016; Zhang et al., 2017). The wide application of useful bio-based chemical 5-HMF can be seen in the conversion of biofuel and other valuable organic substances as fuel additives, polymer, and resin precursors (Delbecq et al., 2017; Libra et al., 2011). Therefore, consequential consideration should also be carried out in the separation and recovery of 5-HMF from the production as a value-added by-product for utilization in other applications.

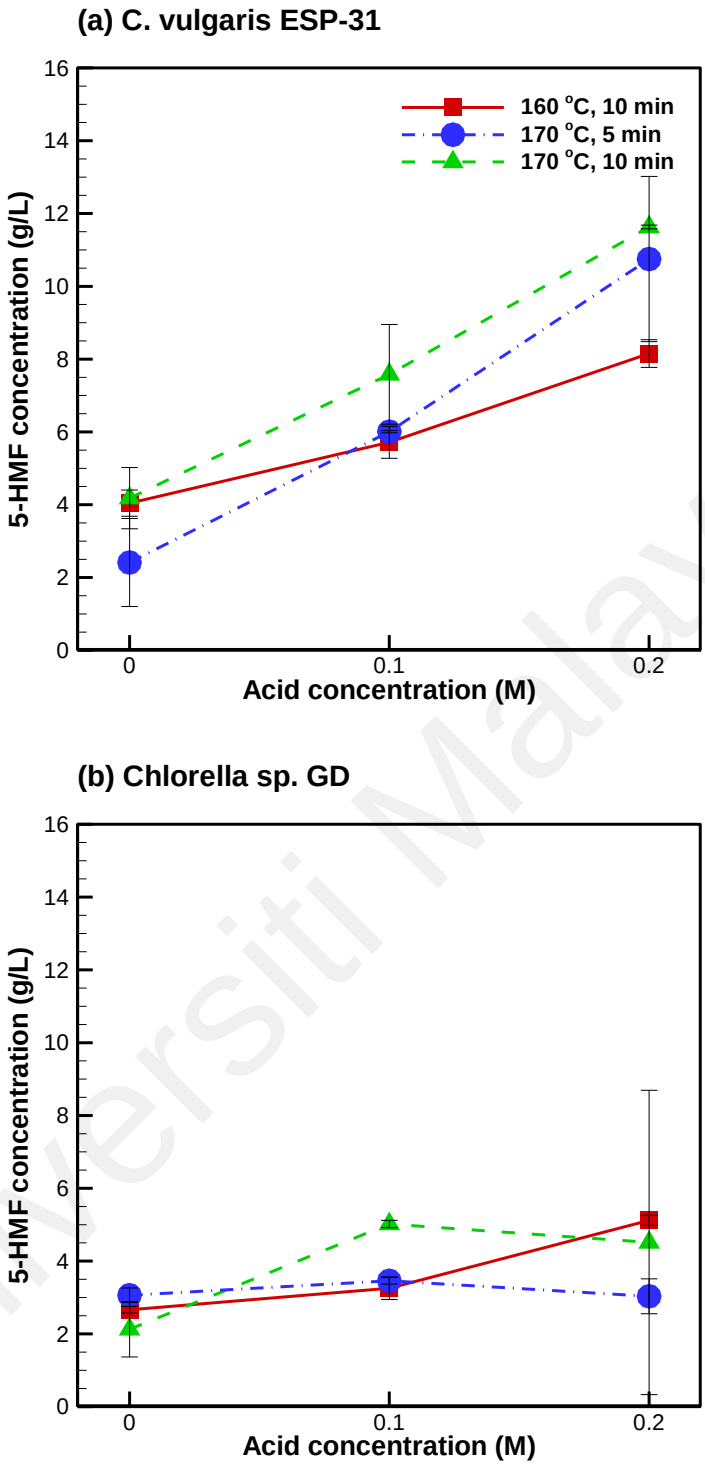

Figure 4.12: The concentration of 5-HMF in microalgal hydrolysates for (a) *C. vulgaris* ESP-31 and (b) *Chlorella* sp. GD after acid pretreatment under several wet torrefaction operating conditions.[1]

[1] All the points are the mean of two independent experimental data sets.

4.3.4 Total reducing sugar of hydrolysates before and after fermentation

The initial and final total reducing sugar concentrations in the *Chlorella* sp. GD and *C. vulgaris* ESP-31 microalgal hydrolysates were obtained throughout the fermentation process to investigate the total fermented sugar used to produce ethanol. Figure 4.13 and Figure 4.14 show the total reducing sugar concentrations in both microalgal hydrolysates over 120 h fermentation time under different pretreatment media. The total fermented sugar in both microalgal hydrolysates after acid pretreatment is presented in Figure 4.15. Overall, the total fermented sugar in *C. vulgaris* ESP-31 hydrolysates (5.14-32.79 g/L) is higher with $p < 0.05$ in comparison with *Chlorella* sp. GD hydrolysates (2.05-5.05 g/L). This might be attributed to the high carbohydrate composition in *C. vulgaris* ESP-31 where more fermentable sugars were produced in the hydrolysates during the acid pretreatment for bioethanol production (Ho et al., 2013). When the acid concentration of the hydrolysis medium increased, the total fermented sugar used for the conversion of bioethanol also increased. This is related to the final ethanol concentration obtained from the fermentation of microalgal hydrolysates as presented in Figure 4.16. From the result, an assumption can be made where the hydrolysates produced under a more severe hydrolysis pretreatment with the acid concentration of 0.2 M tend to play a better role in producing more fermentable sugar for bioethanol production. However, there is an unusual phenomenon for hydrolysate produced at the torrefaction condition of 170 °C, 10 min under 0.2 M acid medium for *C. vulgaris* ESP-31. There was no consumption of reducing sugar throughout the fermentation. This can be predicted by the overproduction of toxic inhibitor compounds such as 5-HMF and furfural during the pretreatment that leads to unfavorable fermentation conditions for bioethanol production (Prasad et al., 2018; Yu et al., 2017). Therefore, further investigation on the optimum conditions for acid pretreatment using wet torrefaction and its impact on the total reducing sugar and toxic inhibitors production in the hydrolysates can be carried out. Moreover, the removal

of inhibitors using charcoal powder can be also carried out to improve the bioethanol yield from the fermentation of hydrolysates (Zhang et al., 2019).

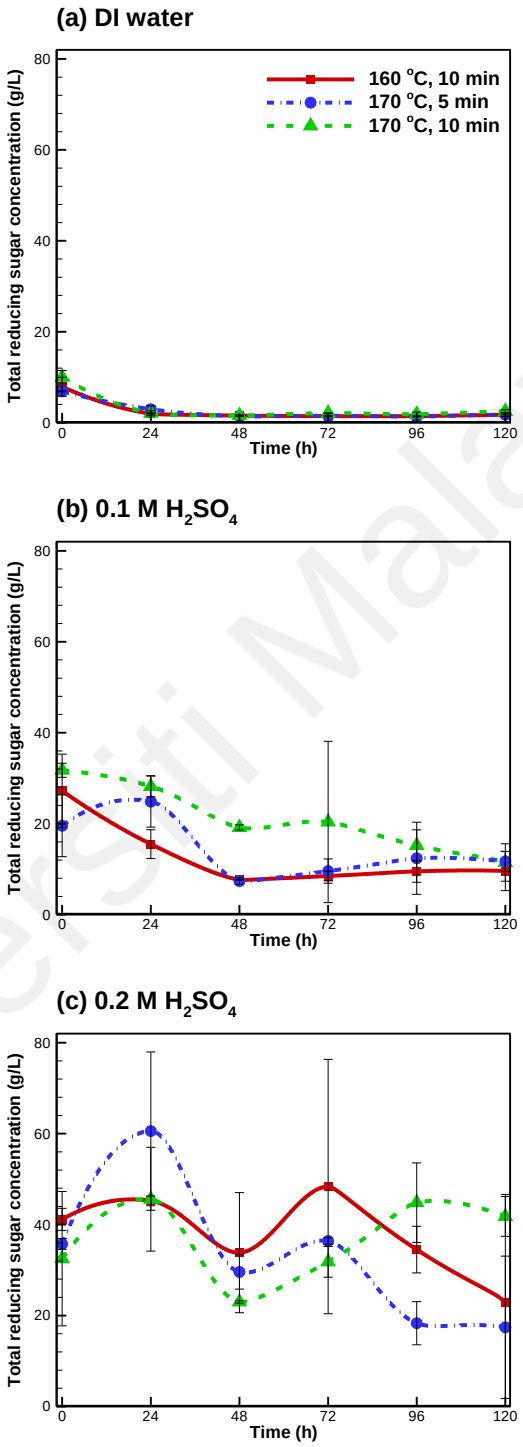

Figure 4.13: Total reducing sugar concentration in microalgal hydrolysates *C. vulgaris* ESP-31 over 120 h fermentation time under hydrolysis medium (a) DI water, (b) 0.1 M H_2SO_4 and (c) 0.2 M H_2SO_4.[1]

[1] All the points are the mean of two independent experimental data sets.

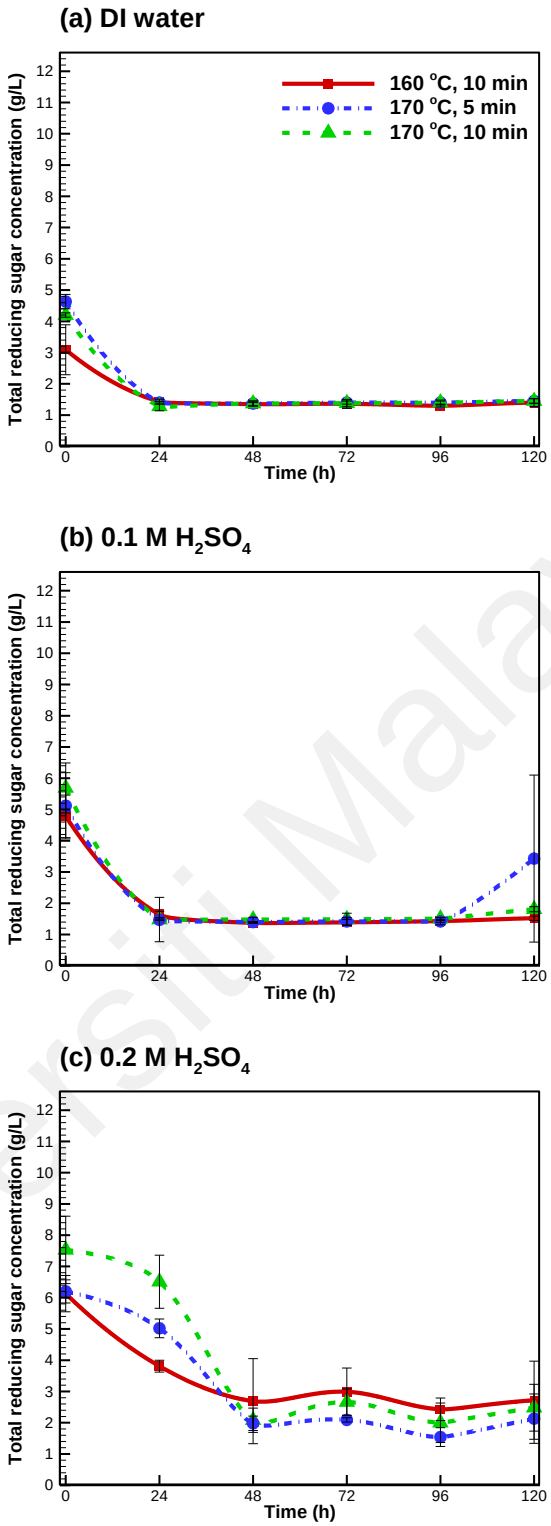

Figure 4.14: Total reducing sugar concentration in microalgal hydrolysates *Chlorella* sp. GD over 120 h fermentation time under hydrolysis medium (a) DI water, (b) 0.1 M H_2SO_4 and (c) 0.2 M H_2SO_4.[1]

[1] All the points are the mean of two independent experimental data sets.

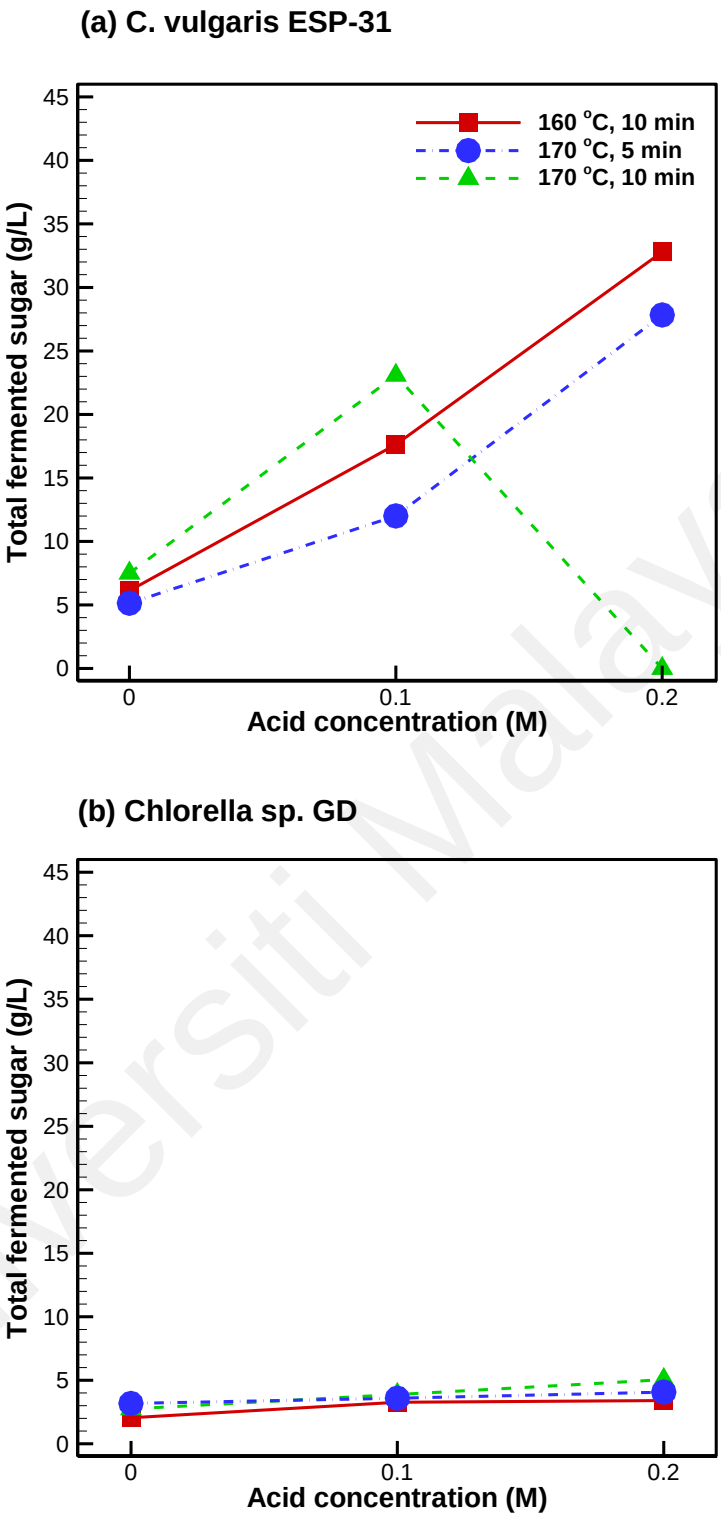

Figure 4.15: Total fermented sugar in microalgal hydrolysates for (a) *C. vulgaris* ESP-31 and (b) *Chlorella* sp. GD after acid pretreatment under several wet torrefaction operating conditions.[1]

[1] All the points are the mean of two independent experimental data sets.

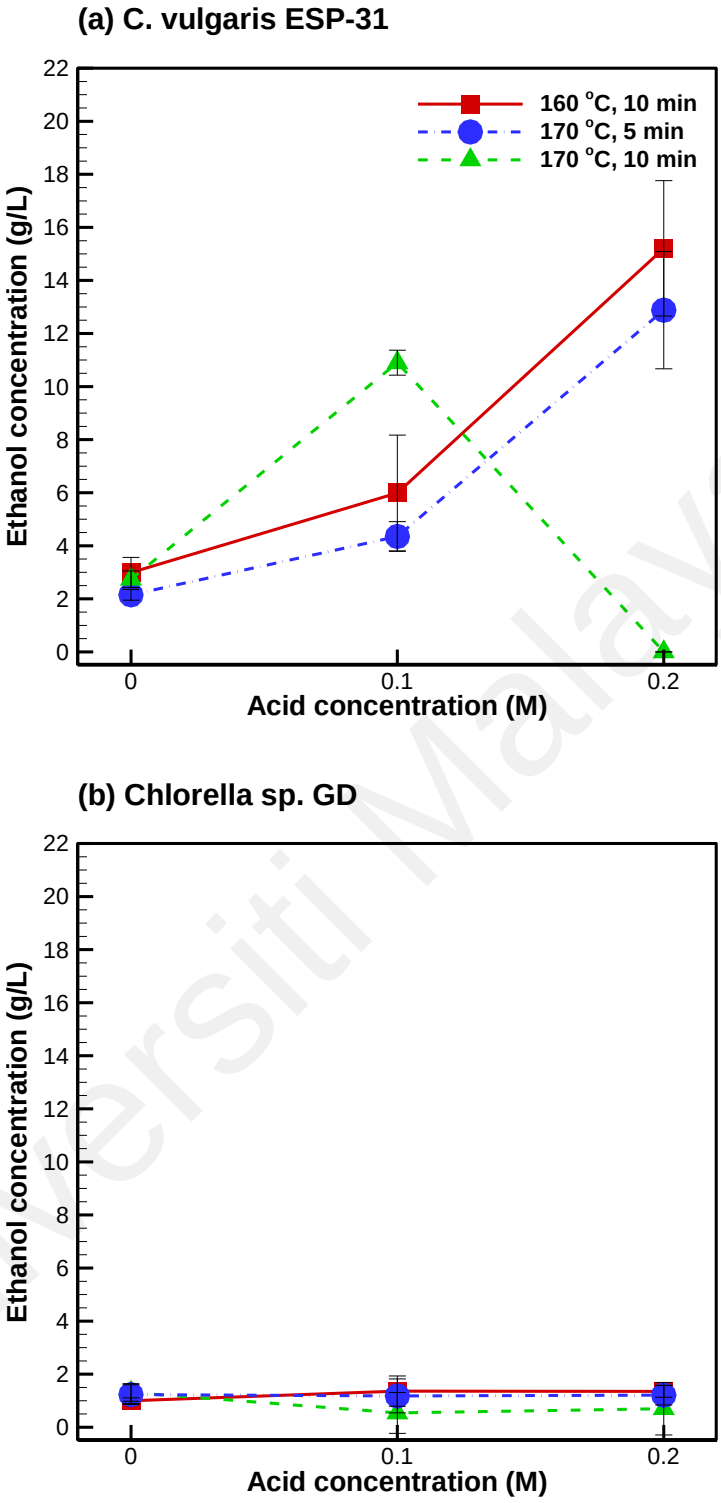

Figure 4.16: Ethanol concentration obtained from the fermentation of microalgal hydrolysates for (a) *C. vulgaris* ESP-31 and (b) *Chlorella* sp. GD produced under several acid wet torrefaction operating conditions.[1]

[1] All the points are the mean of two independent experimental data sets.

4.3.5 Bioethanol yield and productivity

The ethanol concentrations in the microalgal hydrolysates over 120 h fermentation time under several pretreatment media are presented in Figure 4.17 and Figure 4.18, respectively. The ethanol yield and productivity from the fermentation of two microalgal hydrolysates were calculated and presented in Table 4.10. Microalga *C. vulgaris* ESP-31 hydrolysates showed a higher ethanol yield ($p < 0.05$) range of 0.0107-0.0761 g ethanol/ (g microalgae) with a percentage yield of 1.07-7.61% in comparison with *Chlorella* sp. GD microalgal hydrolysates with an ethanol yield range of 0.0027-0.0068 g ethanol/ (g microalgae) which is equivalent to a percentage yield of 0.27-0.68%. As a relative, the ethanol productivity throughout the fermentation is also higher in *C. vulgaris* ESP-31 hydrolysates (0.018-0.127 g/L/h) compared to *Chlorella* sp. GD hydrolysates (0.005-0.011 g/L/h). In comparison to the previous study using different hydrolysis methods with ethanol yield up to around 0.08 g ethanol/ (g microalgae) (Eshaq et al., 2010; Wang et al., 2011), this study managed to show a maximum ethanol yield of 0.0761 g ethanol/ (g microalgae) from *C. vulgaris* ESP-31 microalgal hydrolysate. This shows that wet torrefaction pretreatment using dilute acids on *C. vulgaris* ESP-31 with carbohydrates-rich composition has an applicable performance from reducing sugar production towards the final bioethanol yield. An overview of the comparison of two microalgae species from the carbohydrates content to reducing sugar and the by-product concentration towards the final ethanol yield is shown in Figure 4.19. To obtain ideal ethanol productivity from the current study, further optimization and enhancement of the fermentation conditions such as pH, temperature, agitation rate, and the removal of inhibitors can be carried out to improve the performance of the overall microalgal bioethanol productivity (Harun et al., 2010; John et al., 2011; Láinez et al., 2019; Pejin et al., 2015).

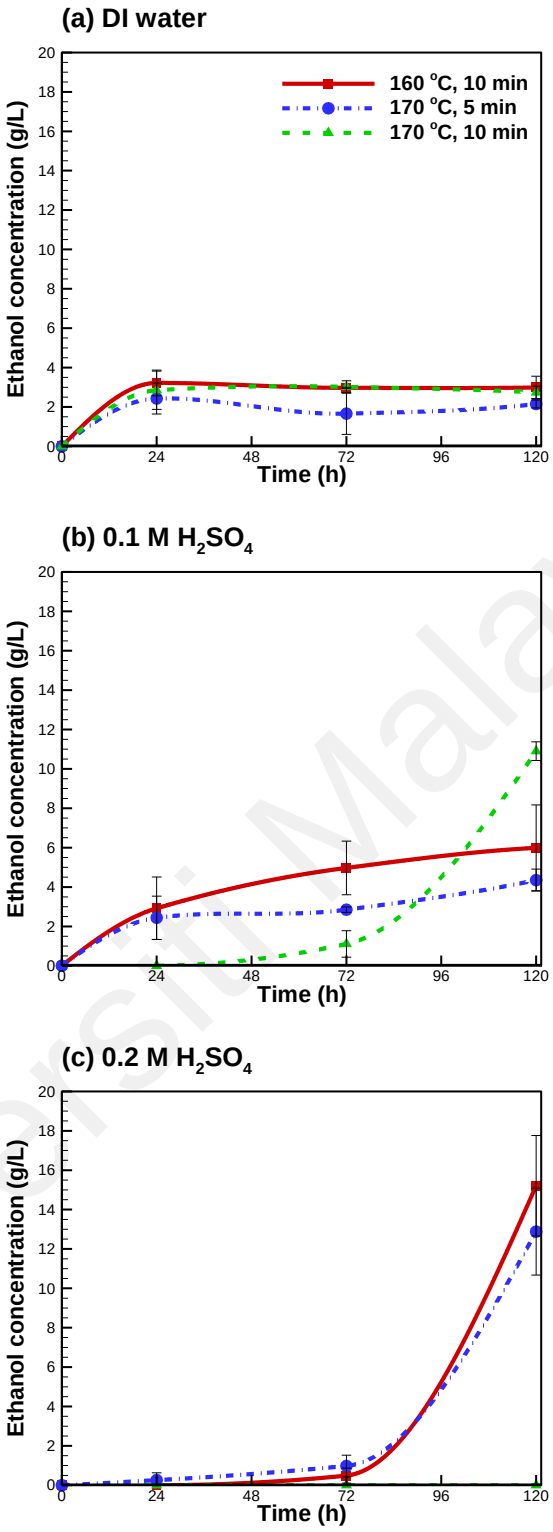

Figure 4.17: Ethanol concentration in microalgal hydrolysates *C. vulgaris* ESP-31 over 120 h fermentation time under hydrolysis medium (a) DI water, (b) 0.1 M H_2SO_4 and (c) 0.2 M H_2SO_4.[1]

[1] All the points are the mean of two independent experimental data sets.

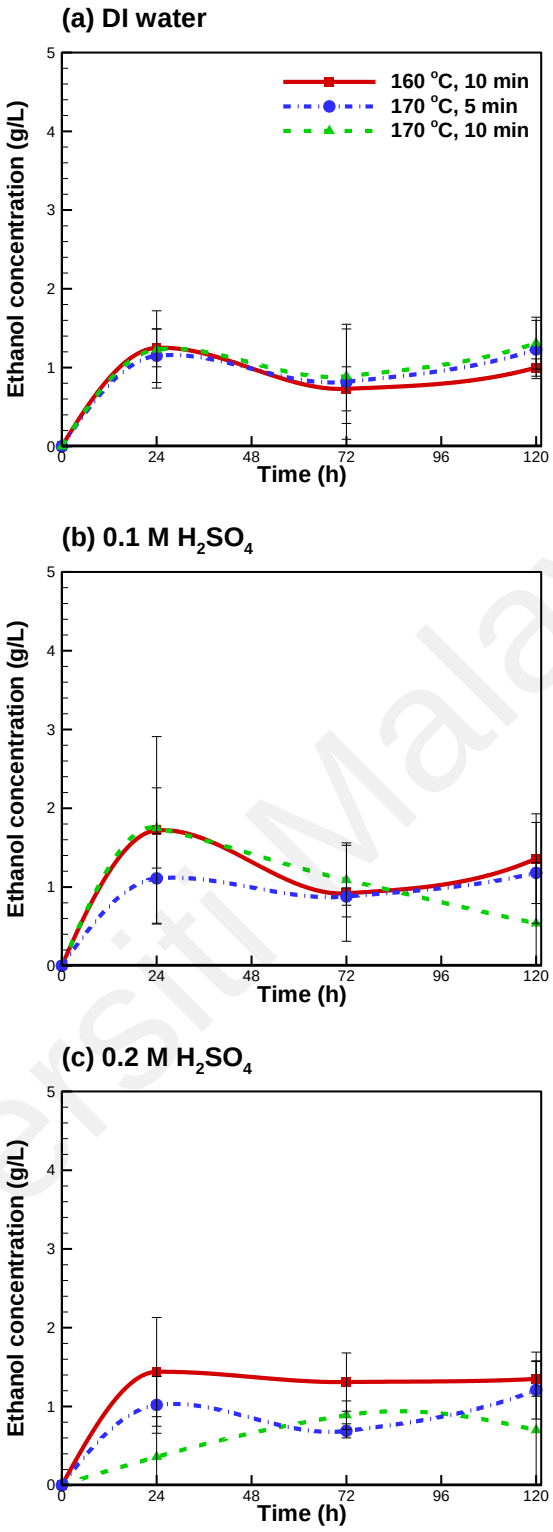

Figure 4.18: Ethanol concentration in microalgal hydrolysates *Chlorella* sp. GD over 120 h fermentation time under hydrolysis medium (a) DI water, (b) 0.1 M H_2SO_4 and (c) 0.2 M H_2SO_4.[1]

[1] All the points are the mean of two independent experimental data sets.

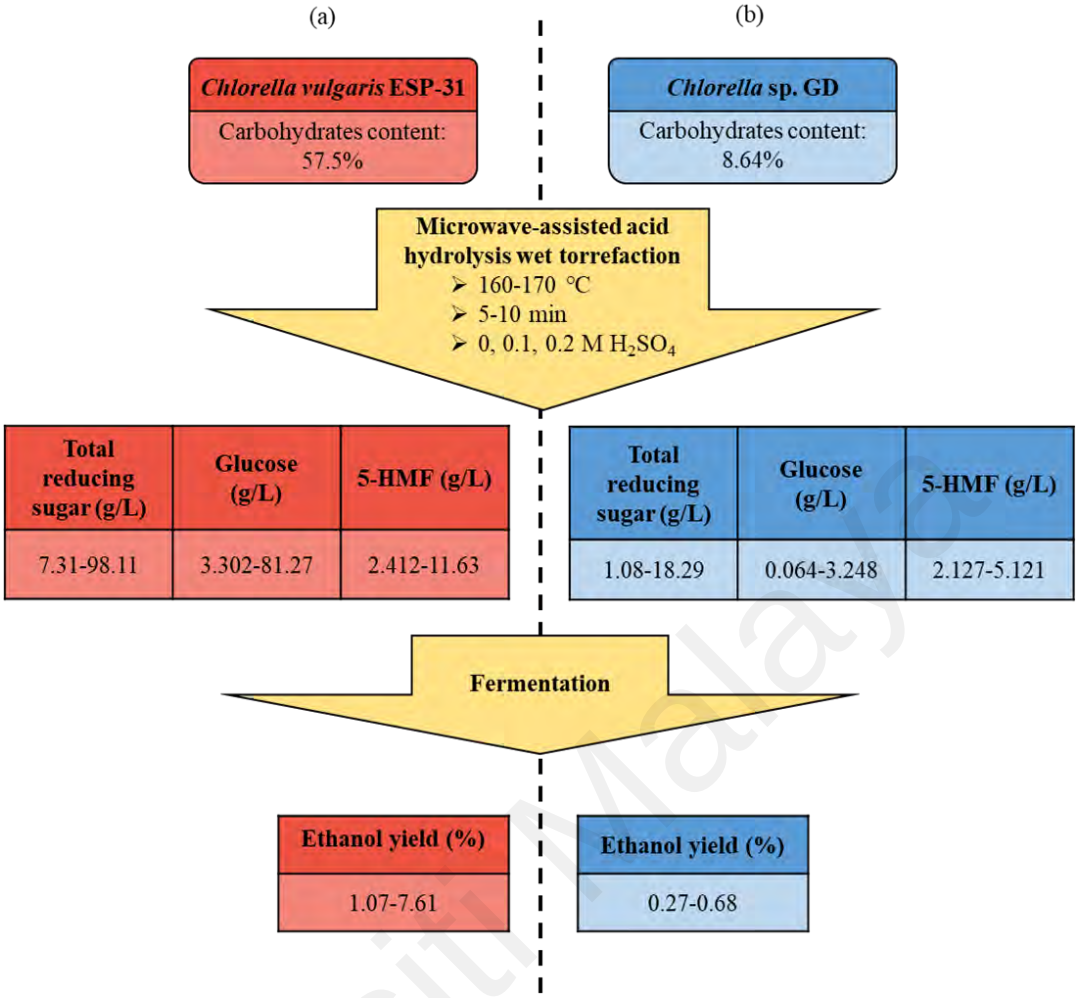

Figure 4.19: Overview of the comparison of (a) *C. vulgaris* ESP-31 and (b) *Chlorella* sp. GD from the carbohydrates content to reducing sugars and the by-product concentration towards the final ethanol yield.

Table 4.10: Ethanol yield and productivity from the fermentation of microalgal hydrolysates produced under several wet torrefaction operating conditions.[1]

Torrefaction condition	Pretreatment medium	*C. vulgaris* ESP-31			*Chlorella* sp. GD		
		Ethanol yield (g ethanol/ g microalgae)	Ethanol yield (%)	Ethanol productivity (g/L/h)	Ethanol yield (g ethanol/ g microalgae)	Ethanol yield (%)	Ethanol productivity (g/L/h)
160 °C,	DI water	0.0149	1.49	0.025	0.0050	0.50	0.008
10 min	0.1 M H_2SO_4	0.0299	2.99	0.050	0.0068	0.68	0.011
	0.2 M H_2SO_4	0.0761	7.61	0.127	0.0068	0.68	0.011
170 °C,	DI water	0.0107	1.07	0.018	0.0061	0.61	0.010
5 min	0.1 M H_2SO_4	0.0217	2.17	0.036	0.0059	0.59	0.010
	0.2 M H_2SO_4	0.0644	6.44	0.107	0.0060	0.60	0.010
170 °C,	DI water	0.0137	1.37	0.023	0.0066	0.66	0.011
10 min	0.1 M H_2SO_4	0.0545	5.45	0.091	0.0027	0.27	0.005
	0.2 M H_2SO_4	n.d.[2]	n.d.	n.d.	0.0035	0.35	0.006

[1] All the data are the mean of two independent experimental data sets.
[2] n.d.: not detected.

Table 4.11: Experimental and theoretical ethanol concentration and the relative experimental conversion probability after the fermentation of microalgal hydrolysates produced under several wet torrefaction operating conditions.[1]

		C. vulgaris ESP-31			*Chlorella* sp. GD		
Torrefaction condition	Pretreatment medium	Ethanol concentration[2] (g/L)	Ethanol concentration[3] (g/L)	Experimental conversion probability (%)	Ethanol concentration[2] (g/L)	Ethanol concentration[3] (g/L)	Experimental conversion probability (%)
160 °C,	DI water	2.99	3.14	95.22	1.00	1.05	95.17
10 min	0.1 M H_2SO_4	5.99	9.02	66.40	1.36	1.67	81.20
	0.2 M H_2SO_4	15.21	16.77	90.70	1.35	1.74	77.58
170 °C,	DI water	2.15	2.63	81.82	1.23	1.63	75.31
5 min	0.1 M H_2SO_4	4.35	6.14	70.81	1.18	1.84	64.36
	0.2 M H_2SO_4	12.88	14.23	90.49	1.21	2.08	58.02
170 °C,	DI water	2.74	3.83	71.50	1.31	1.41	93.21
10 min	0.1 M H_2SO_4	10.90	11.81	92.29	0.54	1.99	27.44
	0.2 M H_2SO_4	n.d.[4]	n.d.	n.d.	0.70	2.58	27.24

[1] All the data are the mean of two independent experimental data sets.
[2] Ethanol concentration from the experimental data.
[3] Ethanol concentration from the theoretical calculation.
[4] n.d.: not detected.

4.3.6 Bioethanol experimental conversion probability

The ethanol concentrations and the relative experimental conversion probability after the fermentation of microalgal hydrolysates produced under several wet torrefaction operating conditions are shown in Table 4.11. From the results, the ethanol experimental probability obtained from *C. vulgaris* ESP-31 was around 66.40-95.22% whereas for *Chlorella* sp. GD was around 27.24-95.17%. The ethanol experimental conversion probability from *C. vulgaris* ESP-31 hydrolysates was relatively higher with $p < 0.05$ in comparison with *Chlorella* sp. GD. This may be due to the larger fermentable sugar amount in the hydrolysates after acid pretreatment and hence the conversion of ethanol can be carried out more effectively (Alfonsín et al., 2019). Other than that, other unfavorable influence factors such as inhibitors in the fermentation environment that would lead to the low efficiency of ethanol conversion should also take into account where further optimization study can be carried out (Zhang et al., 2019). This study is in good agreement with similar literature on microwave-assisted acid hydrolysis using sago pith waste with a fermentation efficiency of 91% (Thangavelu et al., 2019), and thus showing an approachable conversion technique in utilizing microalgal biomass for efficient bioethanol production. Bioethanol production using microwave-assisted heating wet torrefaction for acid pretreatment can be a forthcoming development and cost-effective technology for future large-scale production with lower energy consumption and simple pretreatment using fast and efficient reaction under low temperature. In addition, the maximum ethanol concentration of *C. vulgaris* ESP-31 hydrolysates (15.21 g/L) is also in good agreement with the previous study of *Chlorella* sp. using acid pretreatment for maximum ethanol production of 11.66 g/L (Ho et al., 2013). The conversion of bioethanol utilizing microalgal hydrolysates with total reducing sugar using energy-efficient and simpler technology can be an approach in reducing the operating cost (David et al., 2020; Thangavelu et al., 2019). Furthermore, the co-production of

bioethanol and biochar from microalgal biomass by microwave-assisted heating wet torrefaction using dilute acids can be one of the feasible green technologies for future alternative energy applications (Javed et al., 2019; Teh et al., 2017).

4.4 Adsorptive removal of cationic and anionic dyes using wet-torrefied microalgal biochar

4.4.1 Wet-torrefied microalgal biochar adsorbent characterization

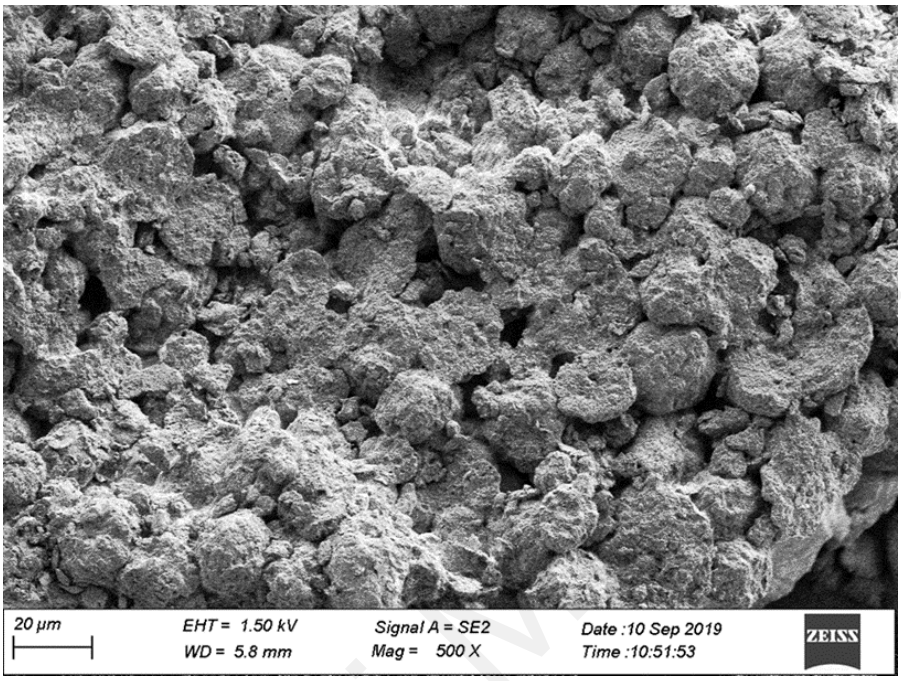

Figure 4.20: FESEM image of *Chlorella* sp. GD wet-torrefied microalgal biochar.

The residue of wet-torrefied biochar where *Chlorella* sp. GD with the high solid yield was further utilized as the adsorbent in the adsorption study for value-added application. The surface morphology of the wet-torrefied microalgal biochar was observed using a field emission scanning electron microscope (FESEM) under 500 × magnification and the image is shown in Figure 4.20. As seen in Figure 4.20, wet-torrefied microalgal biochar exhibited irregular porous structures with rough surfaces. Microalgal biochar with the noticeable coarse and porous surfaces may have provided some active binding sites for the dye adsorption (Gan et al., 2018; Yu et al., 2020). In addition, the surface structure of the adsorbent can be one of the important factors affecting the adsorption process which is correlated to the pore properties such as specific surface area.

The pore properties of the wet-torrefied microalgal biochar were characterized and shown in Table 4.12. The wet-torrefied microalgal biochar shows a BET surface area of 2.66 m^2/g and this is similar to the previous literature on microalgal biochars with a range from 2.1 to 15.0 m^2/g for p-nitrophenols adsorption (Zheng et al., 2017). With the pore diameter, *Chlorella* sp. GD wet-torrefied microalgal biochar can be considered as a microporous material with a pore diameter of <2 nm (Chowdhury et al., 2019). For the determination of dye adsorption capacity, the pore size of adsorbents and the structure of adsorbates will be contributing more than the surface area where the compounds will directly compete for adsorption sites in the accessible micropore region (Li et al., 2016; Pelekani et al., 2001). In addition, the wet-torrefied microalgal biochar also showed alternative potential applications on the natural gas treating or CO_2 capture by selective adsorption with the microporous pore structure (Tagliabue et al., 2009).

The determination of pH_{pzc} is also important to understand the electrostatic interaction mechanism and adsorption favourability by indicating the adsorption ability and active sites of the wet-torrefied microalgal biochar adsorbent (Zhang et al., 2011). The adsorbent is positively charged below pH_{pzc} and negatively charged above the pH_{pzc}. When $pH>pH_{pzc}$, it is favorable for the MB cationic dye adsorption; when $pH<pH_{pzc}$, it will be favorable for the CR anionic dye adsorption (Zhou et al., 2019). The pH_{pzc} value of wet-torrefied microalgal biochar is presented in Table 4.11 and the plot is shown in Figure 4.21.

Table 4.12: Properties of *Chlorella* sp. GD wet-torrefied microalgal biochar.

Properties	
pH_{pzc}	3.7
BET surface area (m^2/g)	2.6578
Total volume pore (cm^3/g)	0.000435
Average pore diameter (nm)	0.65484

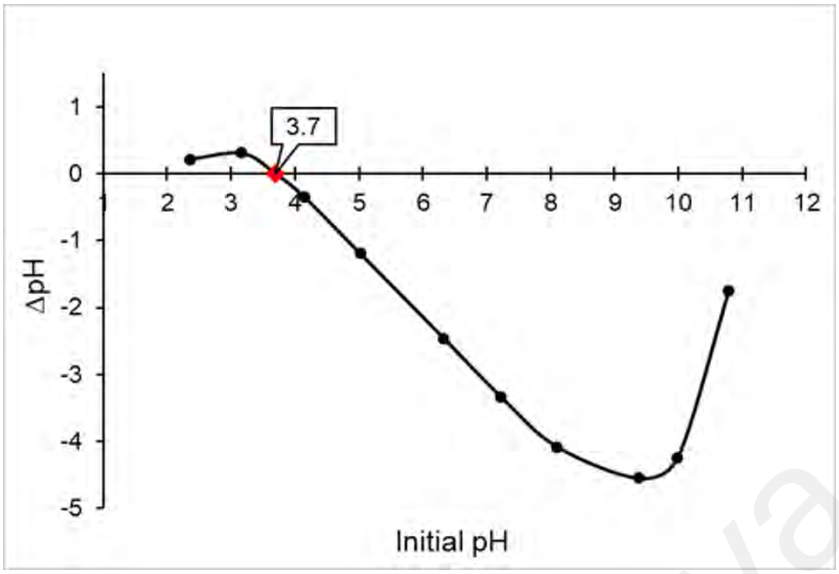

Figure 4.21: Point of zero charge plot for *Chlorella* sp. GD wet-torrefied microalgal biochar.[1]

4.4.2 Adsorption study

4.4.2.1 Effect of adsorbent dosage

The amount of biosorbent dosage can be regarded as one of the important parameters towards the cost-effective performance of batch adsorption study. Figure 4.22 shows the removal percentage and adsorption capacity of MB and CR dyes at different adsorbent dosages. The removal percentage of MB increased from 11.82% to 94.60% with increasing adsorbent dosage from 0.1 g/L to 5 g/L. For CR, the removal percentage increased from 2.16% at 0.1 g/L adsorbent dosage to the highest value of 98.01% at 3 g/L adsorbent dosage, and the removal percentage remains nearly constant after this point. This explains that the number of adsorbent particles increased with the increase of adsorbent dosage and led to the increasing of dye sorption site on the adsorbents (Lee et al., 2016). Other than that, the adsorption capacity decreased with the increasing adsorbent dosage where the adsorption capacity of MB decreased from 54.67 mg/g to 8.70 mg/g with the increase of dosage from 0.1 g/L to 5 g/L. For CR, the adsorption capacity showed the highest value of 34.89 mg/g at 1 g/L adsorbent dosage and the lowest

[1] All the data are the mean of three independent experimental data sets.

value of 9.61 mg/g at 5 g/L adsorbent dosage. The splitting effect of the concentration gradient between the adsorbent and dye adsorbates will be led to a less effective surface with the decrease of driving force towards the adsorption site when the amount of adsorbent increased at a fixed initial dye concentration and volume (Sun et al., 2008). Therefore by considering both the removal percentage and adsorption capacity, the optimum wet-torrefied microalgal biochar adsorbent dosage for MB is around 1 g/L with a removal percentage of 85.47% and adsorption capacity of 39.99 mg/g, while for CR is around 2 g/L with a removal percentage of 95.61% with an adsorption capacity of 23.77 mg/g.

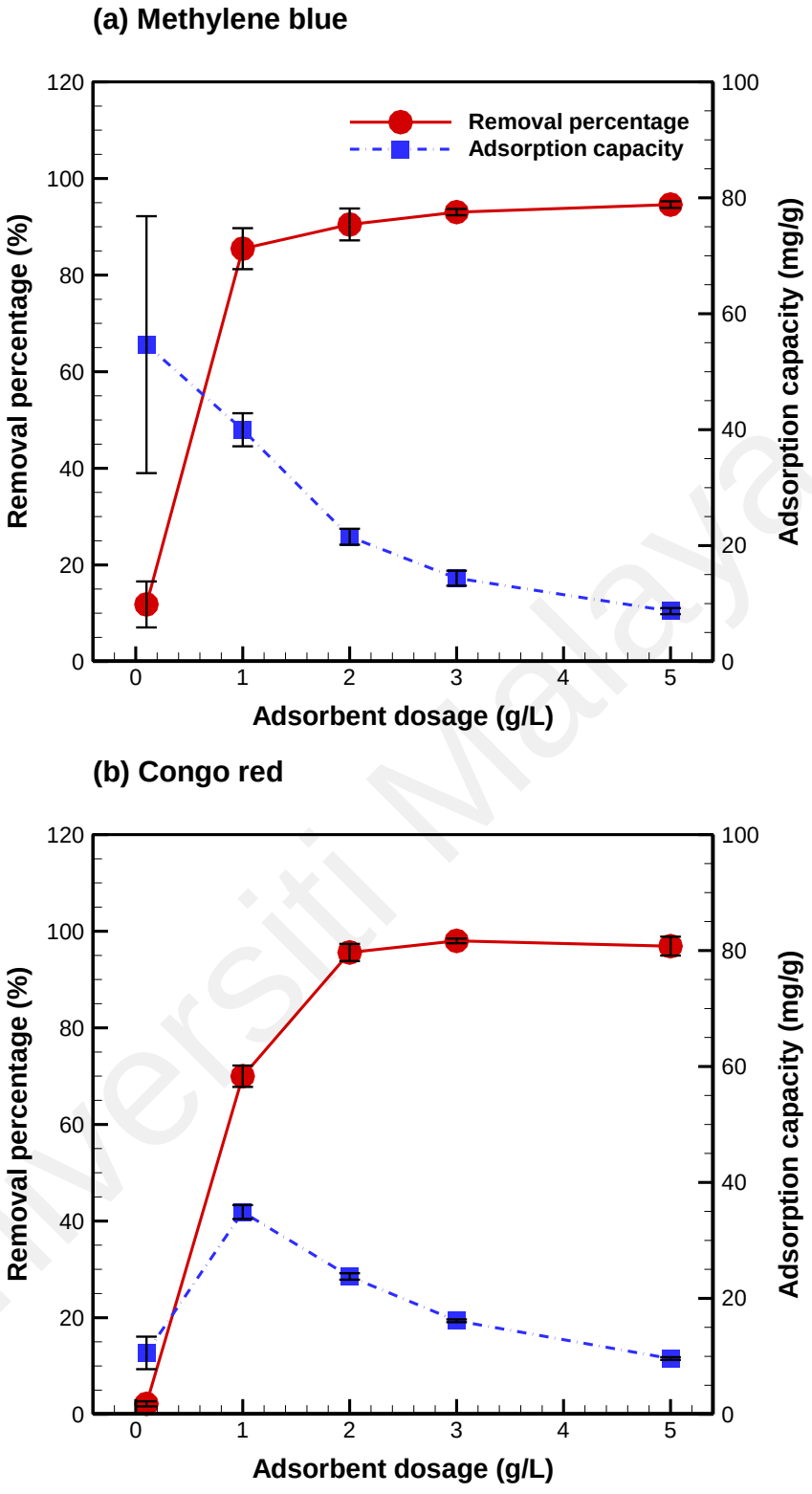

Figure 4.22: Removal percentage and adsorption capacity of (a) MB and (b) CR at different adsorbent dosages.[1]

[1] All the data are the mean of three independent experimental data sets and error bars indicate the standard deviation.

4.4.2.2 Effect of initial pH

Other than adsorbent dosage, another essential parameter in the adsorption process is the initial pH of the adsorbate solution with its effects on the surface condition for interaction between adsorbent and adsorbates (Zheng et al., 2017). In addition, the effects of pH on the adsorption of the dyes also can convey some features of the adsorption mechanisms. Figure 4.23 shows the removal percentage and adsorption capacity of MB and CR at different pH conditions with a control blank test. The result showed a minimal increasing trend in the removal percentage of MB from 93.25% to 94.46% when the pH increased from 2 to 10. For CR, the removal percentage increased from 94.52% to 99.22% when the pH increased from 2 to 8, and the lowest removal percentage of 90.18% was obtained at pH 10. The control test of MB showed no other influencing factors in the removal percentage at the pH range of 2 to 8 and this may be a suitable range for MB adsorption study. For CR, the adjustment of pH to range 2 to 4 might presents a great influence on the adsorption process. Since CR is a pH-sensitive dye and the exposure to HCl acid will cause the color change from red to blue as shown in Figure 4.24, this may affect the overall adsorption process where CR becomes cationic at the lower pH due to protonation (Ahmad et al., 2010). Thus, it is more suitable to control the pH at a range of 6 to 8 for adsorption of CR. With the natural pH for both MB and CR solutions that fall within the preferable adsorption range, operation of the MB and CR adsorption process at their natural pH conditions would be optimum with an approach towards cost-effective treatment without additional chemicals application in the process (Lee et al., 2015).

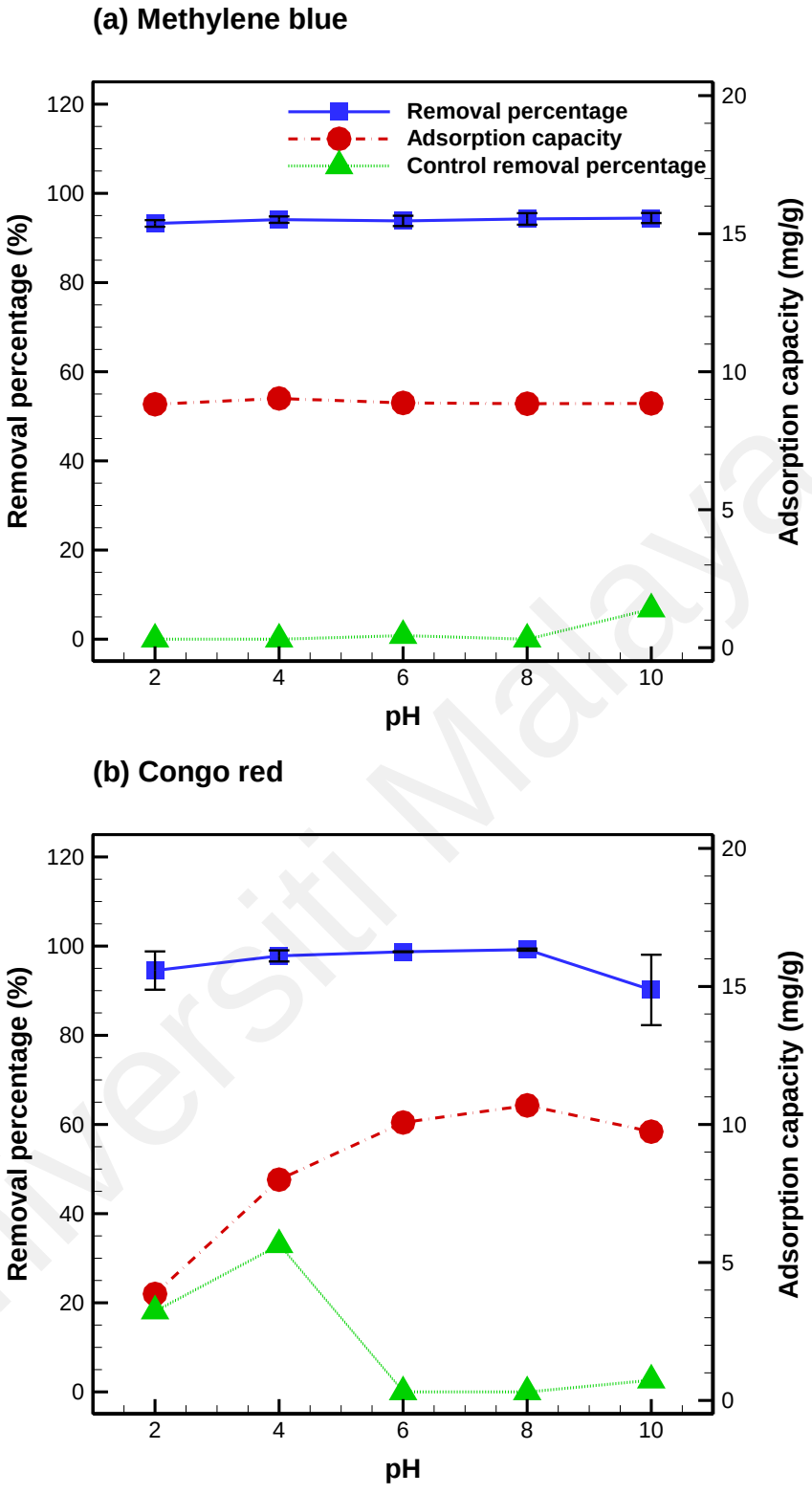

Figure 4.23: Removal percentage and adsorption capacity of MB and CR at different initial pH with control blank test.[1]

[1] All the data are the mean of three independent experimental data sets and error bars indicate the standard deviation.

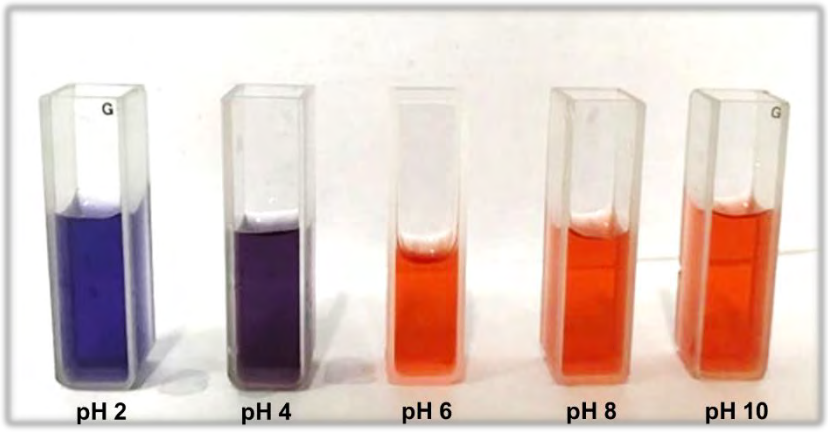

Figure 4.24: The color of CR dye solution at different pH conditions.

4.4.2.3 Effect of contact time

To determine the interaction of adsorbent and adsorbate until reaching the equilibrium state, contact time is the vital factor by providing an evaluation of the adsorbent properties in the adsorption system (Cui et al., 2015; Guo et al., 2019). The removal percentages of MB and CR dyes at different initial concentrations over time are shown in Figure 4.25 to study the effects of contact time and determine the equilibrium time for maximum dye adsorption by wet-torrefied microalgal biochar. Other parameter factors such as adsorbent dosage and initial pH for the dyes were kept at the optimum where the dosage for MB and CR dyes are 1 g/L and 2 g/L, respectively, under natural pH conditions. As seen in Figure 4.25, the removal percentages for both the MB and CR dye increasing with the increase of contact time until the passage of active sites gets occupied to attain equilibrium. The interactions of the dye with the adsorbent behaved uniformly with time until constant where the equilibrium time for the adsorption can be obtained as there is almost no further adsorptive removal reaction (Meroufel et al., 2013). The removal percentage of MB at an initial concentration of 5 ppm to 100 ppm reaching a plateau after a contact time of 120 h and this can be regarded as the equilibrium adsorption time for MB at low to middle concentration environment. For CR, the removal percentage reached the equilibrium state after 4h (240 min) at most of the concentrations. As a comparison,

the time needed for equilibrium adsorption using wet-torrefied microalgal biochar on CR is shorter compared to MB. This provides critical insight on the equilibrium time required for MB and CR, respectively, and could be subsequently applied for kinetics modelling.

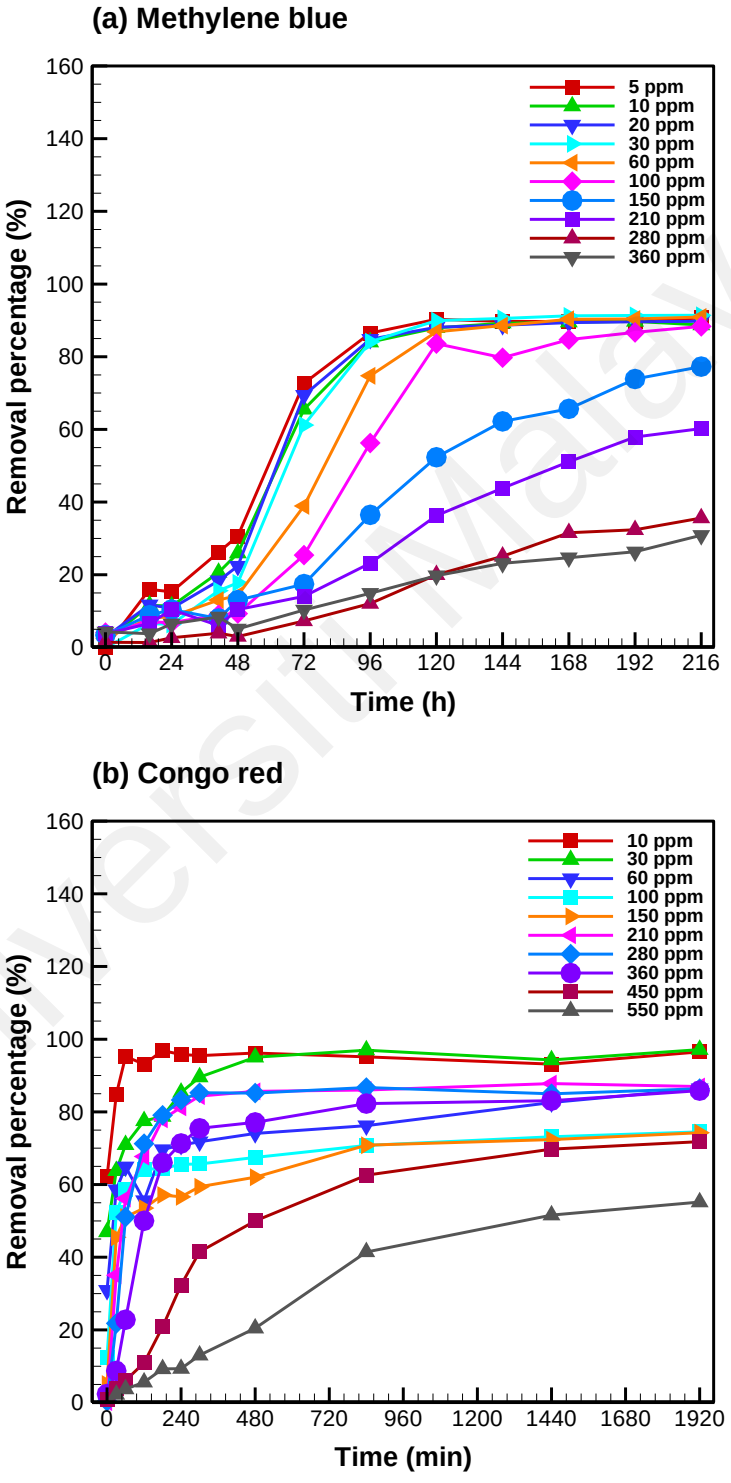

Figure 4.25: Removal percentage of (a) MB and (b) CR over the contact time.[1]

[1] All the data are the mean of three independent experimental data sets.

4.4.2.4 Effect of initial concentration

The initial concentration of the adsorbate plays an important role in its correlation to the availability of sorption sites on the adsorbent surface. In general, the percentage of removal decreases with the increase of initial concentration if the active site on the surface of adsorbent is saturated, whereas the percentage of removal increases with the increase of initial concentration if the active site is unsaturated where the high concentration will provide a large driving force for mass transfer towards adsorption (Eren et al., 2006; Zhou et al., 2019). As observed in Figure 4.26, the removal percentage of MB decreased from 89.78% to 26.32% with increasing of initial concentration from 5 ppm to 360 ppm. A similar trend is also obtained in the adsorption of CR where the removal percentage decreased from 97.10% to 54.72% when the initial concentration increased from 10 ppm to 550 ppm. In addition, the equilibrium adsorption capacity for MB and CR increases with increasing concentration until plateau as shown in Figure 4.27. The maximum equilibrium adsorption capacity obtained for MB is 113.00 mg/g at a concentration of 210 ppm, while CR is 164.35 mg/g at a concentration of 450 ppm. The availability of a sorption site is one of the rate-limiting factors which affects the equilibrium concentration of the adsorbate solution where the high initial concentration caused the saturation of the active site and resulting in lower adsorption capacity. A similar trend is also observed in the previous literature on biosorption of MB using de-oiled algal biomass and algae *Sargassum* sp. with a maximum monolayer adsorption capacity of 139.11 mg/g at 2000 ppm and 107.5 mg/g, respectively (Kumar et al., 2015; Maurya et al., 2014), where the adsorption of MB using wet-torrefied microalgal biochar in this study possesses a greater adsorption capacity compared to the previous study.

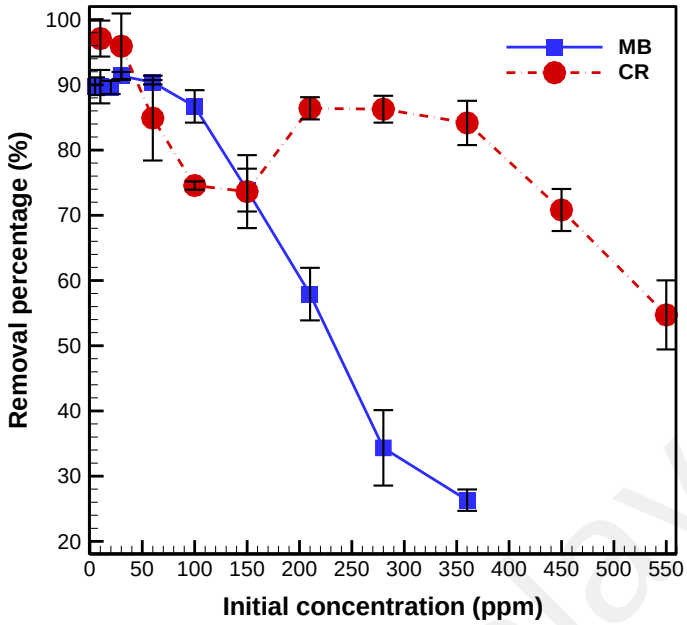

Figure 4.26: Removal percentage of MB and CR at different initial concentrations.[1]

[1] All the data are the mean of three independent experimental data sets and error bars indicate the standard deviation.

4.4.3 Adsorption modeling

4.4.3.1 Adsorption equilibrium isotherm

Three commonly used types of adsorption equilibrium isotherm models namely Langmuir, Freundlich, and Temkin were employed to study the adsorption mechanism of MB and CR with wet-torrefied microalgal biochar as the adsorbent. Langmuir isotherm model predicts that the outer surface of the adsorbent is homogeneous where the dye molecules have completely covered the adsorbent through monolayer formation with the access of only one molecule at a specific site (Li et al., 2016). The Freundlich isotherm model assumes that multilayer adsorption occurs on the uneven surface of the adsorbent and the Temkin isotherm model is used to describe the interaction between dye adsorbate and microalgal biochar adsorbents such as ion exchange and electrostatic attraction where the molecules in the layer will be decreasing in linear with coverage than logarithmic (Ali

et al., 2018). Table 4.13 shows the model parameters of each of the isotherm models with the value of R^2 showing the best model fitting.

As shown in Table 4.13, Langmuir isotherm showed a better model fit compared to Freundlich and Temkin for both MB and CR with R_2= 0.8977 and R_2= 0.9492, respectively, where the adsorption can be described as a monolayer coverage with the availability of adsorption site as the rate-limiting factor. This indicates that when the active site of the adsorbent is occupied by a molecule, no other molecules can be adsorbed onto the surface anymore (Ezzati, 2020; Hafeznezami et al., 2016). The finding is similar to a previous study on the adsorption of MB by modified bamboo hydrochar with the best fit on the Langmuir model (Qian et al., 2018). The previous study on the adsorption of CR using saffron corm also showed a similar finding as compared to this study (Dbik et al., 2020). Other than that, both of the hall separator factors (R_L) for MB and CR were in the range of $0 < R_L < 1$ and this indicates the adsorption process is favorable. Generally, the degree of favourability is related to the irreversibility of the adsorption system and this may provide the qualitative assessment of the interactions between microalgal biochar and both of the MB and CR dyes (Meroufel et al., 2013). The wet-torrefied microalgal biochar can be one of the suitable adsorbents for the adsorption of MB and CR dyes with rate-limiting factors on the availability of adsorption site after reaching equilibrium.

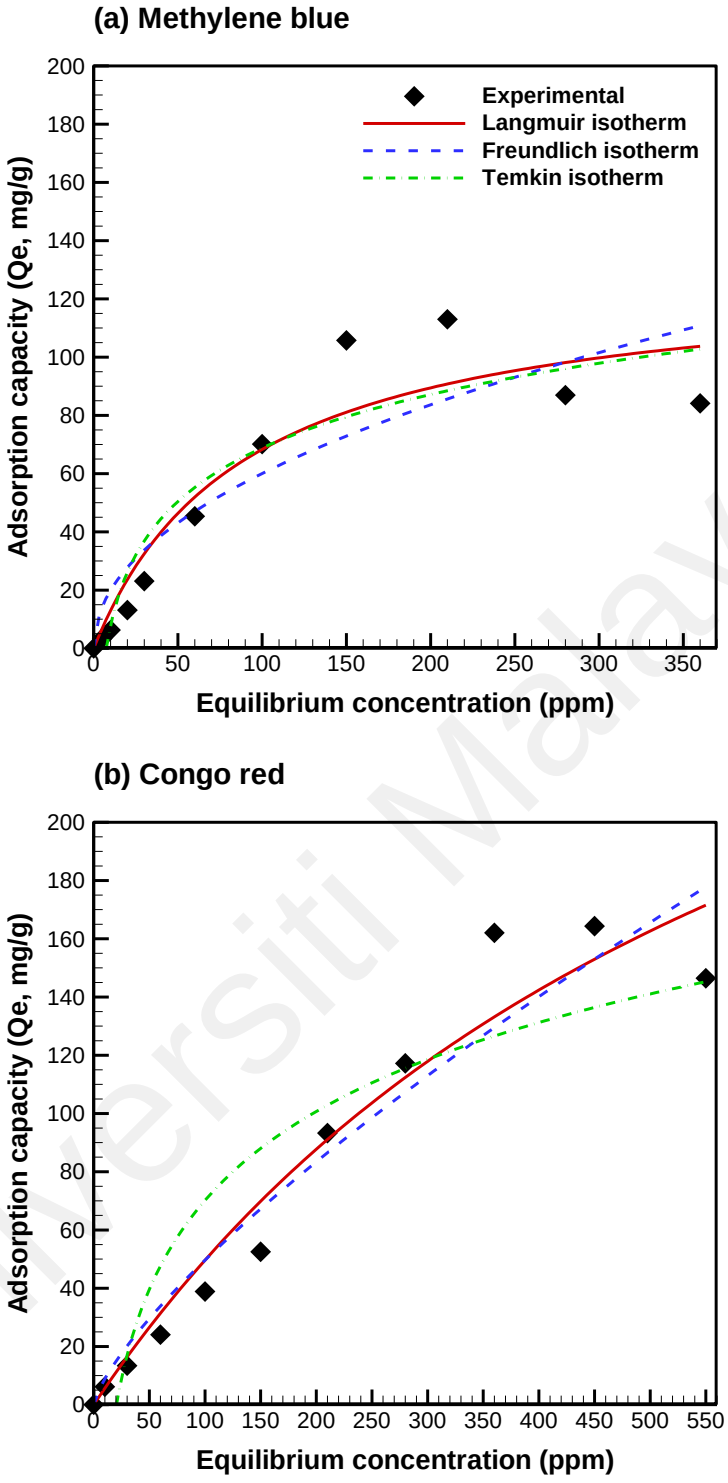

Figure 4.27: The adsorption capacity of (a) MB and (b) CR at different initial concentrations with equilibrium isotherm models fitting.

Table 4.13: Adsorption equilibrium isotherm models on methylene blue and Congo red using wet-torrefied microalgal biochar adsorbent.

Isotherm model	Model parameters	Methylene blue	Congo red
Langmuir	Q_m (mg/g)	129.57	377.67
	K_L (L/mg)	0.0112	0.0015
	R^2	0.8977	0.9492
	R_L	0.014-0.168	0.003-0.354
Freundlich	K_f ((mg/g)(L/mg)$^{1/n}$)	6.63	1.58
	n	0.4786	0.7486
	R^2	0.8177	0.9323
Temkin	B (J/mol)	37.22	22.39
	A (L/mg)	0.1342	0.0492
	R^2	0.8729	0.8465

4.4.3.2 Adsorption kinetics

Other than equilibrium isotherm, the adsorption kinetic is also one of the essential properties to evaluate the effectiveness of adsorbent through the adsorption rate and mechanism (Hafeznezami et al., 2016). To predict and determine the adsorption rate between MB and CR dyes with the wet-torrefied microalgal biochar, pseudo-first-order, pseudo-second-order, and Elovich models as the commonly used rate and diffusion kinetic models were employed with fitting to the experimental kinetic data. Pseudo-first-order kinetic model predicts the adsorption mechanism between the dye adsorbate and adsorbent based on the adsorbent capacity where the adsorption rate is proportional to the availability of active site (Lee et al., 2016). In addition, the pseudo-first-order kinetic model is normally applied at the beginning stage of the adsorption process. Pseudo-second-order kinetic model predicts the chemisorption mechanism over time until reaching an equilibrium state while Elovich kinetic model assumes the heterogeneous-based chemisorption process with the pure assessment of the kinetic behaviors (Guo et al., 2019). The adsorption kinetic models on MB and CR dyes using wet-torrefied

microalgal biochar adsorbent under several initial concentrations were presented in Table 4.14.

As shown in Table 4.14, the adsorption of MB at the initial concentration of 10 and 60 ppm showed the best fit to pseudo-first-order model with R^2 values of 0.9088 and 0.8996, respectively, while the adsorption of MB at the initial concentration of 100 ppm showed the best fit to pseudo-second-order model with an R^2 value of 0.8971. This shows that when the MB concentration at below 100 ppm does not affect the availability of active site with the proportional adsorption rate, while chemisorption process involving the electron exchange between the dye adsorbate and adsorbent as the rate-limiting step may have occurred at the MB concentration of 100 ppm and above (Wu et al., 2009). For CR, the adsorption at the initial concentration of 10 and 100 ppm showed the best fit to pseudo-second-order with R^2= 0.8785 and R^2= 0.9672. However, the CR adsorption at the initial concentration of 60 ppm showed the best fit to the Elovich model with R^2= 0.9358, and it can be assumed that the adsorption system was in the "mild rising" zone at a concentration around 60 ppm (Wu et al., 2009).

4.4.3.3 Adsorption mechanism

To study the adsorption mechanisms of MB and CR dyes with wet-torrefied microalgal biochar as the adsorbent, two types of mechanism models namely intraparticle diffusion and Boyd plots were employed with fitting to the experimental kinetic data. The intraparticle diffusion and Boyd models can be used to determine the rate-limiting steps and the transport mechanism of the adsorption process (Lee et al., 2016). The model parameter of intraparticle diffusion on MB and CR using wet-torrefied microalgal biochar adsorbent under several initial concentrations is presented in Table 4.14 and the Boyd plots of MB and CR under different initial concentrations are shown in Figure 4.28.

Table 4.14: Adsorption kinetic and mechanism models on methylene blue and Congo red using wet-torrefied microalgal biochar adsorbent under several initial concentrations.

Kinetic model	Model parameters	MB initial concentration (ppm)			CR initial concentration (ppm)		
		10	60	100	10	60	100
Pseudo-first-order	$Q_{e,exp}$ (mg/g)[1]	6.26	45.60	71.42	6.18	24.46	38.83
	$Q_{e,cal}$ (mg/g)[2]	7.66	73.05	120.33	5.99	20.12	35.38
	k_1 (1/h)	0.0101	0.0055	0.0046	63.5030	34.1553	2.7739
	R^2	0.9088	0.8996	0.8902	0.8476	0.5982	0.9156
Pseudo-second-order	$Q_{e,cal}$ (mg/g)[2]	12.08	138.92	398.83	6.02	20.43	36.66
	k_2 (g/(mg h))	5.30E-04	1.98E-05	2.92E-06	17.9418	1.8019	0.1621
	R^2	0.8980	0.8965	0.8971	0.8785	0.6546	0.9672
Elovich	β (g/mg)	0.6839	0.0956	0.0647	3.6192	0.5091	0.2462
	α (mg/(g h))	0.3820	2.1888	3.0453	1.29E+08	1.16E+04	3.55E+03
	R^2	0.6838	0.6069	0.5511	0.7296	0.9358	0.9107
Intraparticle diffusion	k_p (mg/(g $h^{0.5}$))	0.4621	3.1273	4.5729	0.2037	2.0828	3.6052
	C_i (mg/g)	1.00E-16	1.00E-14	7.25E-16	5.31	14.10	23.08
	R^2	0.8260	0.7808	0.7452	0.1969	0.6829	0.4317

[1] $Q_{e,exp}$ – Experimental maximum equilibrium adsorption capacity
[2] $Q_{e,cal}$ – Calculated equilibrium adsorption capacity from the equation

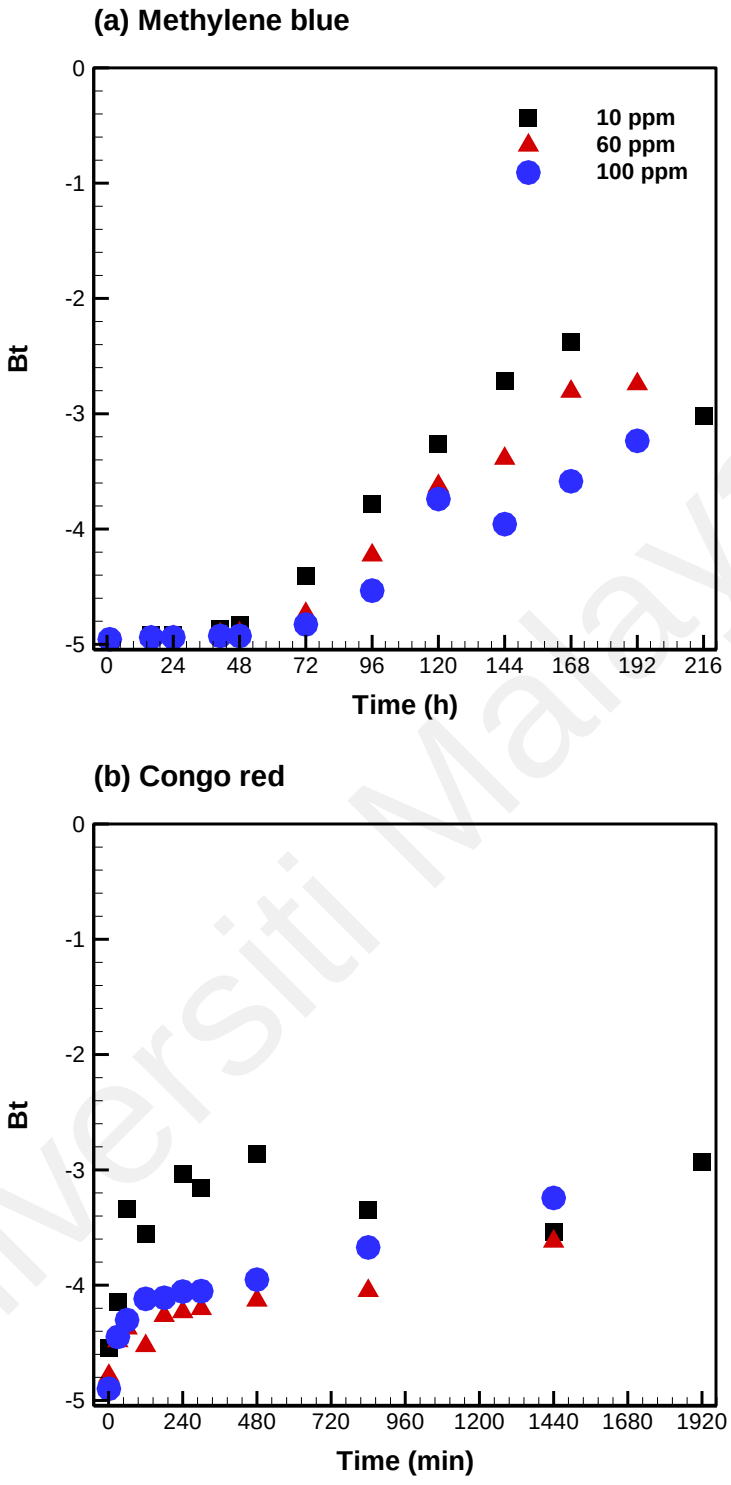

Figure 4.28: Boyd plot of (a) MB and (b) CR under different initial concentrations.

For the intraparticle diffusion mechanism model on MB adsorption, the C_i value (Table 4.14) presented an almost zero value and this indicated the rate is controlled by intra-particle diffusion with the linear plot passing through the origin (Chowdhury et al., 2010). As a contrast, the adsorption of CR showed the C_i value not equal to zero which depicted

a plot not passing through the origin and this could be assumed that the adsorption rate might be limited by two or more steps with the existence of other possible mechanisms such as complexation, diffusion boundary layer, or ion-exchange (Lee et al., 2016; Ozcan et al., 2005). Furthermore, the Boyd plot as shown in Figure 4.28 can be used to predict other rate-controlling steps for the MB and CR dyes adsorption process. Both of the Boyd plots for MB and CR under several initial concentrations did not pass through the origin and this assumes that external mass transfer can be a rate-determining step throughout the adsorption (Lee et al., 2014; Nethaji et al., 2013). As a reference to future modeling and application of wet-torrefied microalgal biochar on dye adsorption, the parameter of initial concentration should be taken into account with the adsorption diffusion rate for better performance in the adsorption system.

4.4.4 Comparison of wet-torrefied microalgal biochar adsorption performance with existing adsorbents

To highlight the strength features of wet-torrefied microalgal biochar in this study, the production of microalgal biochar using wet torrefaction possessed some advantages in term of energy efficiency with the short reaction time (5-10 min) and low-temperature range (160-170 °C) with microwave-assisted heating compared to the conventional pyrolysis (Yu et al., 2020). In addition, no additional drying process is required for processing the microalgae slurry biomass in biochar production through wet torrefaction (Bach et al., 2017). Therefore, this can be an environmental approach with the lower processing cost and utilization of biochar waste derived from the wet torrefaction process for adsorption application (Liew et al., 2018). Table 4.15 shows the comparison of several adsorbents on MB and CR dyes removal adsorption performance. The wet-torrefied microalgal biochar achieved a better adsorption performance for MB with a maximum adsorption capacity of 113.00 mg/g and removal percentages of 26.32-89.78% compared to the oil palm waste biochar produced from microwave pyrolysis (Kong et al., 2019;

Liew et al., 2018). Furthermore, the adsorption performance of CR using wet-torrefied microalgal biochar possessed a maximum adsorption capacity of 164.35 mg/g with removal percentages of 54.72-97.10%, which is slightly higher compared to other similar adsorbents such as microwave-steam activated orange peel waste biochar (Yek et al., 2020). The wet-torrefied microalgal biochar in this study also showed a similar pseudo-second-order kinetics model for CR adsorption analysis with adsorbents such as coffee waste activated biochar and low-rank coal where the adsorption capacity is based on solid phase and the removal of dye is due to the physicochemical interactions between adsorbent and adsorbate (Ausavasukhi et al., 2016; Ho et al., 1998; Lafi et al., 2019). With all the comparisons, the wet-torrefied microalgal biochar could be one of the applicable waste-derived biochar adsorbents in dye wastewater treatment.

Table 4.15: Comparison of several adsorbents on MB and CR dyes removal.

Adsorbent	Adsorption performance	References
Wet-torrefied microalgal biochar	- MB concentration: 5-360 mg/L - Removal percentage: 89.78-26.32% - Max. adsorption capacity: 113.00 mg/g - Isotherm model: Freundlich - Kinetics model: Pseudo-first-order	This study
Wet-torrefied microalgal biochar	- CR concentration: 10-550 mg/L - Removal percentage: 97.10-54.72% - Max. adsorption capacity: 164.35 mg/g - Isotherm model: Temkin - Kinetics model: Pseudo-second-order	This study
Waste palm shell biochar	- MB concentration: 50 mg/L - Adsorption capacity: 20 mg/g	(Kong et al., 2019)
Orange peel waste microwave steam activated biochar	- CR concentration: 500 mg/L - Adsorption capacity: 136 mg/g - Isotherm model: Langmuir - Kinetics model: Pseudo-second-order	(Yek et al., 2020)

Table 4.15, continued.

Orange peel waste microwave CO_2 activated biochar	- CR concentration: 500 mg/L - Adsorption capacity: 91 mg/g - Isotherm model: Freundlich - Kinetics model: Pseudo-second-order	(Yek et al., 2020)
Oil palm waste biochar	- MB concentration: 100 mg/L - Adsorption capacity: 20-48 mg/g	(Liew et al., 2018)
Coffee waste activated biochar	- CR concentration: 50 mg/L - Adsorption capacity: 90.9 mg/g - Isotherm model: Langmuir - Kinetics model: Pseudo-second-order	(Lafi et al., 2019)
Low-rank coal (leonardite)	- CR concentration: 100 mg/L - Adsorption capacity: < 80 mg/g - Isotherm model: Redlich-Peterson - Kinetics model: Pseudo-second-order	(Ausavasukhi et al., 2016)

CHAPTER 5: CONCLUSIONS

This chapter concludes and summarizes the findings from each of the study objectives, from the microalgae cultivation and microalgal biochar production using conventional pyrolysis to the co-production of microalgal biochar and bioethanol using the wet torrefaction, and finally the adsorption application of microalgal biochar on dye pollutants for wastewater treatment. Some future recommendations for each of the studies are discussed.

5.1 Overall conclusion

The study showed the cultivation of microalgae *Chlorella vulgaris* FSP-E and its respective microalgal biochar production through pyrolysis is a potential clean technology for carbon sequestration and microalgal biorefinery approach towards a sustainable environment. Cultivation of *C. vulgaris* FSP-E showed maximum biomass productivity of 0.87 g L^{-1} day^{-1} using 2.5% concentration CO_2 gas supply. The pyrolysis conversion process of microalgal biomass showed 26.9% of total biochar yield. *C. vulgaris* FSP-E biochar has an alkaline pH value with H/C and O/C atomic ratios that are beneficial for carbon sequestration and soil application. The HHV of microalgal biochar also showed potential in the application as alternative coal. Other than that, the irregular porous structure on *C. vulgaris* FSP-E biochar showed an applicable approach for its application in adsorption study in water or soil. Application of microalgal biochar on water treatment may be applicable by applying further treatment into activated biochar.

The microwave-assisted acid hydrolysis pretreatment on two microalgae species with different biomass compositions, namely *Chlorella vulgaris* ESP-31 and *Chlorella* sp. GD is carried to study the biochar and sugar recovery using wet torrefaction. *Chlorella vulgaris* ESP-31 with high carbohydrates composition possesses as a suitable candidate for bioethanol production while *Chlorella* sp. GD can be utilized to produce biochar for

alternative solid fuel applications. In summary, the increasing of wet torrefaction severity with higher temperature, prolonged holding time and higher acid concentration increased the pretreatment effects towards the production of total reducing content in the liquid hydrolysates while vice versa for the solid product yield. The highest solid yield of 54.5% can be obtained from *C. vulgaris* ESP-31 and 74.6% from *Chlorella* sp. GD under a wet torrefaction condition. The proximate and ultimate analysis demonstrates the improvement in the properties of microalgal biochars after wet torrefaction for soil and fuel application. The increase of HHV in the microalgal biochars after wet torrefaction also suggests its application as an alternative solid fuel. Other than that, the microalgal biochar obtained after the pretreatment also possesses additional potential characteristics for application as bio-adsorbent in adsorption study. The co-production of high total reducing sugar content for potential bioethanol production and solid biochar as another value-added product is performed using wet torrefaction. The feasible bioethanol production from microalgal hydrolysate on microwave-assisted heating wet torrefaction using dilute acids is also demonstrated. The carbohydrate-rich microalga *Chlorella vulgaris* ESP-31 showed a better performance in comparison with *Chlorella* sp. GD where higher carbohydrates content produced higher reducing sugar and this aids in the fermentation for bioethanol production. Microalgal hydrolysate obtained after the pretreatment consisted of a total reducing sugar with the highest concentration of 98.11 g/L. The by-product 5-HMF in the *C. vulgaris* ESP-31 hydrolysate (2.41-11.63 g/L) and *Chlorella* sp. GD hydrolysate (2.13-5.12 g/L) might act as the fermentation inhibitor that led to the low ethanol yield, however, this can also be an advantage for the utilization of 5-HMF in industry application after further separation and recovery process. The highest ethanol yield achieved was 0.0761 g ethanol/ (g microalgae) with the maximum experimental conversion probability of 95.22% while the lowest ethanol yield produced was 0.0027 g ethanol/ (g microalgae) with a minimal experimental conversion probability

of 27.24%. In a conclusion, the co-production of bioethanol and biochar from microalgal biomass through microwave-assisted heating wet torrefaction for acid pretreatment can be one of the feasible green technologies for microalgal biorefinery towards the future alternative energy application.

Finally, the adsorption of methylene blue and Congo red has been demonstrated using wet-torrefied microalgal biochar with an approach of the waste-derived and low-cost adsorbent. The wet-torrefied *Chlorella* sp. GD microalgal biochar possessed a pore diameter <2 nm and was regarded as a microporous material. The optimum adsorbent dosage of wet-torrefied microalgal biochar for MB and CR dyes removal was determined at 1 g/L and 2 g/L, respectively. The adsorption process can be performed with the natural pH of MB and CR solutions as the optimum initial pH. The equilibrium adsorption contact time for MB was determined after 120 h while for CR is 4 h. The maximum adsorption capacity for MB using wet-torrefied microalgal biochar was obtained at 113.00 mg/g while for CR was obtained at 164.35 mg/g. The best fit of the Langmuir isotherm model showed the monolayer coverage for the adsorption of MB and CR using wet-torrefied microalgal biochar with the availability of the adsorption site as the rate-limiting factor. Also, the model fitting on the rate and diffusion kinetic models provided additional references to the future modeling and application of wet-torrefied microalgal biochar on dyes adsorption. In conclusion, this study presented the valorization of microalgae by utilizing the wet-torrefied microalgal biochar as the biosorbent for the adsorptive removal of toxic dyes with an approach towards the microalgal biorefinery and value-added application for the environment.

5.2 Future recommendations

Further research on microalgal biochar as an alternative fuel, soil applicant and bio-adsorbent can be carried out in approach to industry application. Furthermore, future

investigation on the recently developed biochar production processes such as torrefaction or hydrothermal carbonization and the optimization of nutrients extracted from microalgal residue can be carried out for microalgal biochar production. In addition, further research can be carried out to optimize the acid pretreatment and fermentation conditions such as the removal of toxic inhibitors for better performance in bioethanol production directly from microalgal hydrolysates. Optimization of bioethanol production through enzymatic hydrolysis and fermentation of microalgal biochar can also be carried out. Furthermore, there are also possible applications of microalgal biochar adsorption on heavy metals for wastewater treatment and natural gas treating or CO_2 capture by selective adsorption. Lastly, it is also recommended to investigate the economically feasible thermochemical conversion technology for large-scale production through energy balance and life cycle analysis (LCA) to enhance the application of the conversion technology towards sustainable energy and the environment.

REFERENCES

Abbasi, T., & Abbasi, S. A. (2010). Biomass energy and the environmental impacts associated with its production and utilization. *Renewable and Sustainable Energy Reviews, 14*(3), 919-937.

Abd-Rahim, F., Wasoh, H., Zakaria, M. R., Ariff, A., Kapri, R., Ramli, N., & Siew-Ling, L. (2014). Production of high yield sugars from *Kappaphycus alvarezii* using combined methods of chemical and enzymatic hydrolysis. *Food Hydrocolloids, 42*, 309-315.

Adnan, N. A. A., Suhaimi, S. N., Abd-Aziz, S., Hassan, M. A., & Phang, L.-Y. (2014). Optimization of bioethanol production from glycerol by *Escherichia coli* SS1. *Renewable Energy, 66*, 625-633.

Agarwal, M., Tardio, J., & Mohan, S. V. (2015). Pyrolysis biochar from cellulosic municipal solid waste as adsorbent for azo dye removal: Equilibrium isotherms and kinetics analysis. *International Journal of Environmental Science and Development, 6*(1), 67.

Ahmad, M., Lee, S. S., Rajapaksha, A. U., Vithanage, M., Zhang, M., Cho, J. S., . . . Ok, Y. S. (2013). Trichloroethylene adsorption by pine needle biochars produced at various pyrolysis temperatures. *Bioresource Technology, 143*, 615-622.

Ahmad, R., & Kumar, R. (2010). Adsorptive removal of congo red dye from aqueous solution using bael shell carbon. *Applied Surface Science, 257*(5), 1628-1633.

Al-Hamamre, Z., Saidan, M., Hararah, M., Rawajfeh, K., Alkhasawneh, H. E., & Al-Shannag, M. (2017). Wastes and biomass materials as sustainable-renewable energy resources for Jordan. *Renewable and Sustainable Energy Reviews, 67*, 295-314.

Alfonsín, V., Maceiras, R., & Gutiérrez, C. (2019). Bioethanol production from industrial algae waste. *Waste Management, 87*, 791-797.

Alhashimi, H. A., & Aktas, C. B. (2017). Life cycle environmental and economic performance of biochar compared with activated carbon: A meta-analysis. *Resources, Conservation and Recycling, 118*, 13-26.

Ali, I., Alharbi, O. M., Alothman, Z. A., Badjah, A. Y., & Alwarthan, A. (2018). Artificial neural network modelling of amido black dye sorption on iron composite nano material: Kinetics and thermodynamics studies. *Journal of Molecular Liquids, 250*, 1-8.

Almeida, J. R. M., Bertilsson, M., Gorwa-Grauslund, M. F., Gorsich, S., & Lidén, G. (2009). Metabolic effects of furaldehydes and impacts on biotechnological processes. *Applied Microbiology and Biotechnology, 82*(4), 625.

Amin, F. R., Huang, Y., He, Y., Zhang, R., Liu, G., & Chen, C. (2016). Biochar applications and modern techniques for characterization. *Clean Technologies and Environmental Policy, 18*(5), 1457-1473.

Anburajan, P., Pugazhendhi, A., Park, J.-H., Sivagurunathan, P., Kumar, G., & Kim, S.-H. (2018). Effect of 5-hydroxymethylfurfural (5-HMF) on high-rate continuous biohydrogen production from galactose. *Bioresource Technology, 247*, 1197-1200.

Anderson, N., Jones, J. G., Page-Dumroese, D., McCollum, D., Baker, S., Loeffler, D., & Chung, W. (2013). A comparison of producer gas, biochar, and activated carbon from two distributed scale thermochemical conversion systems used to process forest biomass. *Energies, 6*(1), 164-183.

Ashokkumar, V., Salam, Z., Tiwari, O., Chinnasamy, S., Mohammed, S., & Ani, F. N. (2015). An integrated approach for biodiesel and bioethanol production from *Scenedesmus bijugatus* cultivated in a vertical tubular photobioreactor. *Energy Conversion and Management, 101*, 778-786.

Ausavasukhi, A., Kampoosaen, C., & Kengnok, O. (2016). Adsorption characteristics of Congo red on carbonized leonardite. *Journal of Cleaner Production, 134*, 506-514.

Aziz, M. (2015). Integrated supercritical water gasification and a combined cycle for microalgal utilization. *Energy Conversion and Management, 91*, 140-148.

Bach, Q.-V., & Chen, W.-H. (2017). A comprehensive study on pyrolysis kinetics of microalgal biomass. *Energy Conversion and Management, 131*, 109-116.

Bach, Q.-V., Chen, W.-H., Lin, S.-C., Sheen, H.-K., & Chang, J.-S. (2017). Wet torrefaction of microalga *Chlorella vulgaris* ESP-31 with microwave-assisted heating. *Energy Conversion and Management, 141*, 163-170.

Bach, Q.-V., Chen, W.-H., Sheen, H.-K., & Chang, J.-S. (2017). Gasification kinetics of raw and wet-torrefied microalgae *Chlorella vulgaris* ESP-31 in carbon dioxide. *Bioresource Technology, 244*, 1393-1399.

Barreiro, D. L., Prins, W., Ronsse, F., & Brilman, W. (2013). Hydrothermal liquefaction (HTL) of microalgae for biofuel production: state of the art review and future prospects. *Biomass and Bioenergy, 53*, 113-127.

Basu, P. (2010). Chapter 2 - Biomass Characteristics. *Biomass Gasification and Pyrolysis*, 27-63.

Basu, P. (2010). Chapter 3 - Pyrolysis and Torrefaction. *Biomass Gasification and Pyrolysis* (pp. 65-96). Boston: Academic Press.

Berndes, G., Hoogwijk, M., & van den Broek, R. (2003). The contribution of biomass in the future global energy supply: A review of 17 studies. *Biomass and Bioenergy, 25*(1), 1-28.

Bharathiraja, B., Chakravarthy, M., Ranjith Kumar, R., Yogendran, D., Yuvaraj, D., Jayamuthunagai, J., . . . Palani, S. (2015). Aquatic biomass (algae) as a future feed stock for bio-refineries: A review on cultivation, processing and products. *Renewable and Sustainable Energy Reviews, 47*, 634-653.

Bibi, R., Ahmad, Z., Imran, M., Hussain, S., Ditta, A., Mahmood, S., & Khalid, A. (2017). Algal bioethanol production technology: A trend towards sustainable development. *Renewable and Sustainable Energy Reviews, 71*, 976-985.

Bird, M., Wurster, C. M., de Paula Silva, P. H., Bass, A. M., & de Nys, R. (2011). Algal biochar – production and properties. *Bioresource Technology, 102*(2), 1886-1891.

Bordoloi, N., Narzari, R., Sut, D., Saikia, R., Chutia, R. S., & Kataki, R. (2016). Characterization of bio-oil and its sub-fractions from pyrolysis of *Scenedesmus dimorphus*. *Renewable Energy, 98*, 245-253.

Bougrier, C., Delgenès, J. P., & Carrère, H. (2008). Effects of thermal treatments on five different waste activated sludge samples solubilisation, physical properties and anaerobic digestion. *Chemical Engineering Journal, 139*(2), 236-244.

Boyd, G. E., Adamson, A. W., & Myers, L. S. (1947). The exchange adsorption of ions from aqueous solutions by organic zeolites. II. Kinetics1. *Journal of the American Chemical Society, 69*(11), 2836-2848.

Brennan, A., Moreno Jiménez, E., Alburquerque, J. A., Knapp, C. W., & Switzer, C. (2014). Effects of biochar and activated carbon amendment on maize growth and the uptake and measured availability of polycyclic aromatic hydrocarbons (PAHs) and potentially toxic elements (PTEs). *Environmental Pollution, 193*, 79-87.

Brennan, L., & Owende, P. (2010). Biofuels from microalgae—a review of technologies for production, processing, and extractions of biofuels and co-products. *Renewable and Sustainable Energy Reviews, 14*(2), 557-577.

Brownsort, P. A. (2009). Biomass pyrolysis processes: review of scope, control and variability. *Edinburgh: UK Biochar Research Center*.

Bryant, H. L., Gogichaishvili, I., Anderson, D., Richardson, J. W., Sawyer, J., Wickersham, T., & Drewery, M. L. (2012). The value of post-extracted algae residue. *Algal Research, 1*(2), 185-193.

Chaiwong, K., Kiatsiriroat, T., Vorayos, N., & Thararax, C. (2012). Biochar production from freshwater algae by slow pyrolysis. *Maejo International Journal of Science and Technology, 6*(2).

Chaiwong, K., Kiatsiriroat, T., Vorayos, N., & Thararax, C. (2013). Study of bio-oil and bio-char production from algae by slow pyrolysis. *Biomass and Bioenergy, 56*, 600-606.

Champagne, P. (2007). Feasibility of producing bio-ethanol from waste residues: A Canadian perspective: feasibility of producing bio-ethanol from waste residues in Canada. *Resources, Conservation and Recycling, 50*(3), 211-230.

Chang, Y.-H., Chang, K.-S., Chen, C.-Y., Hsu, C.-L., Chang, T.-C., & Jang, H.-D. (2018). Enhancement of the efficiency of bioethanol production by *Saccharomyces cerevisiae* via gradually batch-wise and fed-batch increasing the glucose concentration. *Fermentation, 4*(2), 45.

Chang, Y.-M., Tsai, W.-T., & Li, M.-H. (2015). Chemical characterization of char derived from slow pyrolysis of microalgal residue. *Journal of Analytical and Applied Pyrolysis, 111*, 88-93.

Chen, C.-Y., Chang, J.-S., Chang, H.-Y., Chen, T.-Y., Wu, J.-H., & Lee, W.-L. (2013). Enhancing microalgal oil/lipid production from *Chlorella sorokiniana* CY1 using deep-sea water supplemented cultivation medium. *Biochemical engineering journal, 77*, 74-81.

Chen, C.-Y., & Chang, Y.-H. (2018). Engineering strategies for enhancing *C. vulgaris* ESP-31 lipid production using effluents of coke-making wastewater. *Journal of Bioscience and Bioengineering, 125*(6), 710-716.

Chen, C.-Y., Chang, Y.-H., & Chang, H.-Y. (2016). Outdoor cultivation of *Chlorella vulgaris* FSP-E in vertical tubular-type photobioreactors for microalgal protein production. *Algal Research, 13*(Supplement C), 264-270.

Chen, C.-Y., Lee, P.-J., Tan, C. H., Lo, Y.-C., Huang, C.-C., Show, P. L., . . . Chang, J.-S. (2015). Improving protein production of indigenous microalga *Chlorella vulgaris* FSP-E by photobioreactor design and cultivation strategies. *Biotechnology Journal, 10*(6), 905-914.

Chen, C.-Y., Yeh, K.-L., Aisyah, R., Lee, D.-J., & Chang, J.-S. (2011). Cultivation, photobioreactor design and harvesting of microalgae for biodiesel production: A critical review. *Bioresource Technology, 102*(1), 71-81.

Chen, C. Y., Lee, P. J., Tan, C. H., Lo, Y. C., Huang, C. C., Show, P. L., . . . Chang, J. S. (2015). Improving protein production of indigenous microalga *Chlorella vulgaris* FSP‐E by photobioreactor design and cultivation strategies. *Biotechnology journal, 10*(6), 905-914.

Chen, W.-H., Cheng, W.-Y., Lu, K.-M., & Huang, Y.-P. (2011). An evaluation on improvement of pulverized biomass property for solid fuel through torrefaction. *Applied Energy, 88*(11), 3636-3644.

Chen, W.-H., Huang, M.-Y., Chang, J.-S., & Chen, C.-Y. (2014). Thermal decomposition dynamics and severity of microalgae residues in torrefaction. *Bioresource Technology, 169*, 258-264.

Chen, W.-H., Huang, M.-Y., Chang, J.-S., & Chen, C.-Y. (2015). Torrefaction operation and optimization of microalga residue for energy densification and utilization. *Applied Energy, 154*, 622-630.

Chen, W.-H., Huang, M.-Y., Chang, J.-S., Chen, C.-Y., & Lee, W.-J. (2015). An energy analysis of torrefaction for upgrading microalga residue as a solid fuel. *Bioresource Technology, 185*, 285-293.

Chen, W.-H., Lin, B.-J., Huang, M.-Y., & Chang, J.-S. (2015). Thermochemical conversion of microalgal biomass into biofuels: A review. *Bioresource Technology, 184*, 314-327.

Chen, W.-H., Peng, J., & Bi, X. T. (2015). A state-of-the-art review of biomass torrefaction, densification and applications. *Renewable and Sustainable Energy Reviews, 44*, 847-866.

Chen, W.-H., Tu, Y. J., & Sheen, H. K. (2011). Disruption of sugarcane bagasse lignocellulosic structure by means of dilute sulfuric acid pretreatment with microwave-assisted heating. *Applied Energy, 88*(8), 2726-2734.

Chen, W.-H., Wu, Z.-Y., & Chang, J.-S. (2014). Isothermal and non-isothermal torrefaction characteristics and kinetics of microalga *Scenedesmus obliquus* CNW-N. *Bioresource Technology, 155*, 245-251.

Chen, W.-H., Ye, S.-C., & Sheen, H.-K. (2012). Hydrolysis characteristics of sugarcane bagasse pretreated by dilute acid solution in a microwave irradiation environment. *Applied Energy, 93*, 237-244.

Chen, W.-H., Ye, S.-C., & Sheen, H.-K. (2012). Hydrothermal carbonization of sugarcane bagasse via wet torrefaction in association with microwave heating. *Bioresource Technology, 118*, 195-203.

Chen, Y.-C., Chen, W.-H., Lin, B.-J., Chang, J.-S., & Ong, H. C. (2016). Impact of torrefaction on the composition, structure and reactivity of a microalga residue. *Applied Energy, 181*, 110-119.

Cho, D.-W., Kwon, E. E., & Song, H. (2016). Use of carbon dioxide as a reaction medium in the thermo-chemical process for the enhanced generation of syngas and tuning adsorption ability of biochar. *Energy Conversion and Management, 117*, 106-114.

Choi, S. P., Nguyen, M. T., & Sim, S. J. (2010). Enzymatic pretreatment of *Chlamydomonas reinhardtii* biomass for ethanol production. *Bioresource Technology, 101*(14), 5330-5336.

Chowdhury, A. H., Salam, N., Debnath, R., Islam, S. M., & Saha, T. (2019). Chapter 8 - Design and fabrication of porous nanostructures and their applications. In Y. Beeran Pottathara, S. Thomas, N. Kalarikkal, Y. Grohens, & V. Kokol (Eds.), *Nanomaterials Synthesis* (pp. 265-294): Elsevier.

Chowdhury, S., & Saha, P. (2010). Sea shell powder as a new adsorbent to remove Basic Green 4 (Malachite Green) from aqueous solutions: Equilibrium, kinetic and thermodynamic studies. *Chemical Engineering Journal, 164*(1), 168-177.

Christenson, L., & Sims, R. (2011). Production and harvesting of microalgae for wastewater treatment, biofuels, and bioproducts. *Biotechnology Advances, 29*(6), 686-702.

Coates, J. (2006). Interpretation of Infrared Spectra, A Practical Approach, *Encyclopedia of Analytical Chemistry*: John Wiley & Sons, Ltd.

Conti, R., Fabbri, D., Vassura, I., & Ferroni, L. (2016). Comparison of chemical and physical indices of thermal stability of biochars from different biomass by analytical pyrolysis and thermogravimetry. *Journal of Analytical and Applied Pyrolysis, 122*, 160-168.

Coronella, C. J., Yan, W., Reza, M. T., & Vasquez, V. R. (2012). Method for wet torrefaction of a biomass: Google Patents.

Cui, L., Wang, Y., Gao, L., Hu, L., Yan, L., Wei, Q., & Du, B. (2015). EDTA functionalized magnetic graphene oxide for removal of Pb (II), Hg (II) and Cu (II) in water treatment: Adsorption mechanism and separation property. *Chemical Engineering Journal, 281*, 1-10.

Daly, H. (1994). Fossil fuels. *Applied Energy, 47*(2), 101-121.

David, A. N., Sewsynker-Sukai, Y., Sithole, B., & Gueguim Kana, E. B. (2020). Development of a green liquor dregs pretreatment for enhanced glucose recovery from corn cobs and kinetic assessment on various bioethanol fermentation types. *Fuel, 274*, 117797.

Dbik, A., Bentahar, S., El Khomri, M., El Messaoudi, N., & Lacherai, A. (2020). Adsorption of Congo red dye from aqueous solutions using tunics of the corm of the saffron. *Materials Today: Proceedings, 22*, 134-139.

Delbecq, F., Wang, Y., & Len, C. (2017). Various carbohydrate precursors dehydration to 5-HMF in an acidic biphasic system under microwave heating using betaine as a co-catalyst. *Molecular Catalysis, 434*, 80-85.

Demirbas, A. (2008). Biofuels sources, biofuel policy, biofuel economy and global biofuel projections. *Energy Conversion and Management, 49*(8), 2106-2116.

Demirbas, A. (2010). Use of algae as biofuel sources. *Energy Conversion and Management, 51*(12), 2738-2749.

Demirbas, A. (2011). Competitive liquid biofuels from biomass. *Applied Energy, 88*(1), 17-28.

Deng, J., Wang, G.-j., Kuang, J.-h., Zhang, Y.-l., & Luo, Y.-h. (2009). Pretreatment of agricultural residues for co-gasification via torrefaction. *Journal of Analytical and Applied Pyrolysis, 86*(2), 331-337.

Denisov, E., & Shestakov, A. (2013). Free-radical decarboxylation of carboxylic acids as a concerted abstraction and fragmentation reaction. *Kinetics and Catalysis, 54*(1), 22-33.

Dong, T., Gao, D., Miao, C., Yu, X., Degan, C., Garcia-Pérez, M., . . . Chen, S. (2015). Two-step microalgal biodiesel production using acidic catalyst generated from pyrolysis-derived bio-char. *Energy Conversion and Management, 105*, 1389-1396.

Draper, K. (2016). Waste water treatment and biochar. *the Biochar Journal 2016.* Retrieved from www.biochar-journal.org/en/ct/81

Du, Z. (2013). *Thermochemical conversion of microalgae for biofuel production.* University of Minnesota.

El-Dalatony, M. M., Kurade, M. B., Abou-Shanab, R. A., Kim, H., Salama, E.-S., & Jeon, B.-H. (2016). Long-term production of bioethanol in repeated-batch fermentation of microalgal biomass using immobilized *Saccharomyces cerevisiae*. *Bioresource Technology, 219*, 98-105.

El-Hendawy, A.-N. A. (2006). Variation in the FTIR spectra of a biomass under impregnation, carbonization and oxidation conditions. *Journal of Analytical and Applied Pyrolysis, 75*(2), 159-166.

Eloka-Eboka, A. C., & Inambao, F. L. (2017). Effects of CO_2 sequestration on lipid and biomass productivity in microalgal biomass production. *Applied Energy, 195*(Supplement C), 1100-1111.

Ennis, C. J., Evans, A. G., Islam, M., Ralebitso-Senior, T. K., & Senior, E. (2012). Biochar: carbon sequestration, land remediation, and impacts on soil microbiology. *Critical Reviews in Environmental Science and Technology, 42*(22), 2311-2364.

Eren, Z., & Acar, F. N. (2006). Adsorption of Reactive Black 5 from an aqueous solution: Equilibrium and kinetic studies. *Desalination, 194*(1), 1-10.

Eriksen, N. (2008). The technology of microalgal culturing. *Biotechnology letters, 30*(9), 1525-1536.

Erlach, B., Harder, B., & Tsatsaronis, G. (2012). Combined hydrothermal carbonization and gasification of biomass with carbon capture. *Energy, 45*(1), 329-338.

Eshaq, F. S., Ali, M. N., & Mohd, M. K. (2010). *Spirogyra* biomass a renewable source for biofuel (bioethanol) production. *International Journal of Engineering Science and Technology, 2*(12), 7045-7054.

Ezzati, R. (2020). Derivation of pseudo-first-order, pseudo-second-order and modified pseudo-first-order rate equations from Langmuir and Freundlich isotherms for adsorption. *Chemical Engineering Journal, 392*, 123705.

Ferreira, A. F., Dias, A. S., Silva, C. M., & Costa, M. (2015). Evaluation of thermochemical properties of raw and extracted microalgae. *Energy, 92*, 365-372.

Foley, P. M., Beach, E. S., & Zimmerman, J. B. (2011). Algae as a source of renewable chemicals: Opportunities and challenges. *Green Chemistry, 13*(6), 1399-1405.

Freundlich, H. (1906). Over the adsorption in solution. *Journal of Physical Chemistry, 57*(385471), 1100-1107.

Gai, C., Zhang, Y., Chen, W.-T., Zhang, P., & Dong, Y. (2015). An investigation of reaction pathways of hydrothermal liquefaction using *Chlorella pyrenoidosa* and *Spirulina platensis*. *Energy Conversion and Management, 96*, 330-339.

Gan, Y. Y., Ong, H. C., Show, P. L., Ling, T. C., Chen, W.-H., Yu, K. L., & Abdullah, R. (2018). Torrefaction of microalgal biochar as potential coal fuel and application as bio-adsorbent. *Energy Conversion and Management, 165*, 152-162.

García-Martos, C., Rodríguez, J., & Sánchez, M. J. (2013). Modelling and forecasting fossil fuels, CO_2 and electricity prices and their volatilities. *Applied Energy, 101*, 363-375.

Garcia-Perez, M., Lewis, T., & Kruger, C. (2010). Methods for producing biochar and advanced biofuels in Washington State, part 1: Literature review of pyrolysis reactors. *Department of Biological Systems Engineering and the Center for Sustaining Agriculture and Natural Resources. Washington State University, Pullman, WA*.

Ghayal, M. S., & Pandya, M. T. (2013). Microalgae biomass: A renewable source of energy. *Energy Procedia, 32*, 242-250.

Gombert, A. K., & van Maris, A. J. A. (2015). Improving conversion yield of fermentable sugars into fuel ethanol in 1st generation yeast-based production processes. *Current Opinion in Biotechnology, 33*, 81-86.

Gonzalez-Salazar, M. A., Morini, M., Pinelli, M., Spina, P. R., Venturini, M., Finkenrath, M., & Poganietz, W.-R. (2014). Methodology for estimating biomass energy potential and its application to Colombia. *Applied Energy, 136*, 781-796.

Gouveia, L., & Oliveira, A. C. (2009). Microalgae as a raw material for biofuels production. *Journal of Industrial Microbiology & Biotechnology, 36*(2), 269-274.

Goyal, H., Seal, D., & Saxena, R. C. (2008). Bio-fuels from thermochemical conversion of renewable resources: A review. *Renewable and Sustainable Energy Reviews, 12*(2), 504-517.

Grierson, S., Strezov, V., & Bengtsson, J. (2013). Life cycle assessment of a microalgae biomass cultivation, bio-oil extraction and pyrolysis processing regime. *Algal Research, 2*(3), 299-311.

Gronchi, N., Favaro, L., Cagnin, L., Brojanigo, S., Pizzocchero, V., Basaglia, M., & Casella, S. (2019). Novel yeast strains for the efficient saccharification and fermentation of starchy by-products to bioethanol. *Energies, 12*(4), 714.

Gronnow, M. J., Budarin, V. L., Mašek, O., Crombie, K. N., Brownsort, P. A., Shuttleworth, P. S., . . . Clark, J. H. (2013). Torrefaction/biochar production by microwave and conventional slow pyrolysis–comparison of energy properties. *Gcb Bioenergy, 5*(2), 144-152.

Guo, H., Daroch, M., Liu, L., Qiu, G., Geng, S., & Wang, G. (2013). Biochemical features and bioethanol production of microalgae from coastal waters of Pearl River Delta. *Bioresource Technology, 127*, 422-428.

Guo, X., Mu, Q., Zhong, H., Li, P., Zhang, C., Wei, D., & Zhao, T. (2019). Rapid removal of tetracycline by *Myriophyllum aquaticum*: Evaluation of the role and mechanisms of adsorption. *Environmental Pollution, 254*, 113101.

Guo, X., & Wang, J. (2019). A general kinetic model for adsorption: Theoretical analysis and modeling. *Journal of Molecular Liquids, 288*, 111100.

Hafeznezami, S., Zimmer-Faust, A. G., Dunne, A., Tran, T., Yang, C., Lam, J. R., . . . Jay, J. A. (2016). Adsorption and desorption of arsenate on sandy sediments from contaminated and uncontaminated saturated zones: Kinetic and equilibrium modeling. *Environmental Pollution, 215*, 290-301.

Hall, K. R., Eagleton, L. C., Acrivos, A., & Vermeulen, T. (1966). Pore- and solid-diffusion kinetics in fixed-bed adsorption under constant-pattern conditions. *Industrial & Engineering Chemistry Fundamentals, 5*(2), 212-223.

Hallenbeck, P. C., Grogger, M., Mraz, M., & Veverka, D. (2016). Solar biofuels production with microalgae. *Applied Energy, 179*, 136-145.

Harun, R., Danquah, M. K., & Forde, G. M. (2010). Microalgal biomass as a fermentation feedstock for bioethanol production. *Journal of Chemical Technology & Biotechnology, 85*(2), 199-203.

Harun, R., Danquah, M. K., & Thiruvenkadam, S. (2014). Particulate size of microalgal biomass affects hydrolysate properties and bioethanol concentration. *BioMed Research International, 2014*, 8.

Harun, R., Jason, W. S. Y., Cherrington, T., & Danquah, M. K. (2011). Exploring alkaline pre-treatment of microalgal biomass for bioethanol production. *Applied Energy, 88*(10), 3464-3467.

Heilmann, S. M., Davis, H. T., Jader, L. R., Lefebvre, P. A., Sadowsky, M. J., Schendel, F. J., . . . Valentas, K. J. (2010). Hydrothermal carbonization of microalgae. *Biomass and Bioenergy, 34*(6), 875-882.

Hirano, A., Ueda, R., Hirayama, S., & Ogushi, Y. (1997). CO_2 fixation and ethanol production with microalgal photosynthesis and intracellular anaerobic fermentation. *Energy, 22*(2), 137-142.

Ho, S.-H., Chen, C.-Y., Lee, D.-J., & Chang, J.-S. (2011). Perspectives on microalgal CO_2-emission mitigation systems — A review. *Biotechnology Advances, 29*(2), 189-198.

Ho, S.-H., Huang, S.-W., Chen, C.-Y., Hasunuma, T., Kondo, A., & Chang, J.-S. (2013). Bioethanol production using carbohydrate-rich microalgae biomass as feedstock. *Bioresource Technology, 135*, 191-198.

Ho, S.-H., Huang, S.-W., Chen, C.-Y., Hasunuma, T., Kondo, A., & Chang, J.-S. (2013). Characterization and optimization of carbohydrate production from an indigenous microalga *Chlorella vulgaris* FSP-E. *Bioresource Technology, 135*(Supplement C), 157-165.

Ho, S.-H., Li, P.-J., Liu, C.-C., & Chang, J.-S. (2013). Bioprocess development on microalgae-based CO_2 fixation and bioethanol production using *Scenedesmus obliquus* CNW-N. *Bioresource Technology, 145*, 142-149.

Ho, Y. S., & McKay, G. (1998). A comparison of chemisorption kinetic models applied to pollutant removal on various sorbents. *Process Safety and Environmental Protection, 76*(4), 332-340.

Ho, Y. S., & McKay, G. (1998). Sorption of dye from aqueous solution by peat. *Chemical Engineering Journal, 70*(2), 115-124.

Hodgson, E., Lewys-James, A., Ravella, S. R., Thomas-Jones, S., Perkins, W., & Gallagher, J. (2016). Optimisation of slow-pyrolysis process conditions to maximise char yield and heavy metal adsorption of biochar produced from different feedstocks. *Bioresource Technology, 214*, 574-581.

Hoekman, S. K., Broch, A., Robbins, C., Zielinska, B., & Felix, L. (2013). Hydrothermal carbonization (HTC) of selected woody and herbaceous biomass feedstocks. *Biomass Conversion and Biorefinery, 3*(2), 113-126.

Hossain, M. K., Strezov, V., Chan, K. Y., & Nelson, P. F. (2010). Agronomic properties of wastewater sludge biochar and bioavailability of metals in production of cherry tomato (*Lycopersicon esculentum*). *Chemosphere, 78*(9), 1167-1171.

Illman, A., Scragg, A. H., & Shales, S. W. (2000). Increase in *Chlorella* strains calorific values when grown in low nitrogen medium. *Enzyme and Microbial Technology, 27*(8), 631-635.

Ippolito, J. A., Laird, D. A., & Busscher, W. J. (2012). Environmental benefits of biochar. *Journal of Environmental Quality, 41*(4), 967-972.

Jacobson, M. Z. (2009). Review of solutions to global warming, air pollution, and energy security. *Energy & Environmental Science, 2*(2), 148-173.

Javed, F., Aslam, M., Rashid, N., Shamair, Z., Khan, A. L., Yasin, M., . . . Bazmi, A. A. (2019). Microalgae-based biofuels, resource recovery and wastewater treatment: A pathway towards sustainable biorefinery. *Fuel, 255*, 115826.

Jeong, T. S., Choi, C. H., Lee, J. Y., & Oh, K. K. (2012). Behaviors of glucose decomposition during acid-catalyzed hydrothermal hydrolysis of pretreated *Gelidium amansii*. *Bioresource Technology, 116*, 435-440.

Jindo, K., Mizumoto, H., Sawada, Y., Sanchez-Monedero, M. A., & Sonoki, T. (2014). Physical and chemical characterization of biochars derived from different agricultural residues. *Biogeosciences, 11*(23), 6613-6621.

John, R., Anisha, G., Nampoothiri, K. M., & Pandey, A. (2011). Micro and macroalgal biomass: A renewable source for bioethanol. *Bioresource Technology, 102*(1), 186-193.

Joseph, S., & Lehmann, J. (2009). *Biochar for Environmental Management : Science and Technology*. London: Routledge.

Kadhum, H. J., Mahapatra, D. M., & Murthy, G. S. (2019). A comparative account of glucose yields and bioethanol production from separate and simultaneous saccharification and fermentation processes at high solids loading with variable PEG concentration. *Bioresource Technology, 283*, 67-75.

Karatay, S. E., Erdoğan, M., Dönmez, S., & Dönmez, G. (2016). Experimental investigations on bioethanol production from halophilic microalgal biomass. *Ecological Engineering, 95*, 266-270.

Khoja, A. H., Ali, E., Zafar, K., Ansari, A. A., Nawar, A., & Qayyum, M. (2015). Comparative study of bioethanol production from sugarcane molasses by using *Zymomonas mobilis* and *Saccharomyces cerevisiae*. *African Journal of Biotechnology, 14*(31), 2455-2462.

Khoo, H. H., Koh, C. Y., Shaik, M. S., & Sharratt, P. N. (2013). Bioenergy co-products derived from microalgae biomass via thermochemical conversion – Life cycle energy balances and CO_2 emissions. *Bioresource Technology, 143*, 298-307.

Kim, J. K., Um, B.-H., & Kim, T. H. (2012). Bioethanol production from micro-algae, *Schizocytrium* sp., using hydrothermal treatment and biological conversion. *Korean Journal of Chemical Engineering, 29*(2), 209-214.

Kiran, B., Kumar, R., & Deshmukh, D. (2014). Perspectives of microalgal biofuels as a renewable source of energy. *Energy Conversion and Management, 88*, 1228-1244.

Koide, R. T. (2017). Chapter 25 - Biochar—*Arbuscular Mycorrhiza* interaction in temperate soils, *Mycorrhizal Mediation of Soil* (pp. 461-477): Elsevier.

Kołtowski, M., Charmas, B., Skubiszewska-Zięba, J., & Oleszczuk, P. (2017). Effect of biochar activation by different methods on toxicity of soil contaminated by industrial activity. *Ecotoxicology and Environmental Safety, 136*, 119-125.

Kong, S.-H., Lam, S. S., Yek, P. N. Y., Liew, R. K., Ma, N. L., Osman, M. S., & Wong, C. C. (2019). Self-purging microwave pyrolysis: An innovative approach to convert oil palm shell into carbon-rich biochar for methylene blue adsorption. *Journal of Chemical Technology & Biotechnology, 94*(5), 1397-1405.

Kubo, S. (2013). Nanostructured carbohydrate–derived carbonaceous materials. *TANSO, 2013*(258), 232-233.

Kumar, G., Shobana, S., Chen, W.-H., Bach, Q.-V., Kim, S.-H., Atabani, A. E., & Chang, J.-S. (2017). A review of thermochemical conversion of microalgal biomass for biofuels: Chemistry and processes. *Green Chemistry, 19*(1), 44-67.

Kumar, P. S., Pavithra, J., Suriya, S., Ramesh, M., & Kumar, K. A. (2015). *Sargassum wightii*, a marine alga is the source for the production of algal oil, bio-oil, and application in the dye wastewater treatment. *Desalination and Water Treatment, 55*(5), 1342-1358.

Kuo, C.-M., Chen, T.-Y., Lin, T.-H., Kao, C.-Y., Lai, J.-T., Chang, J.-S., & Lin, C.-S. (2015). Cultivation of *Chlorella* sp. GD using piggery wastewater for biomass and lipid production. *Bioresource Technology, 194*, 326-333.

Lafi, R., Montasser, I., & Hafiane, A. (2019). Adsorption of Congo red dye from aqueous solutions by prepared activated carbon with oxygen-containing functional groups and its regeneration. *Adsorption Science & Technology, 37*(1-2), 160-181.

Lagergren, S. K. (1898). About the theory of so-called adsorption of soluble substances. *Sven. Vetenskapsakad. Handingarl, 24*, 1-39.

Láinez, M., Ruiz, H. A., Arellano-Plaza, M., & Martínez-Hernández, S. (2019). Bioethanol production from enzymatic hydrolysates of *Agave salmiana* leaves comparing *S. cerevisiae* and *K. marxianus*. *Renewable Energy, 138*, 1127-1133.

Langmuir, I. (1918). The adsorption of gases on plane surfaces of glass, mica and platinum. *Journal of the American Chemical Society, 40*(9), 1361-1403.

Lawrinenko, M., & Laird, D. A. (2015). Anion exchange capacity of biochar. *Green Chemistry, 17*(9), 4628-4636.

Lee, I., & Yu, J.-H. (2020). The production of fermentable sugar and bioethanol from acacia wood by optimizing dilute sulfuric acid pretreatment and post treatment. *Fuel, 275*, 117943.

Lee, L., Lee, X., Chia, P., Tan, K., & Gan, S. (2014). Utilisation of *Cymbopogon citratus* (lemon grass) as biosorbent for the sequestration of nickel ions from aqueous solution: Equilibrium, kinetic, thermodynamics and mechanism studies. *Journal of the Taiwan Institute of Chemical Engineers, 45*(4), 1764-1772.

Lee, L. Y., Chin, D. Z. B., Lee, X. J., Chemmangattuvalappil, N., & Gan, S. (2015). Evaluation of *Abelmoschus esculentus* (lady's finger) seed as a novel biosorbent for the removal of Acid Blue 113 dye from aqueous solutions. *Process Safety and Environmental Protection, 94*, 329-338.

Lee, L. Y., Gan, S., Yin Tan, M. S., Lim, S. S., Lee, X. J., & Lam, Y. F. (2016). Effective removal of Acid Blue 113 dye using overripe *Cucumis sativus* peel as an eco-friendly biosorbent from agricultural residue. *Journal of Cleaner Production, 113*, 194-203.

Lee, O. K., Seong, D. H., Lee, C. G., & Lee, E. Y. (2015). Sustainable production of liquid biofuels from renewable microalgae biomass. *Journal of Industrial and Engineering Chemistry, 29*, 24-31.

Lee, S., Oh, Y., Kim, D., Kwon, D., Lee, C., & Lee, J. (2011). Converting carbohydrates extracted from marine algae into ethanol using various ethanolic *Escherichia coli* strains. *Applied Biochemistry and Biotechnology, 164*(6), 878-888.

Lee, X. J., Lee, L. Y., Gan, S., Thangalazhy-Gopakumar, S., & Ng, H. K. (2017). Biochar potential evaluation of palm oil wastes through slow pyrolysis: Thermochemical characterization and pyrolytic kinetic studies. *Bioresource Technology, 236*(Supplement C), 155-163.

Lehmann, J. (2007). A handful of carbon. *Nature, 447*(7141), 143-144.

Lei, H., Ren, S., Wang, L., Bu, Q., Julson, J., Holladay, J., & Ruan, R. (2011). Microwave pyrolysis of distillers dried grain with solubles (DDGS) for biofuel production. *Bioresource Technology, 102*(10), 6208-6213.

Li, D., Li, J., Gu, Q., Song, S., & Peng, C. (2016). Co-influence of the pore size of adsorbents and the structure of adsorbates on adsorption of dyes. *Desalination and Water Treatment, 57*(31), 14686-14695.

Li, J., Dai, J., Liu, G., Zhang, H., Gao, Z., Fu, J., . . . Huang, Y. (2016). Biochar from microwave pyrolysis of biomass: A review. *Biomass and Bioenergy, 94*, 228-244.

Libra, J. A., Ro, K. S., Kammann, C., Funke, A., Berge, N. D., Neubauer, Y., . . . Emmerich, K.-H. (2011). Hydrothermal carbonization of biomass residuals: a comparative review of the chemistry, processes and applications of wet and dry pyrolysis. *Biofuels, 2*(1), 71-106.

Liew, R. K., Nam, W. L., Chong, M. Y., Phang, X. Y., Su, M. H., Yek, P. N. Y., . . . Lam, S. S. (2018). Oil palm waste: An abundant and promising feedstock for microwave pyrolysis conversion into good quality biochar with potential multi-applications. *Process Safety and Environmental Protection, 115*, 57-69.

Liu, Y., Zhao, X., Li, J., Ma, D., & Han, R. (2012). Characterization of bio-char from pyrolysis of wheat straw and its evaluation on methylene blue adsorption. *Desalination and Water Treatment, 46*(1-3), 115-123.

Liu, Z., Quek, A., Kent Hoekman, S., & Balasubramanian, R. (2013). Production of solid biochar fuel from waste biomass by hydrothermal carbonization. *Fuel, 103*, 943-949.

Liu, Z., & Zhang, F.-S. (2009). Removal of lead from water using biochars prepared from hydrothermal liquefaction of biomass. *Journal of Hazardous Materials, 167*(1), 933-939.

Mandal, A., Singh, N., & Purakayastha, T. J. (2017). Characterization of pesticide sorption behaviour of slow pyrolysis biochars as low cost adsorbent for atrazine and imidacloprid removal. *Science of the total environment, 577*, 376-385.

Markou, G., Angelidaki, I., Nerantzis, E., & Georgakakis, D. (2013). Bioethanol production by carbohydrate-enriched biomass of *Arthrospira (Spirulina) platensis*. *Energies, 6*(8), 3937-3950.

Mata, T. M., Martins, A. A., & Caetano, N. S. (2010). Microalgae for biodiesel production and other applications: A review. *Renewable and Sustainable Energy Reviews, 14*(1), 217-232.

Maurya, R., Ghosh, T., Paliwal, C., Shrivastav, A., Chokshi, K., Pancha, I., . . . Mishra, S. (2014). Biosorption of methylene blue by de-oiled algal biomass: Equilibrium, kinetics and artificial neural network modelling. *PloS one, 9*(10), e109545.

Meroufel, B., Benali, O., Benyahia, M., Benmoussa, Y., & Zenasni, M. (2013). Adsorptive removal of anionic dye from aqueous solutions by Algerian kaolin: Characteristics, isotherm, kinetic and thermodynamic studies. *Journal of Materials and Environmental Science, 4*(3), 482-491.

Miller, G. L. (1959). Use of dinitrosalicylic acid reagent for determination of reducing sugar. *Analytical Chemistry, 31*(3), 426-428.

Mohan, D., Sarswat, A., Ok, Y. S., & Pittman, C. U. (2014). Organic and inorganic contaminants removal from water with biochar, a renewable, low cost and sustainable adsorbent–a critical review. *Bioresource Technology, 160*, 191-202.

Molina, M., Zaelke, D., Sarma, K. M., Andersen, S. O., Ramanathan, V., & Kaniaru, D. (2009). Reducing abrupt climate change risk using the Montreal Protocol and other regulatory actions to complement cuts in CO_2 emissions. *Proceedings of the National Academy of Sciences, 106*(49), 20616-20621.

Mukome, F. N., Six, J., & Parikh, S. J. (2013). The effects of walnut shell and wood feedstock biochar amendments on greenhouse gas emissions from a fertile soil. *Geoderma, 200*, 90-98.

Mukome, F. N., Zhang, X., Silva, L. C., Six, J., & Parikh, S. J. (2013). Use of chemical and physical characteristics to investigate trends in biochar feedstocks. *Journal of Agricultural and Food Chemistry, 61*(9), 2196-2204.

Mulabagal, V., Baah, D. A., Egiebor, N. O., & Chen, W.-Y. (2017). Biochar from biomass: A strategy for carbon dioxide sequestration, soil amendment, power generation, and CO_2 utilization. In W.-Y. Chen, T. Suzuki, & M. Lackner (Eds.), *Handbook of Climate Change Mitigation and Adaptation* (pp. 1937-1974). Cham: Springer International Publishing.

Mutripah, S., Meinita, M. D. N., Kang, J.-Y., Jeong, G.-T., Susanto, A., Prabowo, R. E., & Hong, Y.-K. (2014). Bioethanol production from the hydrolysate of *Palmaria palmata* using sulfuric acid and fermentation with brewer's yeast. *Journal of Applied Phycology, 26*(1), 687-693.

Mwangi, J. K., Lee, W.-J., Whang, L.-M., Wu, T. S., Chen, W.-H., Chang, J.-S., . . . Chen, C.-L. (2015). Microalgae oil: Algae cultivation and harvest, algae residue torrefaction and diesel engine emissions tests. *Aerosol and Air Quality Research, 15*(1), 81-98.

Nethaji, S., Sivasamy, A., & Mandal, A. (2013). Adsorption isotherms, kinetics and mechanism for the adsorption of cationic and anionic dyes onto carbonaceous particles prepared from *Juglans regia* shell biomass. *International Journal of Environmental Science and Technology, 10*(2), 231-242.

Nhuchhen, D. R., Basu, P., & Acharya, B. (2014). A comprehensive review on biomass torrefaction. *International Journal of Renewable Energy & Biofuels, 2014*, 1-56.

Niazi, N., Murtaza, B., Bibi, I., Shahid, M., White, J. C., Nawaz, M. F., . . . Wang, H. (2016). Chapter 7 - Removal and recovery of metals by biosorbents and biochars derived from biowastes, *Environmental Materials and Waste* (pp. 149-177): Academic Press.

Nizamuddin, S., Baloch, H. A., Griffin, G., Mubarak, N., Bhutto, A. W., Abro, R., . . . Ali, B. S. (2017). An overview of effect of process parameters on hydrothermal carbonization of biomass. *Renewable and Sustainable Energy Reviews, 73*, 1289-1299.

Oasmaa, A., & Peacocke, C. (2001). *A guide to physical property characterisation of biomass-derived fast pyrolysis liquids*: Technical Research Centre of Finland Espoo.

Oncel, S. S. (2013). Microalgae for a macroenergy world. *Renewable and Sustainable Energy Reviews, 26*, 241-264.

Ozcan, A., Ozcan, A., Tunali, S., Akar, T., & Kiran, I. (2005). Determination of the equilibrium, kinetic and thermodynamic parameters of adsorption of copper(II) ions onto seeds of. *Journal of Hazardous Materials, 124*(1-3), 200-208.

Pacheco, R., Ferreira, A. F., Pinto, T., Nobre, B. P., Loureiro, D., Moura, P., . . . Silva, C. M. (2015). The production of pigments & hydrogen through a *Spirogyra* sp. biorefinery. *Energy Conversion and Management, 89*, 789-797.

Paudel, S. R., Banjara, S. P., Choi, O. K., Park, K. Y., Kim, Y. M., & Lee, J. W. (2017). Pretreatment of agricultural biomass for anaerobic digestion: Current state and challenges. *Bioresource Technology, 245*, 1194-1205.

Pejin, J. D., Mojović, L. V., Pejin, D. J., Kocić-Tanackov, S. D., Savić, D. S., Nikolić, S. B., & Djukić-Vuković, A. P. (2015). Bioethanol production from triticale by simultaneous saccharification and fermentation with magnesium or calcium ions addition. *Fuel, 142*, 58-64.

Pelekani, C., & Snoeyink, V. L. (2001). A kinetic and equilibrium study of competitive adsorption between atrazine and Congo red dye on activated carbon: The importance of pore size distribution. *Carbon, 39*(1), 25-37.

Peng, L., Ren, Y., Gu, J., Qin, P., Zeng, Q., Shao, J., . . . Chai, L. (2014). Iron improving bio-char derived from microalgae on removal of tetracycline from aqueous system. *Environmental Science and Pollution Research, 21*(12), 7631-7640.

Petrou, E. C., & Pappis, C. P. (2009). Biofuels: A survey on pros and cons. *Energy & Fuels, 23*(2), 1055-1066.

Phwan, C. K., Ong, H. C., Chen, W.-H., Ling, T. C., Ng, E. P., & Show, P. L. (2018). Overview: Comparison of pretreatment technologies and fermentation processes of bioethanol from microalgae. *Energy Conversion and Management, 173*, 81-94.

Präger, F., Paczkowski, S., Sailer, G., Derkyi, N. S. A., & Pelz, S. (2019). Biomass sources for a sustainable energy supply in Ghana – A case study for Sunyani. *Renewable and Sustainable Energy Reviews, 107*, 413-424.

Prasad, S., Malav, M. K., Kumar, S., Singh, A., Pant, D., & Radhakrishnan, S. (2018). Enhancement of bio-ethanol production potential of wheat straw by reducing furfural and 5-hydroxymethylfurfural (HMF). *Bioresource Technology Reports, 4*, 50-56.

Qian, W.-C., Luo, X.-P., Wang, X., Guo, M., & Li, B. (2018). Removal of methylene blue from aqueous solution by modified bamboo hydrochar. *Ecotoxicology and Environmental Safety, 157*, 300-306.

Rajapaksha, A. U., Chen, S. S., Tsang, D. C. W., Zhang, M., Vithanage, M., Mandal, S., . . . Ok, Y. S. (2016). Engineered/designer biochar for contaminant removal/immobilization from soil and water: Potential and implication of biochar modification. *Chemosphere, 148*, 276-291.

Rashid, N., Rehman, M. S. U., & Han, J.-I. (2013). Recycling and reuse of spent microalgal biomass for sustainable biofuels. *Biochemical Engineering Journal, 75*, 101-107.

Roberts, D. A., Cole, A. J., Paul, N. A., & de Nys, R. (2015). Algal biochar enhances the re-vegetation of stockpiled mine soils with native grass. *Journal of Environmental Management, 161*, 173-180.

Roginsky, S., & Zeldovich, Y. B. (1934). The catalytic oxidation of carbon monoxide on manganese dioxide. *Acta Physicochimica U.R.S.S., 1*(554), 2019.

Rout, P. K., Nannaware, A. D., Prakash, O., Kalra, A., & Rajasekharan, R. (2016). Synthesis of hydroxymethylfurfural from cellulose using green processes: A promising biochemical and biofuel feedstock. *Chemical Engineering Science, 142*, 318-346.

Salgado, M. A. H., Tarelho, L. A. C., & Matos, A. (2020). Analysis of combined biochar and torrefied biomass fuel production as alternative for residual biomass valorization generated in small-scale palm oil mills. *Waste and Biomass Valorization, 11*(1), 343-356.

Sambusiti, C., Bellucci, M., Zabaniotou, A., Beneduce, L., & Monlau, F. (2015). Algae as promising feedstocks for fermentative biohydrogen production according to a biorefinery approach: A comprehensive review. *Renewable and Sustainable Energy Reviews, 44*, 20-36.

Sarkar, O., Agarwal, M., Kumar, A. N., & Mohan, S. V. (2015). Retrofitting hetrotrophically cultivated algae biomass as pyrolytic feedstock for biogas, bio-char and bio-oil production encompassing biorefinery. *Bioresource Technology, 178*, 132-138.

Sebayang, A. H., Hassan, M. H., Ong, H. C., Dharma, S., Silitonga, A. S., Kusumo, F., . . . Bahar, A. H. (2017). Optimization of reducing sugar production from *Manihot glaziovii* starch using response surface methodology. *Energies, 10*(1), 35.

Sheng, C., & Azevedo, J. L. T. (2005). Estimating the higher heating value of biomass fuels from basic analysis data. *Biomass and Bioenergy, 28*(5), 499-507.

Shukla, S., Gita, S., Bharti, V., Bhuvaneswari, G., & Wikramasinghe, W. (2017). Atmospheric carbon sequestration through microalgae: Status, prospects, and challenges, *Agro-Environmental Sustainability* (pp. 219-235): Springer.

Silitonga, A., Masjuki, H., Ong, H. C., Mahlia, T., & Kusumo, F. (2017). Optimization of extraction of lipid from *Isochrysis galbana* microalgae species for biodiesel synthesis. *Energy Sources, Part A: Recovery, Utilization, and Environmental Effects, 39*(11), 1167-1175.

Sirajunnisa, A. R., & Surendhiran, D. (2016). Algae–A quintessential and positive resource of bioethanol production: A comprehensive review. *Renewable and Sustainable Energy Reviews, 66*, 248-267.

Sivaramakrishnan, R., & Incharoensakdi, A. (2018). Utilization of microalgae feedstock for concomitant production of bioethanol and biodiesel. *Fuel, 217*, 458-466.

Slade, R., & Bauen, A. (2013). Micro-algae cultivation for biofuels: Cost, energy balance, environmental impacts and future prospects. *Biomass and Bioenergy, 53*, 29-38.

Sohi, S., Loez-Capel, E., Krull, E., & Bol, R. (2009). Biochar's roles in soil and climate change: A review of research needs. *CSIRO Land and Water Science Report, 5*(09), 1-57.

Spokas, K. A., Novak, J. M., Stewart, C. E., Cantrell, K. B., Uchimiya, M., DuSaire, M. G., & Ro, K. S. (2011). Qualitative analysis of volatile organic compounds on biochar. *Chemosphere, 85*(5), 869-882.

Standard, A. (2007). *A standard test method for gross calorific value of coal and coke*: ASTM International.

Standard, A. (2009). *Standard practice for ultimate analysis of coal and coke*: ASTM International.

Standard, A. (2013). *Standard test methods for proximate analysis of coal and coke by macro thermogravimetric analysis*: ASTM International.

Suganya, T., Varman, M., Masjuki, H., & Renganathan, S. (2016). Macroalgae and microalgae as a potential source for commercial applications along with biofuels production: A biorefinery approach. *Renewable and Sustainable Energy Reviews, 55*, 909-941.

Sun, H., Lu, H., Chu, L., Shao, H., & Shi, W. (2017). Biochar applied with appropriate rates can reduce N leaching, keep N retention and not increase NH_3 volatilization in a coastal saline soil. *Science of the total environment, 575*, 820-825.

Sun, X.-F., Wang, S.-G., Liu, X.-W., Gong, W.-X., Bao, N., Gao, B.-Y., & Zhang, H.-Y. (2008). Biosorption of Malachite Green from aqueous solutions onto aerobic granules: Kinetic and equilibrium studies. *Bioresource Technology, 99*(9), 3475-3483.

Tag, A. T., Duman, G., Ucar, S., & Yanik, J. (2016). Effects of feedstock type and pyrolysis temperature on potential applications of biochar. *Journal of Analytical and Applied Pyrolysis, 120*, 200-206.

Tagliabue, M., Farrusseng, D., Valencia, S., Aguado, S., Ravon, U., Rizzo, C., . . . Mirodatos, C. (2009). Natural gas treating by selective adsorption: Material science and chemical engineering interplay. *Chemical Engineering Journal, 155*(3), 553-566.

Tan, Z., Wang, Y., Kasiulienė, A., Huang, C., & Ai, P. (2017). Cadmium removal potential by rice straw-derived magnetic biochar. *Clean Technologies and Environmental Policy, 19*(3), 761-774.

Teh, Y. Y., Lee, K. T., Chen, W.-H., Lin, S.-C., Sheen, H.-K., & Tan, I. S. (2017). Dilute sulfuric acid hydrolysis of red macroalgae *Eucheuma denticulatum* with microwave-assisted heating for biochar production and sugar recovery. *Bioresource Technology, 246*, 20-27.

Tekin, K., Karagöz, S., & Bektaş, S. (2014). A review of hydrothermal biomass processing. *Renewable and Sustainable Energy Reviews, 40*, 673-687.

Temkin, M. (1940). Kinetics of ammonia synthesis on promoted iron catalysts. *Acta Physicochimica U.R.S.S., 12*, 327-356.

Thangalazhy-Gopakumar, S., Adhikari, S., Chattanathan, S. A., & Gupta, R. B. (2012). Catalytic pyrolysis of green algae for hydrocarbon production using H+ZSM-5 catalyst. *Bioresource Technology, 118*(Supplement C), 150-157.

Thangavelu, S. K., Rajkumar, T., Pandi, D. K., Ahmed, A. S., & Ani, F. N. (2019). Microwave assisted acid hydrolysis for bioethanol fuel production from sago pith waste. *Waste Management, 86*, 80-86.

Titirici, M.-M., White, R. J., Falco, C., & Sevilla, M. (2012). Black perspectives for a green future: Hydrothermal carbons for environment protection and energy storage. *Energy & Environmental Science, 5*(5), 6796-6822.

Torri, C., Samorì, C., Adamiano, A., Fabbri, D., Faraloni, C., & Torzillo, G. (2011). Preliminary investigation on the production of fuels and bio-char from *Chlamydomonas reinhardtii* biomass residue after bio-hydrogen production. *Bioresource Technology, 102*(18), 8707-8713.

Tripathi, M., Sahu, J. N., & Ganesan, P. (2016). Effect of process parameters on production of biochar from biomass waste through pyrolysis: A review. *Renewable and Sustainable Energy Reviews, 55*, 467-481.

Turkcan, A. (2018). Effects of high bioethanol proportion in the biodiesel-diesel blends in a CRDI engine. *Fuel, 223*, 53-62.

Uchimiya, M., Chang, S., & Klasson, K. T. (2011). Screening biochars for heavy metal retention in soil: Role of oxygen functional groups. *Journal of Hazardous Materials, 190*(1), 432-441.

Uemura, Y., Matsumoto, R., Saadon, S., & Matsumura, Y. (2015). A study on torrefaction of *Laminaria japonica*. *Fuel Processing Technology, 138*, 133-138.

Ueno, Y., Kurano, N., & Miyachi, S. (1998). Ethanol production by dark fermentation in the marine green alga, *Chlorococcum littorale*. *Journal of Fermentation and Bioengineering, 86*(1), 38-43.

Ullah, K., Ahmad, M., Sofia, Sharma, V. K., Lu, P., Harvey, A., . . . Sultana, S. (2015). Assessing the potential of algal biomass opportunities for bioenergy industry: A review. *Fuel, 143*, 414-423.

Vassilev, S. V., & Vassileva, C. G. (2016). Composition, properties and challenges of algae biomass for biofuel application: An overview. *Fuel, 181*, 1-33.

Vaughn, S. F., Kenar, J. A., Tisserat, B., Jackson, M. A., Joshee, N., Vaidya, B. N., & Peterson, S. C. (2017). Chemical and physical properties of *Paulownia elongata* biochar modified with oxidants for horticultural applications. *Industrial Crops and Products, 97*, 260-267.

Wan, Y., Chen, P., Zhang, B., Yang, C., Liu, Y., Lin, X., & Ruan, R. (2009). Microwave-assisted pyrolysis of biomass: Catalysts to improve product selectivity. *Journal of Analytical and Applied Pyrolysis, 86*(1), 161-167.

Wang, K., Brown, R. C., Homsy, S., Martinez, L., & Sidhu, S. S. (2013). Fast pyrolysis of microalgae remnants in a fluidized bed reactor for bio-oil and biochar production. *Bioresource Technology, 127*, 494-499.

Wang, N., Tahmasebi, A., Yu, J., Xu, J., Huang, F., & Mamaeva, A. (2015). A comparative study of microwave-induced pyrolysis of lignocellulosic and algal biomass. *Bioresource Technology, 190*, 89-96.

Wang, T., Arbestain, M. C., Hedley, M., & Bishop, P. (2012). Chemical and bioassay characterisation of nitrogen availability in biochar produced from dairy manure and biosolids. *Organic Geochemistry, 51*, 45-54.

Wang, X., Liu, X., & Wang, G. (2011). Two-stage hydrolysis of invasive algal feedstock for ethanol fermentation. *Journal of Integrative Plant Biology, 53*(3), 246-252.

Wang, Y., Ho, S.-H., Cheng, C.-L., Guo, W.-Q., Nagarajan, D., Ren, N.-Q., . . . Chang, J.-S. (2016). Perspectives on the feasibility of using microalgae for industrial wastewater treatment. *Bioresource Technology, 222*, 485-497.

Weber, W. J., & Morris, J. C. (1963). Kinetics of adsorption on carbon from solution. *Journal of the Sanitary Engineering Division, 89*(2), 31-60.

Wei, J., Sun, W., Pan, W., Yu, X., Sun, G., & Jiang, H. (2017). Comparing the effects of different oxygen-containing functional groups on sulfonamides adsorption by carbon nanotubes: Experiments and theoretical calculation. *Chemical Engineering Journal, 312*(Supplement C), 167-179.

Wilk, M., & Magdziarz, A. (2017). Hydrothermal carbonization, torrefaction and slow pyrolysis of *Miscanthus giganteus*. *Energy, 140*(Part 1), 1292-1304.

Wilson, C. A., & Novak, J. T. (2009). Hydrolysis of macromolecular components of primary and secondary wastewater sludge by thermal hydrolytic pretreatment. *Water Research, 43*(18), 4489-4498.

Wu, F.-C., Tseng, R.-L., Huang, S.-C., & Juang, R.-S. (2009). Characteristics of pseudo-second-order kinetic model for liquid-phase adsorption: A mini-review. *Chemical Engineering Journal, 151*(1), 1-9.

Wu, F.-C., Tseng, R.-L., & Juang, R.-S. (2009). Characteristics of Elovich equation used for the analysis of adsorption kinetics in dye-chitosan systems. *Chemical Engineering Journal, 150*(2), 366-373.

Wu, K.-T., Tsai, C.-J., Chen, C.-S., & Chen, H.-W. (2012). The characteristics of torrefied microalgae. *Applied Energy, 100*, 52-57.

Wu, Z., Yang, W., Tian, X., & Yang, B. (2017). Synergistic effects from co-pyrolysis of low-rank coal and model components of microalgae biomass. *Energy Conversion and Management, 135*, 212-225.

Xiao, L.-P., Shi, Z.-J., Xu, F., & Sun, R.-C. (2012). Hydrothermal carbonization of lignocellulosic biomass. *Bioresource Technology, 118*, 619-623.

Xiao, R., Chen, X., Wang, F., & Yu, G. (2010). Pyrolysis pretreatment of biomass for entrained-flow gasification. *Applied Energy, 87*(1), 149-155.

Xu, N., Tan, G., Wang, H., & Gai, X. (2016). Effect of biochar additions to soil on nitrogen leaching, microbial biomass and bacterial community structure. *European Journal of Soil Biology, 74*, 1-8.

Yadav, A., Ansari, K. B., Simha, P., Gaikar, V. G., & Pandit, A. B. (2016). Vacuum pyrolysed biochar for soil amendment. *Resource-Efficient Technologies, 2, Supplement 1*, S177-S185.

Yan, W., Acharjee, T. C., Coronella, C. J., & Vásquez, V. R. (2009). Thermal pretreatment of lignocellulosic biomass. *Environmental Progress & Sustainable Energy, 28*(3), 435-440.

Yek, P. N. Y., Peng, W., Wong, C. C., Liew, R. K., Ho, Y. L., Wan Mahari, W. A., . . . Lam, S. S. (2020). Engineered biochar via microwave CO_2 and steam pyrolysis to treat carcinogenic Congo red dye. *Journal of Hazardous Materials, 395*, 122636.

Yu, Y., & Christopher, L. P. (2017). Detoxification of hemicellulose-rich poplar hydrolysate by polymeric resins for improved ethanol fermentability. *Fuel, 203*, 187-196.

Yuan, T., Tahmasebi, A., & Yu, J. (2015). Comparative study on pyrolysis of lignocellulosic and algal biomass using a thermogravimetric and a fixed-bed reactor. *Bioresource Technology, 175*, 333-341.

Zama, E. F., Zhu, Y.-G., Reid, B. J., & Sun, G.-X. (2017). The role of biochar properties in influencing the sorption and desorption of Pb (II), Cd (II) and As (III) in aqueous solution. *Journal of Cleaner Production, 148*, 127-136.

Zhang, D., Pan, B., Wu, M., Wang, B., Zhang, H., Peng, H., . . . Ning, P. (2011). Adsorption of sulfamethoxazole on functionalized carbon nanotubes as affected by cations and anions. *Environmental Pollution, 159*(10), 2616-2621.

Zhang, K., Wells, P., Liang, Y., Love, J., Parker, D. A., & Botella, C. (2019). Effect of diluted hydrolysate as yeast propagation medium on ethanol production. *Bioresource Technology, 271*, 1-8.

Zhang, L., Xi, G., Chen, Z., Qi, Z., & Wang, X. (2017). Enhanced formation of 5-HMF from glucose using a highly selective and stable SAPO-34 catalyst. *Chemical Engineering Journal, 307*, 877-883.

Zhang, X., Wang, H., He, L., Lu, K., Sarmah, A., Li, J., . . . Huang, H. (2013). Using biochar for remediation of soils contaminated with heavy metals and organic pollutants. *Environmental Science and Pollution Research, 20*(12), 8472-8483.

Zheng, H., Guo, W., Li, S., Chen, Y., Wu, Q., Feng, X., . . . Chang, J.-S. (2017). Adsorption of p-nitrophenols (PNP) on microalgal biochar: Analysis of high adsorption capacity and mechanism. *Bioresource Technology, 244*, 1456-1464.

Zhou, J., Chen, H., Huang, W., Arocena, J. M., & Ge, S. (2015). Sorption of Atrazine, 17α-Estradiol, and Phenanthrene on Wheat Straw and Peanut Shell Biochars. *Water, Air, & Soil Pollution, 227*(1), 7.

Zhou, N., Zhang, Y., Wu, X., Gong, X., & Wang, Q. (2011). Hydrolysis of *Chlorella* biomass for fermentable sugars in the presence of HCl and $MgCl_2$. *Bioresource Technology, 102*(21), 10158-10161.

Zhou, Y., Lu, J., Zhou, Y., & Liu, Y. (2019). Recent advances for dyes removal using novel adsorbents: A review. *Environmental Pollution, 252*, 352-365.

Ziolkowska, J., & Simon, L. (2014). Recent developments and prospects for algae-based fuels in the US. *Renewable and Sustainable Energy Reviews, 29*, 847-853.